DEGRADATION OF ENGINEERED POLYURETHANE HEART VALVES IN A MECHANICALLY DEMANDING ENVIRONMENT WITH VARIABLE MIXING OF POLYESTER AND POLYCARBONATE SOFT SEGMENTS

by

Samuel Kevin Luketich

B.S. Bioengineering, University of Pittsburgh, 2015

Submitted to the Graduate Faculty of

Swanson School of Engineering in partial fulfillment

of the requirements for the degree of

Master of Science

University of Pittsburgh

2018

UNIVERSITY OF PITTSBURGH

SWANSON SCHOOL OF ENGINEERING

This thesis was presented

by

Samuel Kevin Luketich

It was defended on

March 27, 2018

and approved by

Harvey S. Borovetz, Ph.D.
Distinguished Professor, Department of Bioengineering
Robert L. Hardesty Professor, Department of Surgery
Professor, Department of Chemical and Petroleum Engineering

Youngjae Chun, Ph.D.
Associate Professor, Departments of Industrial Engineering and Bioengineering

Antonio D'Amore, Ph.D.
Research Assistant Professor, Departments of Surgery and Bioengineering

Thesis Advisor: William R. Wagner, Ph.D.
Professor, Departments of Surgery, Bioengineering, and Chemical and Petroleum Engineering
Director, McGowan Institute for Regenerative Medicine

DEGRADATION OF ENGINEERED POLYURETHANE HEART VALVES IN A MECHANICALLY DEMANDING ENVIRONMENT WITH VARIABLE MIXING OF POLYESTER AND POLYCARBONATE SOFT SEGMENTS

Samuel Kevin Luketich, M.S.

University of Pittsburgh, 2018

Valvular heart disease (VHD) is a major source of morbidity and mortality leading to approximately 290,000 valve replacement surgeries worldwide each year. Current replacement prosthetics include mechanical and bioprosthetic heart valves, which are burdened by chronic anticoagulation therapy and tissue degeneration, respectively, as well as an inability to grow and remodel. Tissue engineered heart valves (TEHVs) have been proposed to overcome these limitations by providing a scaffold that is designed to be gradually replaced by autologous functional tissue. As such, TEHVs should degrade at a rate matching new tissue formation to achieve proper function and avoid structural failure.

Biodegradable polyurethane elastomers are suitable candidates for TEHVs and offer tunable degradability based on soft segment chemistry. Polyester soft segments in poly(ester urethane)urea (PEUU) generate faster degradation than polycarbonate soft segments in poly(carbonate urethane)urea (PCUU). These biodegradable polyurethanes can be electrospun into fully assembled, fibrous TEHVs. The objectives of this study were to evaluate the *in vitro* degradation profile of three polyurethane soft segment mixing strategies and the effects of a mechanically demanding environment on the degradation rate. Equal ratios of faster-degrading polyester and slower-degrading polycarbonate segments were mixed into polyurethanes using three strategies: 1) soft segment mixing during synthesis to form poly(ester carbonate urethane)urea, 2) physical blending of PEUU and PCUU polymers during solvation to form a

single solution, and 3) electrospinning from two independent streams of PEUU and PCUU solutions. These mixing strategies varied the chemical composition of the polymer chains and electrospun fibers between groups.

Electrospun TEHVs from each mixing strategy were subjected to accelerated degradation in a pulse duplicator with enzymatic solution for two weeks. Relative degradation rates were quantified based on scaffold mass and thickness loss, macro- and microscopic structural changes, and viscosity reduction. Additionally, biaxial mechanical compliance was monitored throughout degradation and initial scaffold blood compatibility was assessed. Soft segment mixed TEHVs had the most degradation while co-spun TEHVs degraded very little. Additionally, mechanical strength was maintained for each mixing strategy throughout degradation. Findings of this study are instrumental in efficiently designing TEHVs where tunable degradation is critical to match the *in vivo* tissue formation rate.

TABLE OF CONTENTS

LIST OF TABLES

LIST OF FIGURES

PREFACE

I would first like to thank my thesis advisor, Dr. William R. Wagner, and committee members, Dr. Harvey Borovetz, Dr. Youngjae Chun, and Dr. Antonio D'Amore, for their support and guidance with this thesis. The many opportunities provided to me by Dr. Wagner and Dr. D'Amore to perform cardiovascular research are truly appreciated. I am thankful for the time and efforts of the many other co-workers who trained and assisted me on the various aspects of this project, especially Rich Hoff, Dr. Sang-Ho Ye, Dan McKeel, Dr. Xinzhu Gu, and Salim Olia. The numerous University of Pittsburgh and visiting students have provided me with both friendship and assistance, and I appreciate the contributions of Chiara Dal Zovo, Tamir Grunberg, Gabriele Nasello, Andrea De Nicola, and Drake Pedersen, among many others, to this work. I would also like to acknowledge the University of Pittsburgh Center for Biologic Imaging for providing access to their scanning electron microscope and thank Dr. Marina Kameneva for the equipment used in the pulse duplicator. This work was supported by the RiMED Foundation, the Coulter Foundation, and the Clinical and Translational Science Institute (CTSI) at the University of Pittsburgh.

1.0 INTRODUCTION

1.1 PROSTHETIC HEART VALVES

1.1.1 Epidemiology and etiology of heart valve disease

Cardiovascular disease is the leading cause of death in the United States [1] and includes diseases that affect either the heart or blood vessels. Diseases involving the heart include cardiomyopathy, heart failure, cardiac dysrhythmias, and valvular heart disease. Valvular heart disease (VHD) is a major source of morbidity and mortality in the United States and around the world [2]. While VHD affects 2.5% of the United States population [2], there are approximately 90,000 valve replacement surgeries in the United States [3] and 290,000 worldwide each year [4], and this number is expected to increase with the aging population. Additionally, valvular defects are present in 1% of newborns [5]. The market for heart valve repair and replacement is estimated at $2.8 billion with an anticipated growth rate of 9.1% annually [6].

VHD is classified as dysfunction in any of the four heart valves: aortic, mitral, pulmonary, and tricuspid, which typically arises from either valvular stenosis or regurgitation. Valvular stenosis is the inability of the valve to fully open, resulting in a narrow opening for blood flow, often caused by stiffening of the leaflets. Alternatively, valvular regurgitation, or insufficiency, is characterized by the inability of the valve to close completely and results in the

backflow of blood [7]. Both scenarios force the heart to work harder to either pump enough blood through a small opening or sufficiently overcoming a backflow of blood. The high pressures on the left side of the heart make those valves more susceptible, and consequently, aortic and mitral valve stenosis and regurgitation are the most common forms of VHD [8].

Rheumatic heart disease is the major cause of VHD in developing countries. Industrialized countries, which have had a major reduction in rheumatic disease, still have a large occurrence of VHD typically caused by degenerative processes [2, 9]. Other mechanisms such as endocarditis, inflammatory processes, congenital malformations, and ischemia can also contribute [8]. Although valve repair is the preferred surgical treatment for patients with VHD, some valves cannot be repaired and require replacement surgery [10], typically with a prosthetic heart valve.

1.1.2 Current heart valve technology: mechanical and bioprosthetic

Current technologies for heart valve replacement surgeries include two categories of prosthetic heart valves: mechanical and bioprosthetic. Mechanical heart valves are produced from synthetic materials such as polymer and metal (e.g. stainless steel, titanium). Traditionally, bileaflet, monoleaflet, and ball-in-cage are the three common mechanical prosthetic valve designs [3], shown in **Figure 1**. The bileaflet valve, produced by St. Jude Medical, is the most common mechanical prosthesis and operates by the opening and closing of semicircular leaflets that form three orifices. The monoleaflet, or single-tilting-disk valve, manufactured by Medtronic-Hall, functions by a single disk tilting between two struts to create two orifices. The ball-in-cage valve, manufactured by Starr-Edwards, operates by a ball moving forward or backward in a cage as the valve opens and closes [11].

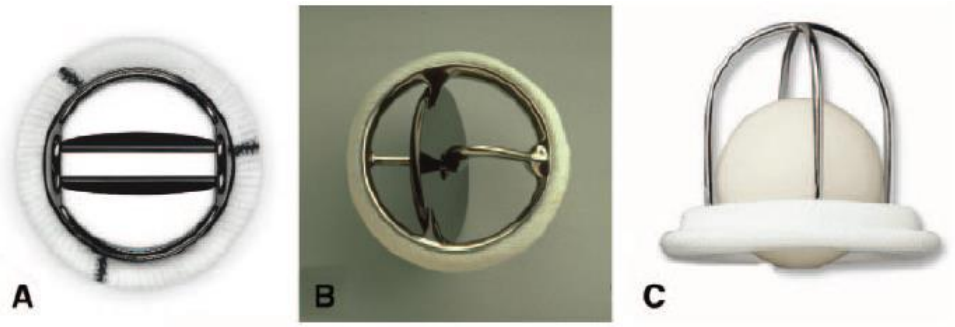

Figure 1. Mechanical heart valves. A) Bileaflet, B) monoleaflet, and C) ball-in-cage (from [3]).

Alternatively, bioprosthetic heart valves are constructed using homogeneic (autologous or allogeneic) or xenogeneic tissue sources. An autologous valve is used in the Ross procedure when a patient has the pulmonary valve removed and repositioned in the aortic root [7]. For humans, allogeneic heart valves from cadavers have many desirable properties. However, xenogeneic tissue valves, harvested from porcine or bovine, are by far the most common and are typically in the form of porcine aortic valves or bovine pericardium [12]. Bioprosthetic heart valves are usually fixed in glutaraldehyde to cross-link the collagen and lyse the cells to decrease the chance of an immune reaction [12].

Medtronic (Minneapolis, MN), St. Jude Medical (St. Paul, MN), and Edwards Lifesciences (Irvine, CA) are the three major bioprosthetic valve manufactures that produce several types of bioprosthetic valves. For example, the Medtronic Mosaic, Medtronic Hancock II, St. Jude Medical Epic, and Edwards Lifesciences Carpentier-Edwards porcine are stent valves from porcine leaflets. Bovine pericardium is used with the St. Jude Medical Trifecta and Edwards Lifesciences Carpentier-Edwards Perimount to form a stented valve. As a stentless approach, the Medtronic Freestyle, St. Jude Medical Toronto SPV, and Edwards Lifesciences Prima use porcine root leaflets [13]. **Figure 2** shows an example of the bioprosthetic valves

listed above. Another manufacturer, Sorin (Milan, Italy) produces the Mitroflow and Soprano Armonia valves, both of which are stented bovine pericardium [13].

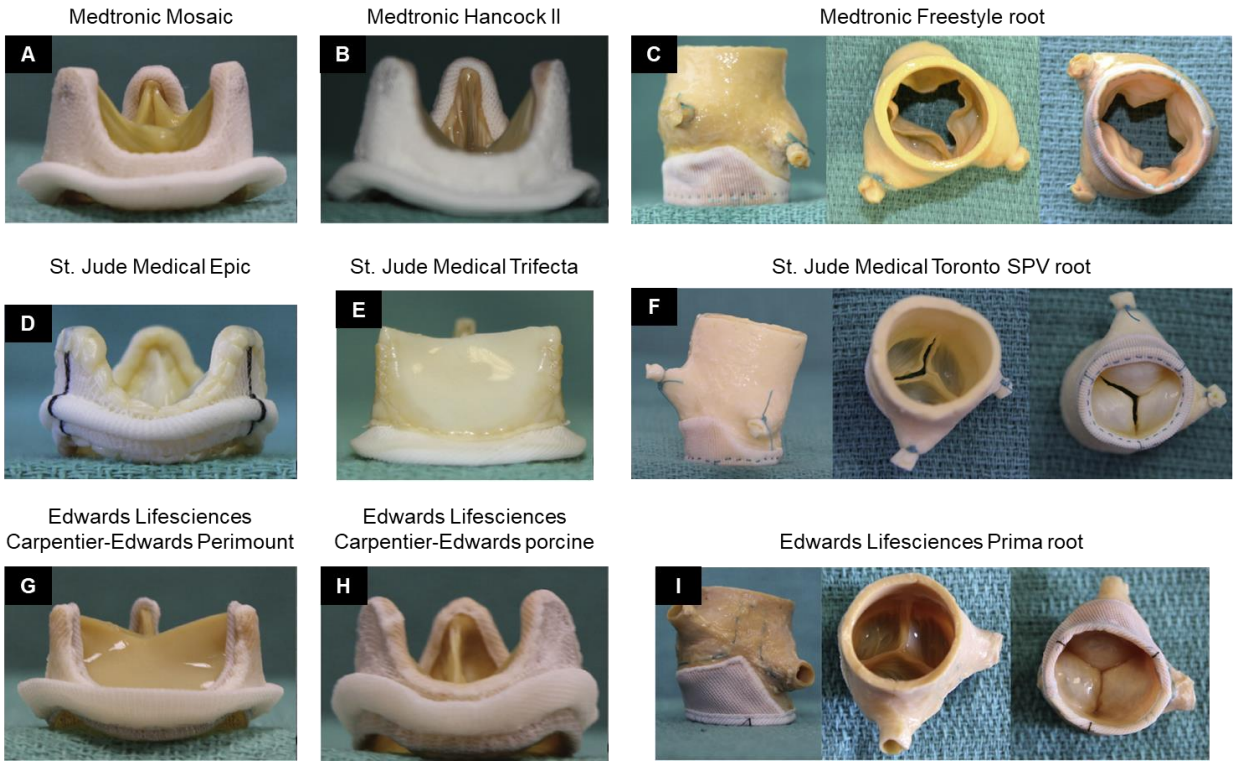

Figure 2. Bioprosthetic heart valves. Examples of porcine and bovine stented and stentless bioprosthetic valves from A-C) Medtronic, D-F) St. Jude Medical, and G-I) Edwards Lifesciences (from [13]).

1.1.3 Limitations of prosthetic heart valves

Prosthetic heart valves are burdened with a number of issues related to the long-term use of the device. One major problem that exists in both types of prostheses is the inability to grow and adapt with the patient. This is particularly problematic for the pediatric population as prostheses can reduce pediatric life expectancy by 50% while subjecting them to lifetime valve morbidity [14]. Because these valves cannot grow with the patient, a child receiving a prosthetic valve will

undergo replacement surgery every few years to increase the size until he or she is fully grown [15].

Mechanical prostheses require chronic anticoagulation therapy, such as warfarin, to control thromboembolism from blood contact with the synthetic surface [3]. Consequently, hemorrhages can form as a result of the therapy, and this puts the patient at an increased risk for excessive bleeding [16]. This prosthesis is particularly difficult for younger patients as it limits their activity. Prosthetic endocarditis is also possible with these valves as bacteria enters the blood stream through incomplete sterilization of the prostheses or other points of entry in the body [4]. In addition, the various geometries and different orifices cause suboptimal hemodynamic performance, which can lead to stagnant blood or poor perfusion [4, 17].

Bioprosthetic heart valves are limited in their durability as the biological tissue leaflets typically begin to degenerate after 7-8 years [3, 12] and will completely degenerate in 10-20 years [7]. The rate of degeneration is higher in younger patients, particularly those under the age of 40, due to higher stresses and pressures on the prosthesis [3]. Degeneration is characterized by tearing, thickening, or stiffening of the leaflets, and there are several mechanisms for bioprosthetic degeneration including infective endocarditis, calcification, thrombosis, pannus formation, and pressure.

Infective endocarditis of the bioprostheses can result from bacteria entering the bloodstream or a previous case of endocarditis, where the tissue leaflet supports the growth of bacteria, which can lead to tearing or stenosis [12, 17]. Glutaraldehyde fixation of the xenogeneic tissue releases calcium from lysed cells in the tissue causing calcium nucleation as well as other components to react with circulating calcium ions, all of which reacts with phospholipids to cause calcification of the prosthesis. This can lead to either regurgitation from

leaflet tears or stenosis associated with leaflet stiffening [12, 17]. Thrombus formation, although infrequent in bioprostheses, can occur from a lack of short-term anticoagulation therapy or asymmetrical valves resulting in static blood [12, 17]. Pannus formation can lead to leaflet stiffening and displaced stress loads when cells at the site of the injury (e.g. myofibroblasts, fibroblasts) overextend onto the leaflets. Although some pannus formation can assist in healing and reduce thrombogenicity, it can also cause stenosis, regurgitation, and calcification [12, 17]. High pressures within the heart can also lead to degeneration, particularly at the commissures, where there is a high stress concentration [12, 17].

The specific drawbacks of each of these prostheses have led to the development of criteria for identifying the best option for the patient. Age and life expectancy are major factors in determining the prosthesis, and it is typically recommended that patients under the age of 65 and with a longer life expectancy receive a mechanical prosthesis. However, a woman of child bearing age that may become pregnant is advised for a bioprosthetic valve. Additionally, those already on warfarin therapy would be advised for a mechanical valve while others with a contra-indication for warfarin would be directed toward a bioprosthetic valve [3].

1.2 TISSUE ENGINEERED HEART VALVES

Tissue engineered heart valves (TEHVs) have been proposed as a solution to overcome the existing limitations of mechanical and bioprosthetic heart valves. These valves are targeted toward a younger patient population with engineering focused on tissue remodeling and growth over time. Specifically, engineered valves are being designed to mimic the native physiological functions of a heart valve with proper hemodynamic performance, support new tissue growth and

corresponding scaffold degradation, reduce thrombogenicity and calcification, and/or be delivered percutaneously with a catheter. Research is being conducted on numerous tissue designs involving decellularized tissues, synthetic polymers, or biologic materials for structurally robust tissue combined with a cell source, growth factors, and/or other synthetic materials to promote growth and remodeling [4, 18]. There have been numerous strategies for developing TEHVs over the past 20 years, and the two main approaches to engineering these constructs are *in vitro* or *in situ* tissue growth [19].

1.2.1 Review of tissue engineered heart valves

The *in vitro* approach to TEHVs generates a construct with new tissue prior to implantation by seeding cells onto a scaffold and then incubating or conditioning them in a bioreactor. With this method, various autologous cell sources have been identified and harvested, expanded in cell culture, and then seeded onto the scaffold matrix. Bioreactors with pulsatile flow are often used to simulate the pressures and mechanical conditions experienced by the valves in the body. For example, Flanagan et al. [20] seeded fibrin heart valves with ovine carotid artery cells and conditioned the construct on a bioreactor to increase cell attachment and extracellular matrix (ECM) production. The drawbacks of this approach are lengthy production times for one scaffold and the complexity of the process which increases regulatory difficulty [19].

The alternative TEHV approach is *in situ* engineering where heart valve scaffolds are not incubated or conditioned prior to implantation. This simpler approach involves implanting scaffold matrices, which may or may not be seeded with cells, directly into the heart of a recipient and using the body as a bioreactor to populate the scaffold and regenerate tissue. An example is the synthetic scaffold with a nitinol stent in Emmert et al. [21] which was seeded with

autologous bone marrow mononuclear cells and implanted immediately. These scaffolds benefit from decreased manipulation prior to implantation and a quicker production process with less stringent regulatory approvals. The main disadvantage with this approach is that the recipient must have the ability to regenerate tissue [19].

Scaffold materials for these approaches are typically derived from two sources: decellularized heart valves or artificial materials. Decellularization of valves prevents an immune response in the recipient by removing all cells, but maintains the components of the ECM that provide structural support. Decellularized heart valves can be either allogenic [22, 23], such as a decellularized pulmonary valve from the same species, or xenogeneic [24-27], like decellularized pulmonary valves from a different species. Artificial materials range from synthetic to natural polymers and can be either fibrous, porous, or a hydrogel [28], each having specific benefits. Porous scaffolds serve to create a network of pores for nutrients and waste to flow thorough in order to support tissue growth and vascularization [28], and can be formed with methods such as thermally induced phase separation, particulate leaching, and solvent casting. Meanwhile, fibrous scaffolds, which can be produced by electrospinning, are assembled to resemble ECM structure to promote cell adhesion to the surface, migration along the scaffold, and differentiation into specific cell types.

Dohmen et al. [22, 23] employed an allogeneic approach by decellularizing pulmonary valves from other humans. These decellularized valves were repopulated with autologous vascular endothelial cells from the human recipient before implantation. Using a xenogeneic method, Metzner et al. [25] developed a decellularized porcine pulmonary valve with an expandable nitinol stent. Endothelial cells and myofibroblasts from the recipient sheep were loaded onto the decellularized tissue and delivered percutaneously. This xenogeneic approach

was applied to humans by Perri et al. [26] who replaced pulmonary valves in patients with decellularized porcine pulmonary valves without the addition of cells before implantation. Similarly, Simon et al. [27] studied Synergraft™, a decellularized porcine heart valve without a cell source, in pediatric patients. Decellularized porcine pericardium was used by Tedder et al. [24], and penta-galloyl glucose, as opposed to glutaraldehyde, was used to stabilize collagen. These scaffolds were seeded with rat aortic fibroblasts before implanting them into a rat model.

Rotary jet spinning was used by Badrossamay et al. [29] to create constructs from blends of polycaprolactone (PLC) and gelatin or collagen before seeding them with several cell types. Capulli et al. [30] modified these scaffolds to contain poly-4-hydroxybutyrate (P4HB) and gelatin. Addition of a nitinol stent provided the ability for a minimally invasive delivery in an ovine model. Molding was used by Syedain et al. [31] to create a fibrin gel seeded with neonatal human dermal fibroblasts, and the scaffold was cultured for 5 weeks before implanting in the pulmonary position in an ovine model. Syedain et al. [32] then moved to the aortic position with a tube matrix consisting mostly of collagen. Ovine and human dermal fibroblasts were temporarily used to produce the matrix and were eventually removed from the scaffold as a stent was added. In comparison, Reimer et al. [33] used ovine fibroblasts in a mold to produce a tubular, stentless collagen matrix which was ultimately decellularized. Molded hyaluronan hydrogels were produced by Puperi et al. [34] and seeded with porcine aortic valve interstitial cells.

Early studies by Shinoka et al. [35, 36] used woven polyglactin and polyglycolic acid (PGA) as a single leaflet scaffold seeded with ovine endothelial cells and fibroblasts. Other early studies using synthetic scaffolds involve the work by Zund et al. [37], which produced biodegradable PGA and poly(lactic-co-glycolic acid) (PLGA) scaffolds with *in vitro* seeding of

sheep myofibroblasts and endothelial cells, and Sodian et al. [38], which involved seeding autologous arterial valvular cells onto molded polyhydroxyalkanoate (PHA) scaffolds. A PGA valve with a P4HB coating and seeded with human marrow stromal cells was developed by Hoerstrup et al. [39, 40]. This work was expanded upon by Mol et al. [41] as the design was modified with cells from the human vena saphena magna and a Fastacryl stent, and then Emmert et al. [42] altered the design with a nitinol stent and autologous bone marrow mononuclear cells for *in vivo* studies which could be delivered with a transcatheter delivery system. Recently, Moreira et al. [43] developed a knit polyethylene terephthalate (PET) tubular mesh and seeded it with ovine smooth muscle cells and fibroblasts. Kidane et al. [44] demonstrated the possibility of using polyhedral oligomeric silsesquioxanes with polycarbonate soft segments for engineered valves.

Other popular heart valve production methods include 3D printing and electrospinning. Hockaday et al. [45] 3D printed an aortic valve and root from poly(ethylene glycol) (PEG) diacrylate and seeded it with porcine aortic valve interstitial cells. Methacrylated hyaluronic acid and methacrylated gelatin were 3D printed to encapsulate human aortic valve interstitial cells by Duan et al. [46]. Electrospun heart valves were introduced by van Lieshout et al. [47] as multiple layers of PCL were electrospun onto a mold and then seeded with human myofibroblasts. Similarly, Del Gaudio et al. [48] electrospun PCL into a trileaflet valve without a stent. Recently, Tseng et al. [49] modified electrospun PCL and embedded it within a PEG hydrogel before seeding with valvular interstitial cells. An acellular approach by Kluin et al. [50] electrospun polycarbonate on a supporting polyether ether ketone stent which was implanted in an ovine model for up to 12 months. Finally, D'Amore et al. [51] electrospun fully assembled biodegradable valves using a mandrel with heart valve anatomical geometry.

With the acellular *in situ* approaches, scaffolds must be populated with endogenous cells from the surrounding tissue and circulating blood. This can be achieved with both biological scaffolds, as Tudorache et al. [52] demonstrated with the repopulation of decellularized pulmonary allografts, and synthetic scaffolds, demonstrated by Kluin et al. [50] with electrospun bis-urea modified polycarbonate into a pulmonary valve. Use of an acellular, synthetic heart valve with the *in situ* approach allows for control over a number of other valve properties (e.g. mechanics, size, geometry), does not require complex and time consuming processing, and donors are not needed for the scaffold material. A visual representation of these TEHV devices are included in **Figure 3**.

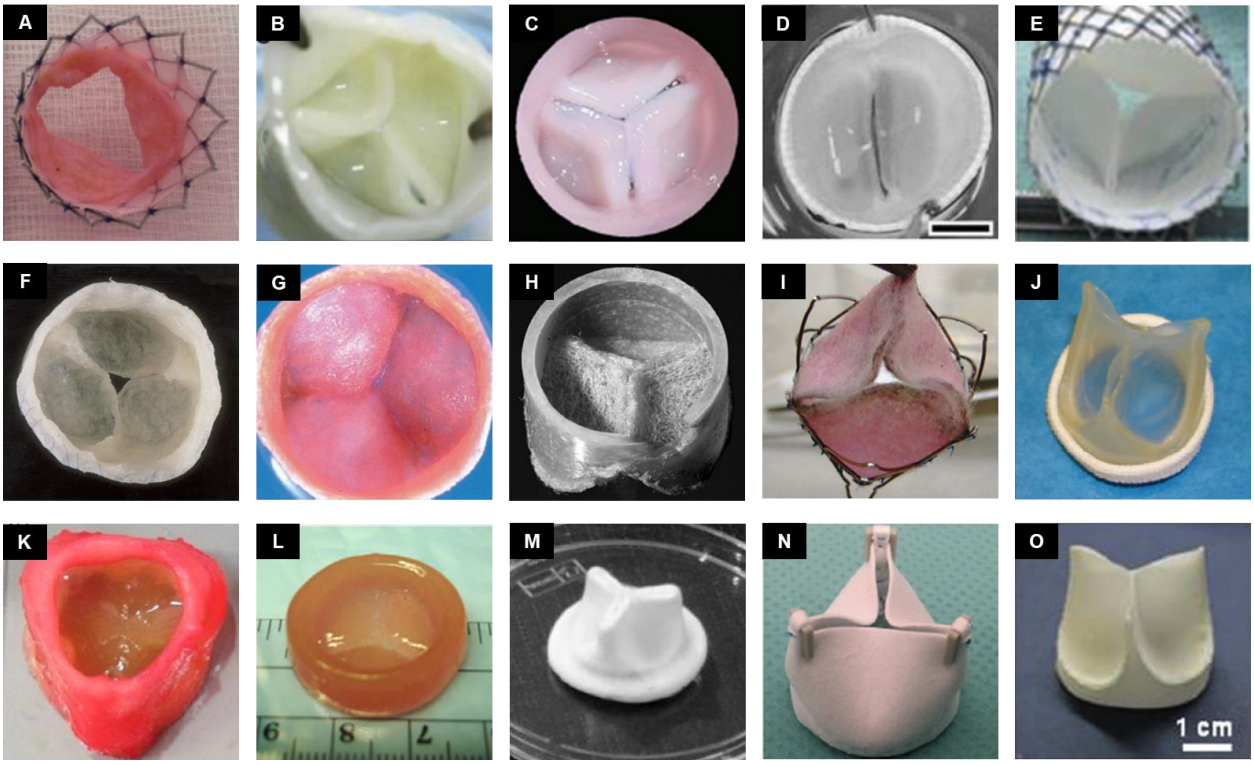

Figure 3. Tissue engineered heart valves. Valves from decellularized xenografts A) from [25]; natural materials B) from [33], C) from [20], D) from [31]; combinations of natural and synthetic materials E) from [30]; synthetic materials F) from [40], G) from [39], H) from [41], I) from [42], J) from [44]; 3D printing K) from [45], L) from [46]; and electrospinning M) from [48], N) from [50], O) from [51].

1.2.2 Mechanical properties of tissue engineered heart valves

Heart valves function in a mechanically demanding environment with cyclic loading throughout their lifetime. Valves are subjected to complex forces and stresses, rapid blood velocity, and high pressures that are constantly changing [15]. TEHVs must be able to function immediately upon implantation and support these complex loads without failure. Therefore, mechanical properties of TEHVs are important for temporarily supporting the mechanical load and directing new tissue development as remodeling occurs. When a valve construct is implanted to augment or replace the native tissue, the construct should be load bearing until new tissue begins forming and then gradually transfers the stress to the new tissue. Although the construct needs sufficient strength to prevent mechanical failure, mechanical mismatch in scaffolds which are too stiff will limit movement and cause discomfort. Additionally, the scaffolds should have appropriate mechanics to direct cell growth, movement, and differentiation. Mechanical signals can direct ECM remodeling at the site of the scaffold [53], and as appropriate *de novo* collagen synthesis occurs, the mechanical load can be transferred from the scaffold. Characterizing the native tissue mechanics and then recapitulating those properties in engineered constructs is essential when designing TEHVs.

Mechanical properties which are critical to and often employed in the design of TEHVs are uniaxial mechanics, biaxial mechanics, flexural mechanics, and mechanical fatigue [15, 54]. Simple material properties like Young's modulus or ultimate tensile strength of heart valve tissues can be evaluated with uniaxial mechanical testing. The stress-stretch curve for these native tissues display a non-linear response due to the stretching of crimped collagen fibers in the leaflets [15]. Stradins et al. [55] characterized the modulus of elasticity for human aortic and pulmonary valves at different anatomical locations on the leaflets. While testing human aortic

valve leaflets, Balguid et al. [56] reported differences in tensile properties in the radial and circumferential directions of the leaflet. Although uniaxial properties are often evaluated in TEHV constructs and are important in understanding strength and failure properties in one direction of a tissue, the dynamic motion and complex performance requirements necessitate an understanding of the in-plane and out-of-plane mechanics.

Merryman et al. [54] argues the importance of biaxial and flexural mechanics as they relate to heart valve mechanics. Biaxial mechanics of the heart valve leaflet is used to evaluate the simultaneous bidirectional (radial and circumferential) in-plane mechanics. The planar mechanics are important for the valve when it is coapting and preventing regurgitation. Christie and Barratt-Boyes biaxially tested porcine aortic and pulmonary valves [57] and the aortic valve from human hearts [58] and found the radial direction of the leaflets to be more compliant than the circumferential direction. Recently, the anisotropy ratio of the biaxial mechanics of porcine tricuspid valve leaflets was matched in a heart valve scaffold produced by electrospinning with a rotating, valve-shaped mandrel [51].

Flexural mechanics is another important property as it involves the bending of the valve leaflets. These out-of-plane mechanics are important as the valve must open and close 60-100 times per minutes without failing. The flexure test evaluates the stiffness of the leaflets, and depending on which direction the valve is bent, with or against curvature, the leaflet should be less stiff and more stiff, respectively [54]. Three-point bending [59] or cantilever bending [60] are two methods to understand flexural properties. A complete characterization by Brazile et al. [61] presented the flexural rigidity of porcine heart valves at all four valve positions, with- and against-curvature. Electrospinning with a low translation speed created a scaffold with similar flexural mechanics to a native porcine tricuspid valve [51].

Heart valves are subjected to cyclical loading and unloading with dynamic motion for the lifespan of a person, so fatigue testing is critical to evaluate construct durability. Fatigue testing can identity stress concentrations or weak point in a heart valve scaffold prior to implantation [5]. In one year, the heart will beat over 30 million times and valves will experience continuous stresses from leaflet stretching, flexing, or shearing [15]. Gloeckner et al. [62] studied changes in leaflet flexural mechanics after fatiguing porcine aortic valves with accelerated durability testing and found that the bending stiffness decreased over time.

Understanding the effects that fatigue has on the aforementioned mechanical properties of the heart valves, especially valves on the left side of the heart under greater pressures, is critical when designing TEHVs. Although engineered heart valves are not intended to experience years of fatigue (e.g. they degrade as new tissue forms), they must maintain their mechanical properties before new tissue forms. This emphasizes the importance of understanding mechanical degradation, as well as other forms of degradation [63], in biodegradable tissues which could accelerate the fatiguing process. Consequently, early losses of scaffold tissue at the site could lead to a loss in mechanical strength and eventually tissue mechanical failure [64].

1.3 ELECTROSPUN POLYMER PROCESSING

Electrospinning is a polymer processing technique used to generate fibrous scaffolds for various applications. The main feature of this processing method is the ability to produce fibers on a submicron scale, which is physiologically relevant for biological scaffolds. Additionally, the adaptability of electrospinning allows it to be used in a wide range of applications, including

drug delivery and tissue engineering. The ease of use and specific control over scaffold geometry make electrospinning an appealing technique for TEHVs.

1.3.1 Fundamentals of electrospinning

The basic electrospinning setup, shown in **Figure 4**, involves a high voltage power source, a metal capillary connected to a polymer solution, and a collecting surface [65]. The polymer solution, often loaded in a syringe, is forced through the metal capillary by a syringe pump or gravity at a certain rate. During this time, an electrode from the high voltage source is connect to the capillary and provides the polymer solution with a charge of one polarity. As it is forced out of the capillary, the charged polymer solution travels through the air and deposits on the collecting surface of opposite polarity as solid fibers. Voltage difference, type and concentration of polymer, and shape of the collecting surface are all variables which can be easily modified by the user to generate numerous scaffold specifications [65].

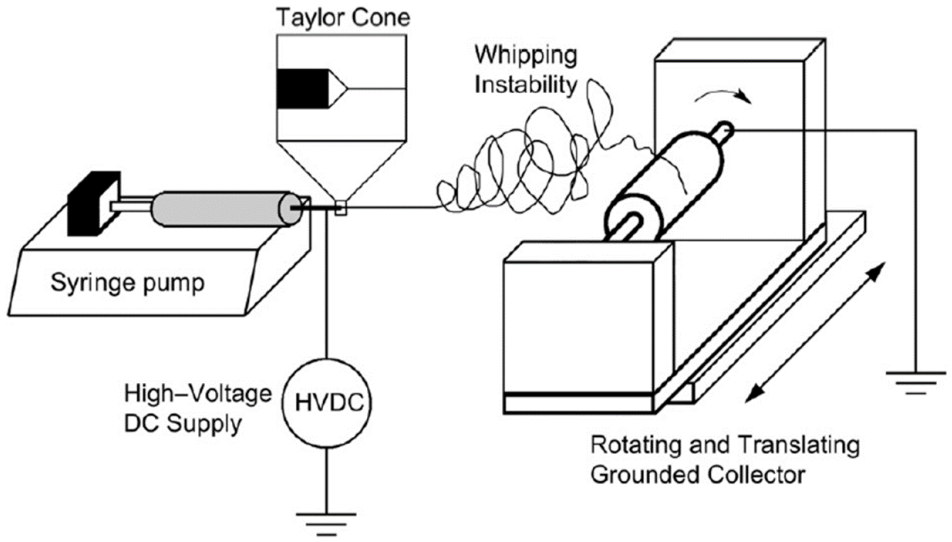

Figure 4. Schematic of a general electrospinning setup with a single polymer stream (from [65]).

The theory behind the polymer solution exiting the capillary tube and accumulating on the collecting surface is based on electrostatic force. As the polymer solution is being forced through the capillary tube, prior to the initiation of the high voltage power source, a pendant drop forms from the end of the capillary tube. Once the power sources are turns on, an electric field is created between the capillary tube and the collecting surface. As described in Sill and von Recum [65], repulsive forces form within the charged polymer solution while attractive forces are created between the polymer solution and collecting surface. Consequently, tensile forces begin to stretch the drop of polymer solution. However, these electrostatic forces are competing against the surface tension of the solution causing a Taylor cone to form at the tip of the capillary when these two forces are equal [65]. If the electric field is then increased further, a jet will erupt from the cone and be directed toward the collecting surface of opposite polarity. During this time, the jet undergoes bending instability due to the similar charges in the solution. The solvent evaporates as the jet moves toward the collector, eventually depositing polymer fibers on the collecting surface [65].

1.3.2 Desirable characteristics of electrospun scaffolds

Fibers produced during electrospinning are typically submicron, although they are often referred to as nanofibers, and range from 100 to 500 nm [65]. Production of fibrous scaffolds which are physiologically relevant is important for directing cell migration and differentiation [66]. Orientation of the fibers in a scaffold is relevant as highly aligned fibers produce mechanical anisotropy while isotropic mechanical properties result from a random fiber orientation [67]. Additionally, an increase in fiber intersections decreases the flexural mechanical stiffness of a

scaffold [68]. Although electrospun scaffolds are not highly porous, porosity and pore size can be moderately controlled for cell infiltration into the scaffold [65].

The electrospinning process has a variety of parameters within the control of the user to manipulate the electric field and alter the properties mentioned above and are summarized in Sill and von Recum [65]. The voltage of the polymer solution and collecting surface are important parameters for generating a sufficient electric field, and increasing the voltage sources can decrease fiber diameter [51]. Increasing the flow rate of the polymer solution results in an increase in fiber diameter. Fiber diameter can also be increased with an increase in polymer concentration and consequential increase in solution viscosity. Increasing the distance between the tip of the capillary and collecting surface results in a decrease in fiber diameter [51]. Finally, microtexture on the fibers can be created by increasing solvent volatility [65].

Tissue engineered scaffolds are often made of multiple biomaterials, and the capillary nozzle configuration can be adjusted for either single or multiple polymer streams during the electrospinning process. Three main spinneret configurations include: single capillary, dual capillaries, and co-axial capillaries. Single capillary technique, the most frequently employed, is used in fabrications in which a solution consists of a single polymer [51] or a blend of miscible polymers [69-71]. Dual capillaries can be set in a side-by-side configuration, to combine two separate polymer streams from adjacent capillaries into a single jet [65], or independently, where two jets form and deposit on the collecting surface [72, 73]. Coaxial configuration is another approach which positions one capillary inside another and allows for the entrapment of smaller fibers in the polymer stream [65].

Control of the fabricated scaffold geometry exists through the type of collecting surface on which the polymer is deposited. These collecting surfaces range from solid surfaces where

fibers can directly deposit to wire and edges between which fibers forms; other methods use ring structures of similar polarity to the polymer to direct the assembly of fibers [74]. When the collecting surface performs dynamic motions like rotation, it is often referred to as a mandrel. Translation and rotation can add extra complexity to the mandrel and assist in fiber deposition. The rotating drum is one of the more common mandrels used for generating flat scaffolds and has shown the ability to produce diverse scaffold properties based on the rotational and translational speeds [67, 68]. D'Amore et al. [51] introduced a new mandrel with a complex geometry using a double component deposition (DCD) technique.

The various types of materials which can be electrospun into scaffolds provide users with another level of control in scaffold design. Current electrospun scaffolds for tissue engineering applications are derived from either natural and synthetic polymers, and recent approaches have used synthetic copolymers, blended natural polymers, blended synthetic polymers, and blended natural and synthetic polymers [75]. Natural polymers, such as proteins, polysaccharides, DNA, and lipids, benefit from a decreased immune response and increased biocompatibility [75], with collagen being the most frequently employed [65]. In contrast, synthetic materials are cheaper and have properties which are more easily controlled [75]. Typical synthetic polymers used in electrospinning include PCL, PEG, PGA, poly(lactic acid) (PLA), PLGA, and poly(L-lactide-*co*-ϵ-caprolactone) (PLCL) [65, 75] as well as a variety of polyurethanes [51, 76].

The main drawback of scaffolds produced by electrospinning is the low porosity with smaller pore size and less interconnected pores. Additionally, the fabrication method produces sample to sample variability and is more difficult to scale up for larger production, especially for more complex constructs like heart valves which are produced one at a time. However, the ability to produce submicron diameter fibers is a major benefit of electrospinning, as these fibers

are close to the physiologically relevant range. The fibrous structure produces robust mechanical properties by achieving relevant fiber alignment and intersection density. In addition, electrospinning is a fairly inexpensive technique for quick prototyping and production.

1.3.3 Electrospun scaffolds for tissue engineered heart valves

Having the ability to control fiber diameter, scaffold geometry, mechanical response, and applicable polymers, electrospinning has been used in the fabrication of a number of TEHVs [47-51]. Van Lieshout et al. [47] used a combination of four stainless steel mandrels as collecting surfaces for electrospun PCL. Three of the mandrels each represented one of the valve leaflets, and two coatings of polymer were electrospun onto each of the pieces. The three pieces were then brought together with a fourth piece that had complementary geometry, and an electrospun layer on the outside of the assembled four-piece mandrel represented the aortic root. Del Gaudio et al. [48] used a single aluminum mandrel with a complex geometry to collect PCL during electrospinning. However, the mandrel was rotated at a very low velocity which did not provide fiber alignment and anisotropy.

Tseng et al. [49] used a flat copper collector and an aluminum drum to collect PCL isotropic and anisotropic fibers, respectively. These constructs were added into PEG hydrogels and seeded with valvular interstitial cells. Although aligned fibers were produced in this study, the simple collecting surfaces did not produce a scaffold with anatomical geometry. D'Amore et al. [51] produced fully assembled, trileaflet valves from electrospun poly(ester urethane)urea using a double component collecting surface and complex geometry. Modification of the electrospinning parameters demonstrated control over the mechanical properties and fiber diameter of the engineered valve. Kluin et al. [50] electrospun bis-urea-modified polycarbonate

into a tube with aligned fibers, and a support ring made from polyether ether ketone was added to the construct. This acellular scaffold was implanted for up to 12 months in ovine and demonstrated the ability to degrade at a rate equivalent to ECM formation.

1.4 POLYMERS FOR TISSUE ENGINEERED SCAFFOLDS

Synthetic polymers are often used in TEHVs because they do not require a donor tissue source and the properties of the polymer are well known and have been extensively characterized. A number of factors can be controlled in the design on polymers including: copolymerization, molecular weight, stereospecificity, branching, cross-linking, and biodegradability. The degradability depends on the chemistry of the polymer and is determined by the number and type of labile bonds as well as the hydrophilicity of the molecule.

1.4.1 Nondegradable polymers

Nondegradable polymers are used in a number of medical applications [77], but are undesirable and counterproductive in tissue engineering. Medical products made from nondegradable polymers such as polyethylene (PE), polypropylene (PP), and polysulfone include catheters, sutures, and hollow fibers, respectively [77]. Other nondegradable polymers like polytetrafluoroethylene (PTFE) and polyurethanes are used as materials in vascular grafts [78] and heart valves [79]. These polymers are expected to last for much longer periods of time than would be required for a degradable tissue engineered scaffold.

1.4.2 Degradable polymers

Polymers with anhydride, ester, or amide groups are often thought of as degradable. Polyanhydrides are very susceptible to degradation due to the labile anhydride bonds and have very fast degradation rates [63]. Therefore, the hydrolysable bonds in polyanhydrides cause them to undergo surface degradation which makes them a good source for drug delivery [80].

Polyesters have longer degradation times than polyanhydrides, but still degrade on a relatively quick timescale making them suitable for tissue scaffolds. PGA, PLA, and PCL are a few examples of frequently used polyesters in tissue engineering. For TEHV applications, PGA [35, 36, 39, 41, 42], PLGA [37], PLC [29, 47-49], P4HB [30, 39, 41, 42], PHA [38], and PET [43] have all been used in. Difference in degradation rates of these polymers depend on the hydrophobicity and length of the carbon chain in the polymer backbone. Polyamides degrade much slower than polyesters [63] and have chemistry similar to proteins with variation in the R-group. These polyamides, or polyaminoacids, are susceptible to degradation at the peptide bond.

Other polymers which could potentially degrade but are less susceptible include polycarbonates and polyurethanes. Polycarbonates have also been used in TEHVs [44, 50] and polyurethanes will be discussed in more detail in the next section.

1.4.3 Degradable polyurethanes

The variable chemical, mechanical, and biological properties make polyurethanes excellent materials for medical and tissue engineered products [81]. Polyurethanes, which are typically nondegradable, have been used in a number of cardiovascular soft tissue applications including cardiac patches [76, 82], vascular grafts [83, 84], and heart valves [51]. To achieve

biodegradability, polyurethanes were modified to incorporate soft segments with labile bonds into their backbone. Alternating hard and soft segments in the polyurethane provided both flexibility and degradability for the polymer. These linear elastic polyurethanes were formed from the synthesis of polyester, polyether, or polycarbonate soft segments, diisocyanate hard segments, and a chain extender.

Guan et al. [85] introduced poly(ester urethane)urea (PEUU) with PCL as the labile segment. Switching or copolymerizing the soft segment in PEUU allows for variations of the degradation rate. Guan et al. [86] increased the rate of degradation with the addition of PEG to form poly(ether ester urethane)urea (PEEUU), while Hong et al. [64] slowed the degradation rate by adding poly(1,6-hexamethylene carbonate) (PHC) to form poly(ester carbonate urethane)urea (PECUU). Other attempts [87-89] to slow degradation incorporated poly(trimethylene carbonate) soft segments into the polyurethane backbone. To further increase degradability, Guan et al. [90] adopted Ala-Ala-Lys (AAK) as the chain extender to add elastase lability to the polyurethane.

Changing the ratios of the soft segments during synthesis allows for tuning of the degradation rate as well as other properties. As the ratio of polyester to polycarbonate decreased, the degradation rate decreased [64]. At the two extremes, PEUU degraded significantly faster and was mechanically stronger than PCUU while PCUU was less viscous and less thrombogenic than PEUU. **Figure 5** is a representation of the bonding between the soft segments, hard segments, and chain extenders for PEUU, PCUU, and PECUU.

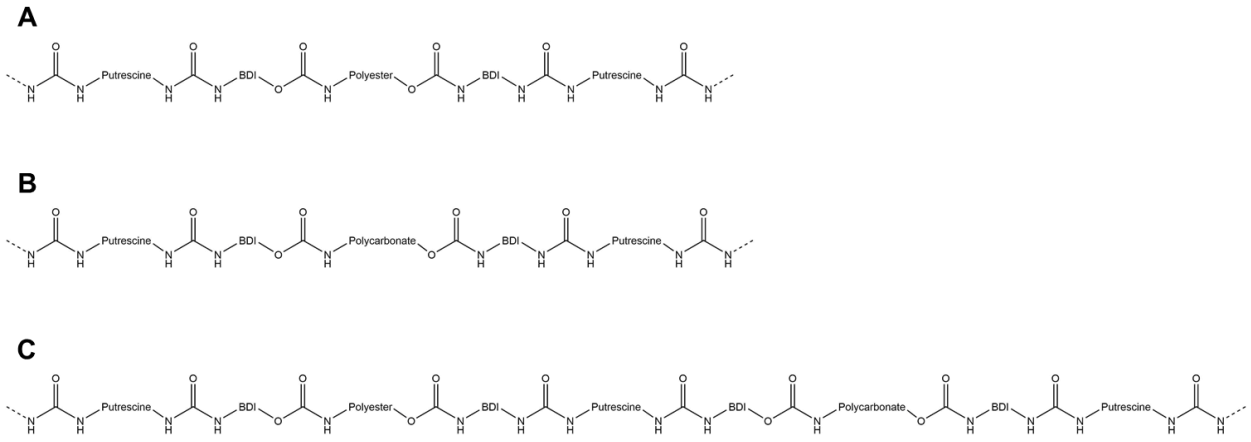

Figure 5. Representative polymer chain segments of the biodegradable polyurethanes showing soft segments (polyester and polycarbonate), hard segments (BDI), and chain extended (putrescine) and the urethane and urea bonds. A) poly(ester urethane)urea (PEUU), B) poly(carbonate urethane)urea (PCUU), and C) poly(ester carbonate urethane)urea (PECUU).

1.5 DEGRADATION OF POLYMER SCAFFOLDS

Degradability is a major component of most tissue engineered scaffolds as these constructs are designed to degrade and be replaced by new tissue at the site of application. Scaffolds with biodegradable polymers avoid additional surgeries to remove temporary support and prevent infection from a permanent scaffold. Understanding the ability of the scaffold to degrade, the time frame for degradation, the mechanisms through which the scaffold is broken down, and the products of degradation are critical in the selection of materials. Inappropriate degradation rates or the release of toxic products during degradation can be extremely harmful in the local environment of the body [91].

Biodegradation and bioerosion are common terms used to describe the breakdown of a biological scaffold. Although they are often used interchangeably, bioerosion typically involves

the passive breakdown of a substance through the loss of monomers and oligomers while biodegradation is a more active form of the breakdown and results from polymer chain scission [63]. All materials degrade over time, but it is the time-scale on which these materials degrade that define them as degradable or nondegradable polymers [63].

Degradation rates which do not coincide with new tissue formation can have detrimental effects. Fast degradation times can lead to a failure in proper stress transfer which results in mechanical failure, while slow degradation times (or no degradation at all) could result in inadequate tissue formation or fibrosis [64, 92]. In addition, degradation of a polymer chain results in the formation of new, smaller products with different chemistries which may be toxic in the body [63]. Depending on the molecular weight of the degradation product, toxic buildup in the kidney is possible. Consequently, *in vitro* or *in vivo* degradation studies are often performed on a material before employing that material in a long term preclinical study.

1.5.1 Mechanisms of degradation

Polymers have a number of different degradation mechanisms which include chemical, mechanical, oxidative, thermal, and photo degradation [63]. Ultraviolet (UV) light and γ-radiation, both relevant for sterilization, can cause photodegradation of a polymer. Thermal degradation is important when processing or working with polymers at high temperatures as free radicals can form. High temperatures can also play a role in oxidative degradation, where oxygen from the atmosphere attacks the polymer at a carbon-carbon double bond. Stresses within a polymer scaffold, such as those in a dynamic environment, can cause mechanical degradation. A study by Li et al. [93] of electrospun PLGA scaffolds found increased degradation with tensile

loading. Chemical degradation results from hydrolysis of hydrolysable bonds in a polymer [63]. Enzymes are used in enzymolysis to catalyze a hydrolysis reaction.

Polymer scaffold degradation typically ranges from surface to bulk degradation, with specific polymer constructs typically existing somewhere between the two extremes. With surface degradation, scaffolds only lose polymer at the surface; over time, the volume of the scaffold decreases, but the shape is maintained. Conversely, bulk degradation is when the degrading agents can penetrate the scaffold and form fractures throughout, yet maintain the original shape and volume for some time [63]. Molecular weight of the polymer initially decreases due to chain scission, but the mass of the scaffold is maintained for a longer time until the fragments are washed away.

Degradation typically occurs by cleaving bonds in the backbone of the polymer, although it is possible for cleavage of cross-links or side chains. With regard to backbone chemistry, polyanhydrides degrade faster than polyesters which degrade faster than polyamides [63]. **Figure 6** shows the general hydrolysis reaction of polyanhydrides. The hydrolysis of polyesters and polycarbonates (e.g. the soft segments in PECUU) is in **Figure 7** and **Figure 8**, respectively [94]. Polyesters are more susceptible to acid-hydrolysis whereas polycarbonates are more vulnerable to alkaline-hydrolysis. Therefore, production of carboxylic acid in polyester hydrolysis results in a positive feedback loop for degradation. This is not the case with polycarbonates which yield CO_2 and a molecule with hydroxyl groups on the ends [94].

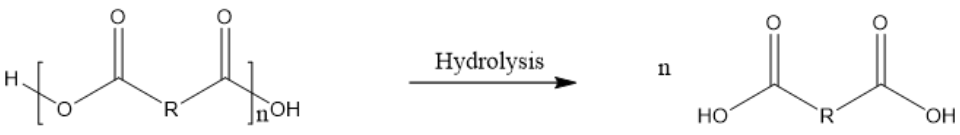

Figure 6. General hydrolysis reaction of polyanhydrides.

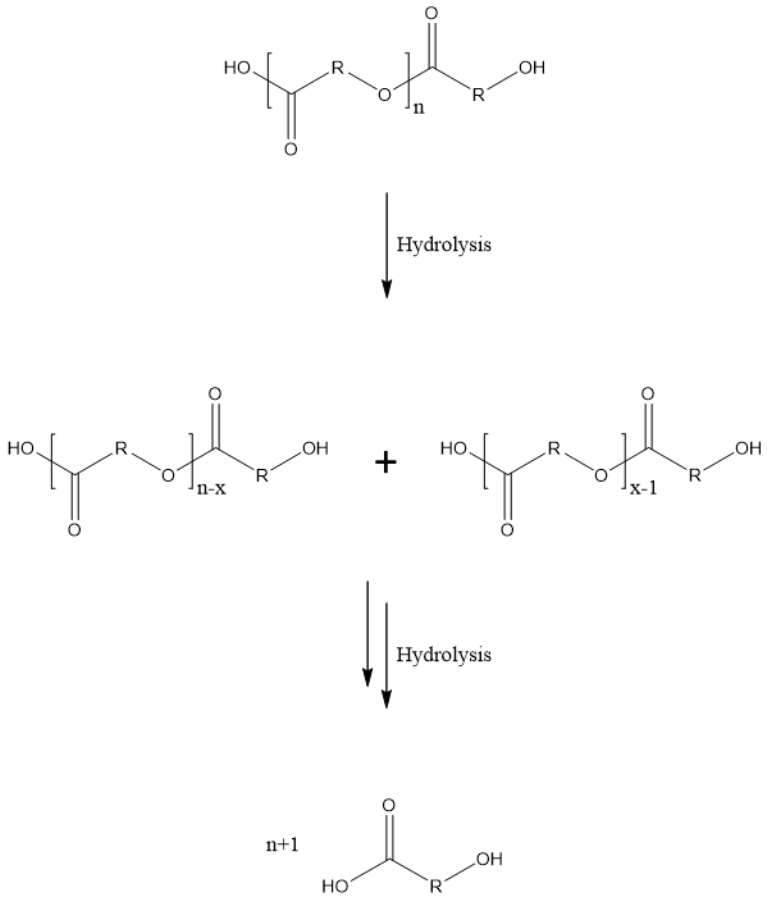

Figure 7. General hydrolysis reaction of polyesters.

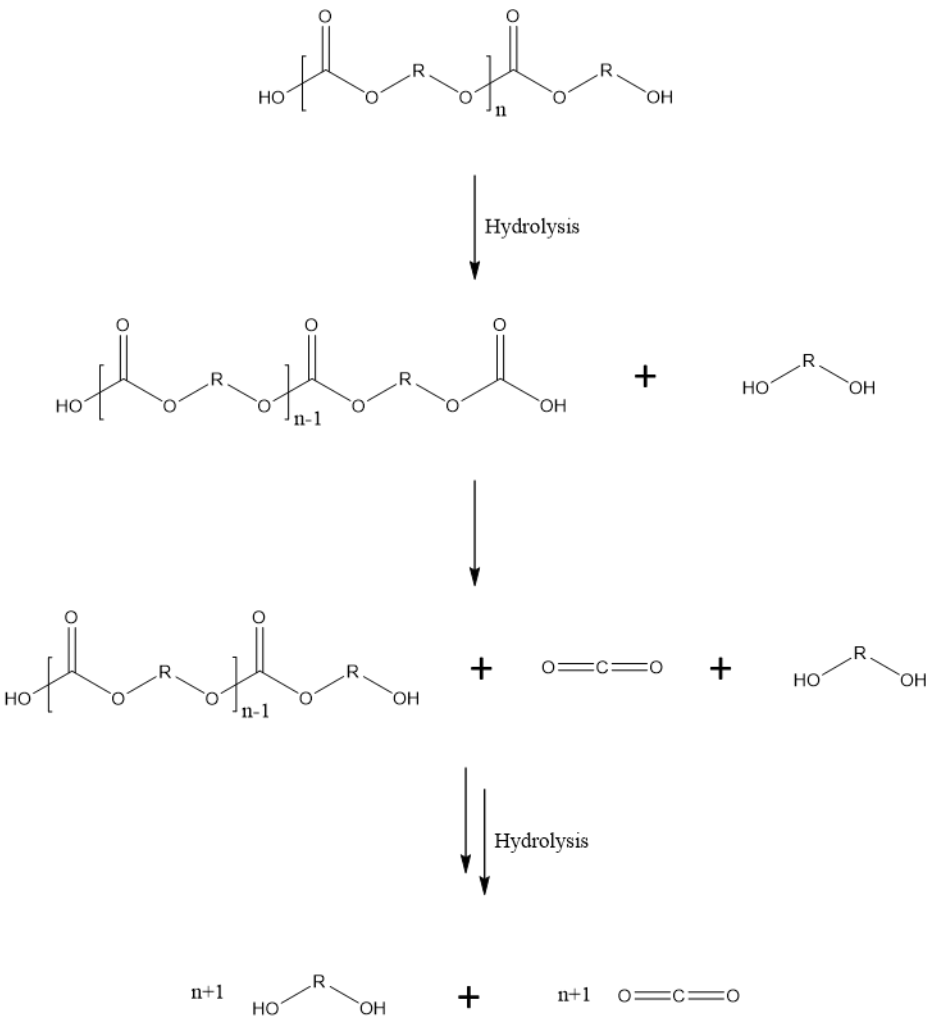

Figure 8. General hydrolysis reaction of polycarbonates.

1.5.2 Degradation of polymer scaffolds

There are a number of factors which can influence the degradation of a polymer scaffold, often involving the ability of water or solution to access the polymer. The hydrophobicity or hydrophilicity of the surrounding groups affects the ability of the polymer to take-up water and alters the degradation time [63, 95]. Less crystalline and amorphous polymers degrade at a faster

rate than highly crystalline polymers [95, 96]. As would be expected, polymers that start off at a lower molecular weight will degrade faster.

Scaffold surface area also influences degradation rate as larger surface to volume ratios lead to faster degradation. This is influenced by scaffold geometry and the fabrication method, as electrospinning produces fibers that result in a large surface area [95]. Finally, as mentioned above, mechanical stresses on the polymer scaffold can increase the degradation rate [63, 95]. *In vivo*, the local environment can also affect degradation; cells, pH, and enzymes can all increase the degradation rate of scaffolds [95].

Scaffolds are often designed to degrade by certain enzymes or processes. A study by West and Hubbell [97] used ABA block copolymers with oligopeptides capped with acrylate groups as the A block and PEG as the B block. Crosslinking via photopolymerization was used to created hydrogels which could be degraded by collagenase and plasmin. Further work by Lutolf et al. [98] studied proteolytic degradation with matrix metalloproteinases of hydrogel scaffolds based on the oligopeptide amino acid sequence from end-functionalized PEG and how the degraded hydrogel affected cell infiltration.

1.5.3 Enzymatic degradation

Many studies have been conducted to characterize the degradation of polyurethanes with a number of different variations including backbone chemistry [64, 82, 85, 90, 99], polymer concentrations [66, 100], collagen/ECM concentrations [101, 102], surface modification [86, 103], functionalization [104, 105], growth factor loading [106], and stent coatings [107]. *In vitro* testing in phosphate buffered saline (PBS) [64, 85-87, 100, 102, 103, 106, 108] is a relatively inexpensive method to find comparative degradation rates between different polymers, but

degradation is more time intensive due the absence of many environmental factors (e.g. mechanical stress, enzymes, cells). *In vivo* testing in an animal model [64, 82] evaluates a polymer scaffold in the native environment producing faster and more accurate degradation rates, but is more cost intensive. Accelerated degradation, an alternative to these two methods, performs degradation analysis *in vitro* using an enzyme solution [66, 90, 99, 101, 104, 105, 107] to increase the degradation rate and more accurately recapitulate the native environment. While this method will not exactly replicate the *in vivo* degradation, it provides a more accurate representation of how a polymer scaffold will perform in the body.

The benefits of accelerated degradation with enzymes *in vitro* make it a useful method for evaluating biodegradable scaffolds. Several studies [66, 90, 101] have shown a significant increase in degradation rate when employing an enzyme as opposed to only using PBS. Polymers will respond to specific enzymes based on their chemistry, and scission of the backbone, cross-links, or side groups can be controlled. Because of this specificity, *in vitro* experiments have adopted a number of different enzymes to analyze polymer scaffold degradation. These enzymes include elastase [90], collagenase [101], and lipase [66, 99, 104, 105, 107] which break down proteins, collagen, and lipids, respectively. Specifically, lipase is a type of esterase which catalyzes the hydrolysis of a labile ester bonds. Thus, the possibility exists to tailor the polymer chemistry with an enzyme specific functional group to control degradation.

1.5.4 Degradation of tissue engineered heart valves

A TEHV is intended to act as a temporary mechanical support and scaffold for cell attachment. Providing a scaffold on which cells can proliferate, differentiate, and produce ECM [92] is critical to generating new functional tissue. Understanding and controlling the degradation rate is

critical in the design of the scaffold materials, and degradation rate should be matched to rate of new ECM production on the scaffold. If the degradation is too fast, the valve could fail mechanically due to inadequate tissue formation; leaflet stiffening and the inability for proper coaptation can result from slow degradation [92].

Initial approaches to engineered heart valves used biodegradable polymers with rapid degradation rates like PGA and P4HB [35-37, 39-41]. Hoerstrup et al. [40] determined total degradation time for these two polymers to be 4 and 8 weeks, respectively, in the valve construct. Other early work by Sodian et al. [38] found polyhydroxyoctanoate (PHO) to have a longer degradation period as scaffolds explants from *in vivo* studies still had scaffold present at 17 weeks. More recent attempts [47-49] have used PCL to increase the degradation time and prevent mechanical failure. Although each of these studies utilize known biodegradable polymers, degradation rates were not extensively studied to analyze the effect of multiple polymers, valve position, cell type, etc.

Recent studies involving TEHVs have included characterization of material degradation rates. Badrossamay et al. [29] studied the degradation rate of different combinations of PCL with collagen or gelatin. Degradation and the corresponding mechanical properties were studied for the bis-urea-modified polycarbonate leaflets presented in Kluin et al. [50]. Furthermore, Sant et al. [109] studied the degradation of blended poly(glycerol sebacate) (PGS) and PCL, and specifically analyzed the interplay between scaffold degradation, ECM synthesis, and mechanical properties. The addition of the faster degrading PGS led to a slight decrease in the mechanical properties of the scaffolds.

Brugmans et al. [110] studied the effects that the slower degrading PCL had on valve leaflet retraction as compared to PLA/P4HB. After culturing the polymer scaffolds with cells for

4 weeks, PCL scaffolds showed significantly less retraction, which would lead to less regurgitation in the valve construct. Additionally, Brugmans et al. [111] cultured the PCL and PLA/P4HB scaffolds as cellular and acellular constructs. In the acellular scaffolds, PLA/P4HB degraded significantly faster than PCL. Cellular scaffolds demonstrated tissue growth in both groups, with PLA/P4HB scaffolds generating slightly more initial tissue, but at the end of the study, PCL scaffolds produced more total tissue.

Reimer et al. [33] fatigued a TEHV in a pulse duplicator for 2 weeks to evaluate the effects of the mechanical stresses experienced by heart valves. The stentless construct showed no significant tearing in the valve or valve leaflet after more than 2 million cycles. There is a need for biodegradable TEHVs within the pediatric population, and understanding the degradation rates and new tissue formation is important in the design. Tunable elastomers provide the possibility of controlling degradation rates in TEHVs [92]. Segmented polyurethanes [64, 85, 86] provide this ability and can be electrospun into scaffolds with controllable fiber populations and mechanical properties [51, 67, 68, 112] providing the possibility of creating an entire valve construct with appropriate mechanics, function, and degradation.

1.6 MIXING OF POLYMERS IN ELECTROSPUN SCAFFOLDS

Polymer scaffolds often combine polymers with different properties to achieve desired characteristics of the scaffolds such as appropriate degradability, mechanics, and blood compatibility. Additionally, natural materials are often integrated into the synthetic scaffold through electrospinning to increase the biocompatibility [113]. This combination of polymers can be achieved several different ways: bonding the scaffolds together during synthesis to form a

copolymer, blending miscible polymers together in a solvent to form a single solution, or electrospinning different streams of polymers together into a scaffold.

1.6.1 Copolymerization

Copolymerization is a synthesis technique which combines multiple units together into a single chemical structure. Depending on the form of synthesis, the copolymers could have a random, alternating, block, or graft structure. PLGA is a frequently used copolymer in biomaterials applications and is used in products approved by the Food and Drug Administration (FDA). Zund et al. [37] used a PLGA copolymer woven mesh in the design of a TEHV. For designed drug release, different ratios of lactic and glycolic acid in the PLGA copolymer can control the release profile of drugs [114].

Polyurethanes with soft segments can be used to generate a desired response within a polymer. Guan et al. [86] used PCL and PEG to produce PEEUU, a triblock copolymer, with tunable degradation rates. Likewise, Hong et al. [64] incorporated PCL and PHC into the polyurethane backbone to produce variations of PECUU with slower degradation rates. The scaffold with the moderate degradation rate, 50/50 PECUU, was found to be optimal by Hashizume et al. [82] during an *in vivo* study with a temporary cardiac patch.

1.6.2 Polymer blends

Polymer blending is the physical mixing of two independent polymers together into a solvent to form a single polymer solution. A solvent which can dissolve all of the selected polymers is

required for this process. This approach is a common way of combining natural and synthetic polymers into an electrospun scaffold.

In TEHV applications, PCL was blended with collagen or gelatin in varying ratios in a solvent before rotary jet spinning [29]. Similarly, P4HB and gelatin were blended at different ratios with the same production process [30]. Blends of P4HB, chitosan, and fibroblast growth factor were electrospun onto decellularized porcine aortic valve leaflets [115]. Hinderer et al. [69] blended PEG dimethacrylate and PLA in solvent before electrospinning into a heart valve using a custom device. Likewise, Sant et al. [70] electrospun blends of PGS and PCL at various ratios.

There have also been applications of polyurethane blends with natural materials to form small diameter vascular grafts. Wang et al. [71] electrospun blends of polyurethane and PEG into vascular grafts with increased blood compatibility due to the PEG incorporation. Thermoplastic polyurethane was blended with collagen and chitosan in Huang et al. [116] and electrospun into vascular grafts. Furthermore, Hong et al. [84] blended PEUU with 2-methacryloyloxyethyl phosphorylcholine (MPC) to form a vascular graft by electrospinning the blended solution.

1.6.3 Dual-stream electrospinning

Dual-stream electrospinning utilizes two independent polymer solutions to create two streams of polymer fibers being deposited on the collecting surface. Scaffolds produced with this method have two independent fiber populations intertwined in the scaffold. This technique can be applied to polymers which do not dissolve in similar solvents and need to be combined in a scaffold [65]. Gupta and Wilkes [117] electrospun two polymer solutions onto a collector using a bicomponent technique where the two polymer solutions were adjacent to one another. Mixing

electrospinning was introduced by Kidoaki et al. [72] who deposited polyurethane and poly(ethylene oxide) (PEO) on a rotating mandrel to create a mesh with mixed fibers.

Multiple jet configurations were studied by Theron et al. [118] through experimental and modeling analysis with a single polymer, PEO. A multicomponent electrospinning setup in Ding et al. [119] presented different ratios of electrospinning jets producing polymer poly(vinyl alcohol) and cellulose acetate. A scaffold with sacrificial fibers was co-electrospun in Baker et al. [73] from PCL and PEO, and the PEO fibers were removed by submerging the scaffolds in water following the fabrication.

The presence of multiple capillary tubes with similar polarities close to one another may influence the electric field and electrospinning jet [74]; therefore, positioning the capillaries on opposite sides of the rotating mandrel can limit this problem. The dual-stream process has been applied to electrospraying as well to create scaffolds with combinations of synthetic polymers and cell culture medium [120], cells [121], and ECM [76].

1.7 STUDY RATIONALE

1.7.1 Purpose of this study

A novel TEHV and fabrication method was introduced by D'Amore et al. [51] to overcome many of the obstacles faced by prosthetic heart valves as well as other TEHVs. Biodegradable, elastomeric, trileaflet heart valves were produced as fully assembled constructs without a stent. The acellular structures were designed to have appropriate geometry, corresponding mechanical properties, and similar fiber diameter to a native heart valve.

To de-risk the first preclinical studies, the valve should be tailored toward a lower pressure location (e.g. the right side of the heart in the tricuspid or pulmonary position). With an interest in the atrioventricular valves, the tricuspid valve was selected due to the lower transvalvular pressure [15]. Although the incidence with the tricuspid valve is much lower than the mitral valve [1], initial *in vivo* assessment should evaluate the valve in the tricuspid position.

Acellular TEHVs are designed to recruit endogenous cells from the body to support endogenous tissue growth *in situ* [50]. Using the body as a bioreactor to support new ECM production, the degradation rate of the scaffold should match that of the new tissue formation in order to avoid detrimental effects [92]. **Figure 9** shows the desired response from an acellular valve where endogenous cells populate the scaffold and remodel. Matching rates of material degradation and formation will allow for appropriate stress transfer and avoid mechanical failure or fibrosis at the site [64].

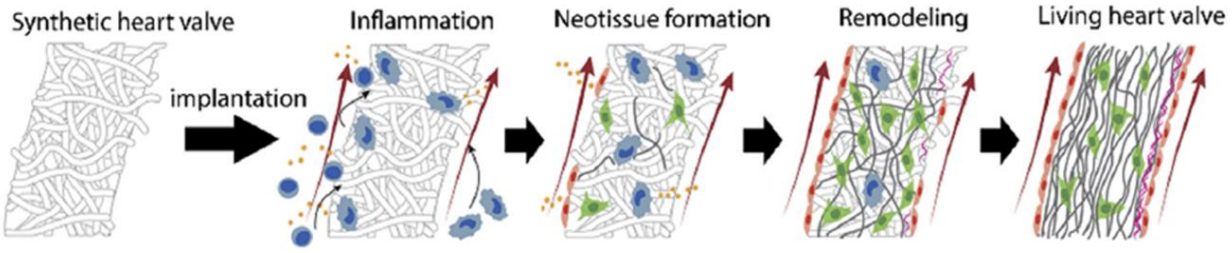

Figure 9. Desired response of an acellular TEHV which relies on endogenous cells for new tissue growth and remodeling (from [50]).

This study is intended to investigate the degradation rates and corresponding changes in mechanical properties of electrospun TEHVs produced with the three mixing strategies introduced in Section 1.6. These strategies could potentially provide tunable degradation rates of the biodegradable heart valves based on the polyurethane soft segment mixing strategy. For *in*

vivo preclinical studies, TEHV degradation rates can be matched to the new tissue formation in order to prevent mechanical failure in the animal.

1.7.2 Study design

An accelerated *in vitro* degradation study was designed to evaluate the degradation rates of biodegradable polyurethanes using the three mixing strategies. Incorporating polyester and polycarbonate soft segment into the backbone of polyurethanes has been shown to change the degradation rate [64, 99]; an increase in polycarbonate segments decreases the degradation rate. This study will consider a 50/50 ratio of polyester to polycarbonate soft segments combined in three different ways, shown in **Figure 10**. The soft segment mixed (chemical) TEHV group was formed by synthesizing a mixture of polyester and polycarbonate segments into the backbone of polyurethane urea to form PECUU, dissolving the polymer in HFIP, and electrospinning heart valves using a single polymer stream. The physically blended TEHV group was formed by synthesizing PEUU and PCUU by incorporating polyester and polycarbonate segments, respectively, into the polyurethane urea backbone, dissolving the PEUU and PCUU together in HFIP, and electrospinning using a single polymer stream. The co-stream electrospun TEHV group was formed by dissolving PEUU and PCUU in HFIP in separate solutions and electrospinning using two polymer streams. A depiction of the polymer chain and fiber composition for the three mixing strategies is shown in **Figure 11**. The soft segment mixed group should have polymer chains consisting of both polyester and polycarbonate soft segments in all electrospun fibers. The physically blended group should have individual polymer chains of either polyester or polycarbonate soft segments, but the electrospun fibers should have both soft

segments. The co-spun group should have polymer chains with either polyester or polycarbonate soft segments and each fiber should only contain either polyester or polycarbonate soft segments.

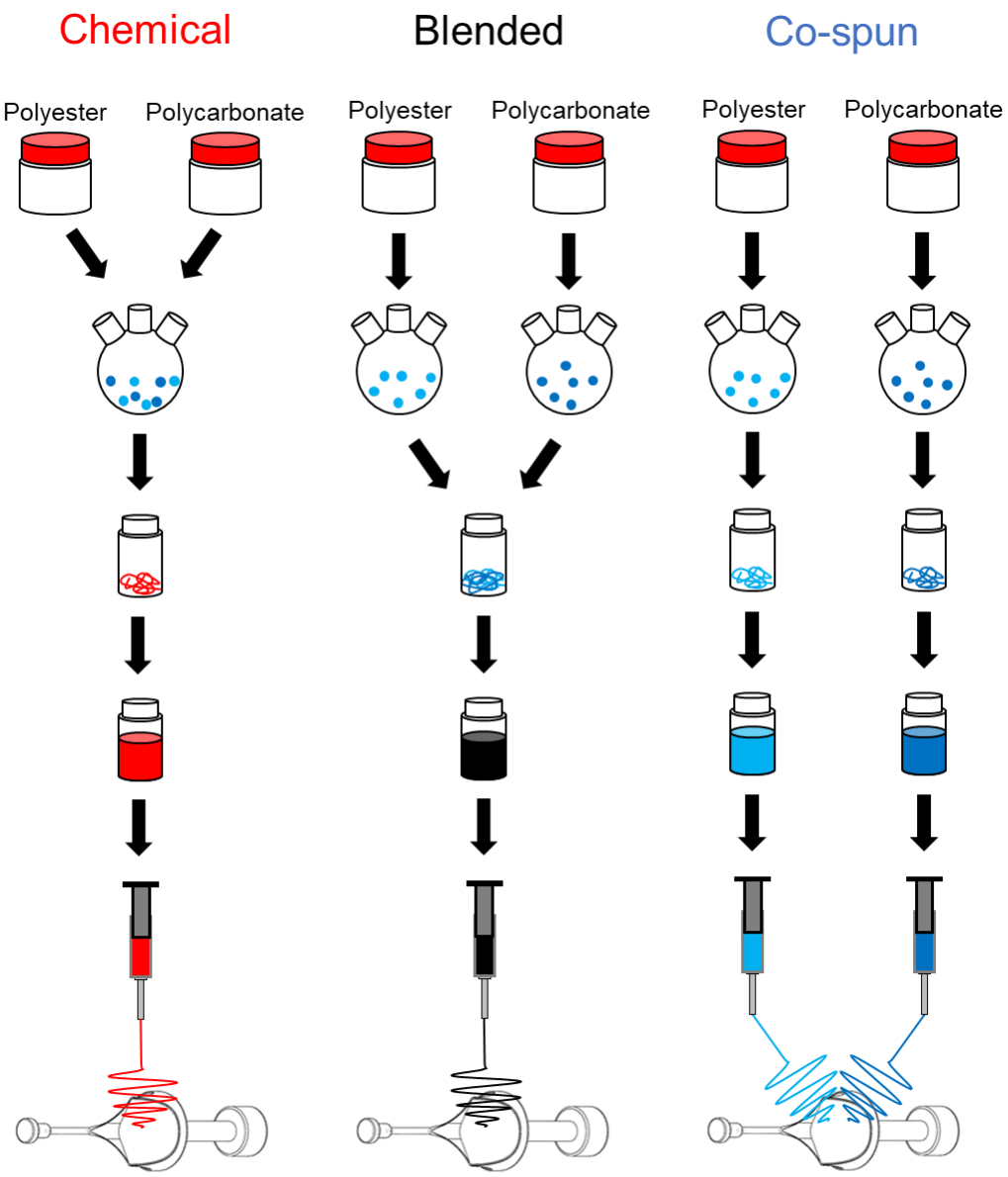

Figure 10. Schematic of polyurethane soft segment mixing strategies: soft segment mixing (chemical), physical blending (blended), and co-stream electrospinning (co-spun).

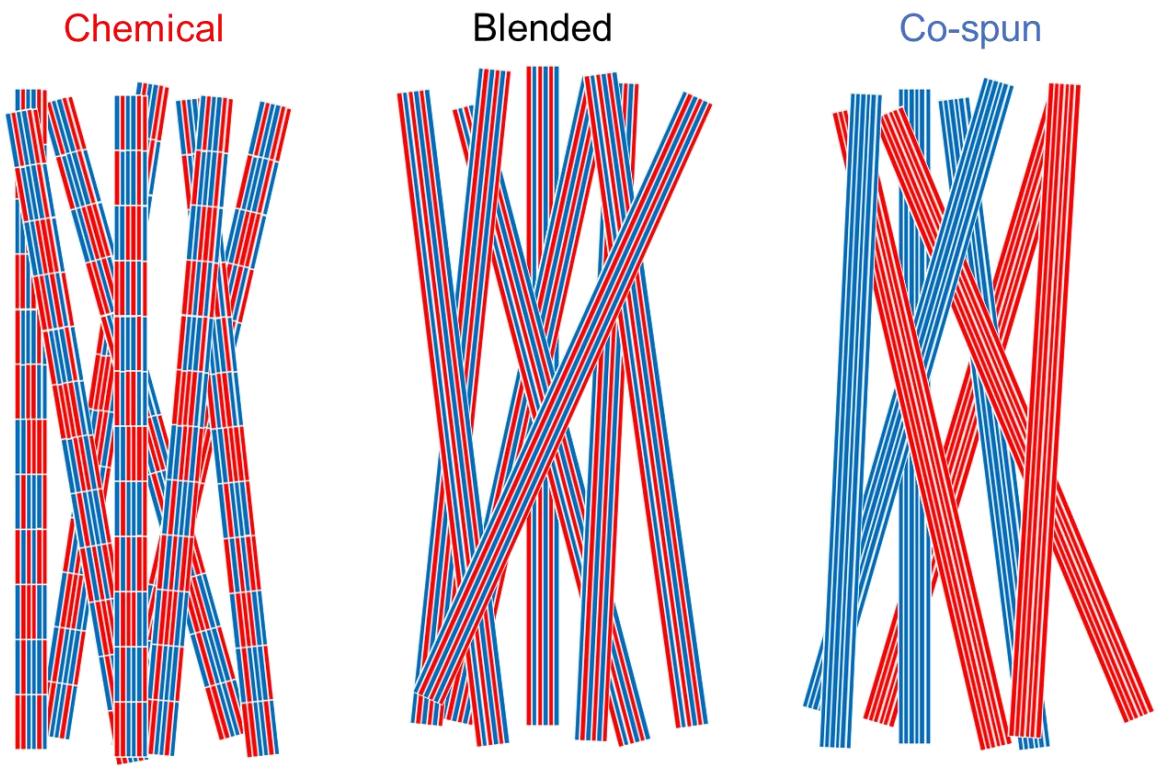

Figure 11. Depiction of the polymer chain and electrospun fiber composition for the three mixing strategies where red represents the polyester segments and blue represents the polycarbonate segments.

An accelerated degradation study was performed on TEHVs from the three mixing strategies to more accurately represent the *in vivo* environment. Hydrolytic, enzymatic, and mechanical degradation were performed on the TEHVs by using a lipase/PBS solution in a pulse duplicator shown in **Figure 12**. The results of lipase in degradation studies has been shown in [66, 99, 104, 105], and to evaluate the degradation effect of pulsatile mechanical forces, a comparison study was completed on a rocker with a lipase/PBS solution. Degradation of the TEHVs was performed for up to 2 weeks in the pulse duplicator [33]. Valve mass, leaflet thickness, surface morphology, mechanical response, and polymer viscosity were evaluated throughout the study to determine the effects of degradation. Additionally, blood compatibility

was considered for the three mixing strategies to assess if the polymer chemistry or fiber population had a significant effect.

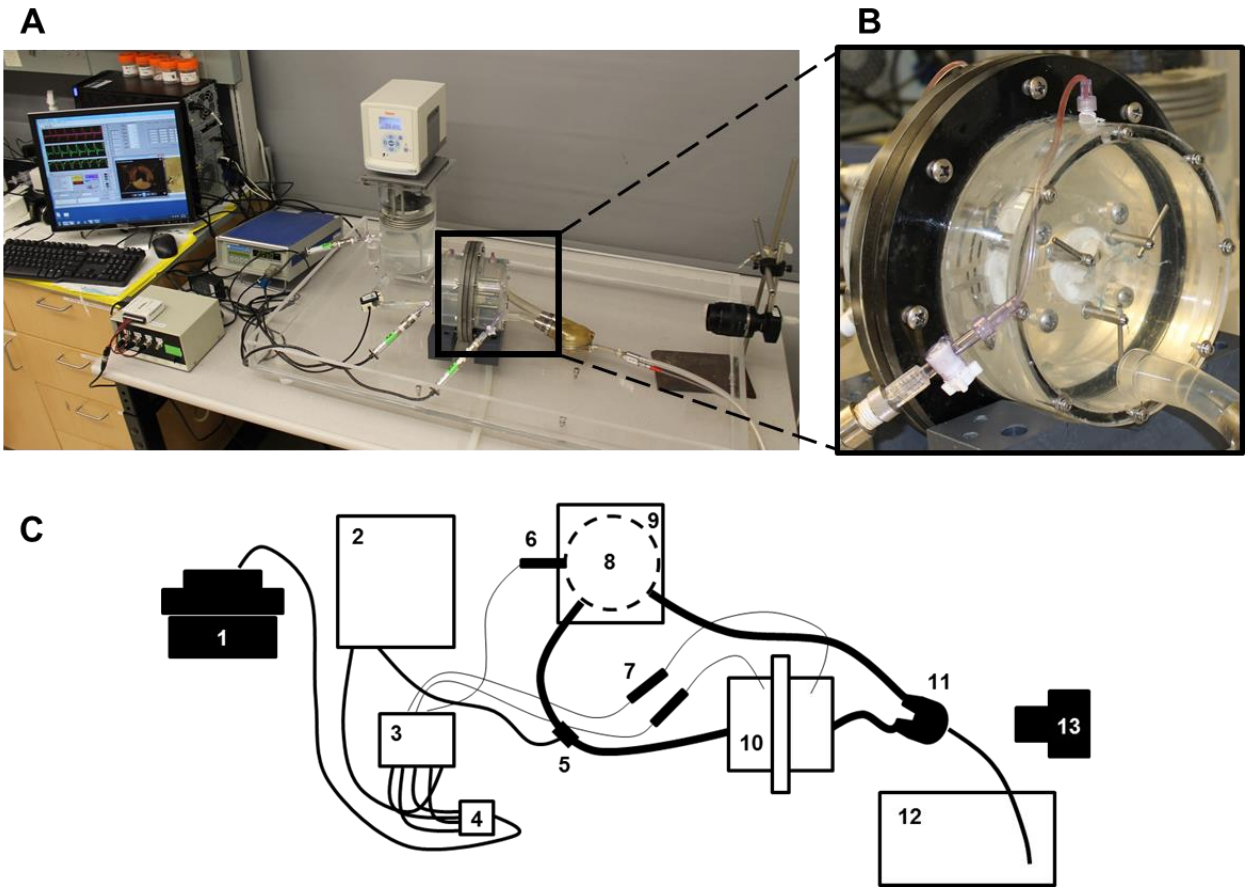

Figure 12. Pulse duplicator and schematic. A) Pulse duplicator for the accelerated degradation study with tissue engineered heart valves. B) Valve holder with the valve positioning apparatus. C) Schematic of the pulse duplicator layout.

1.8 OBJECTIVES

1.8.1 Objective #1: Characterize the degradation profile of engineered polyurethane heart valves with variable soft segment mixing strategies

As discussed previously, tissue engineered scaffolds are often produced from multiple polymers combined through copolymerization, blending, or dual-stream electrospinning to attain desirable performance. To our knowledge, there has not been a comparative study evaluating these three combination methods. Therefore, the first objective in this study is to characterize the degradation profile of each mixing strategy applied to a biodegradable TEHV in a mechanically demanding environment.

1.8.2 Objective #2: Determine the effect of a mechanically demanding and dynamic environment on the degradation rate

Polymers can undergo numerous types of degradation (e.g. mechanical, chemical, thermal) simultaneously, but most *in vitro* degradation studies only consider hydrolytic or enzymatic degradation. Since a TEHV will undergo cyclical mechanical stress *in vivo*, degradation studies should be extended to consider mechanical degradation as well in order to more accurately represent the native environment. The next objective in this study is to evaluate the effect a mechanically demanding environment has on a TEHV with respect to a valve leaflet without mechanical loading.

1.8.3 Objective #3: Investigate the mechanical properties of the engineered heart valves following degradation

Degradable tissue engineered scaffolds should mechanically support damaged tissue while new tissue forms. Ideally, the rate of scaffold degradation and new tissue formation should be equivalent for proper stress transfer from the scaffold to the new tissue. Fast degradation rates of the scaffold and corresponding mechanical properties can lead to mechanical failure at the site of the scaffold. In this objective, the intent is to investigate if and how the in-plane mechanical properties of the TEHV change during degradation.

1.8.4 Objective #4: Determine the effects of the mixing strategies on blood compatibility

Tissue engineered scaffolds in applications with continuous blood contact should have sufficient blood compatibility in order to minimize the chance of thrombus formation. Although polymer chemistry has been shown to affect the blood compatibility, this study uses an equivalent amount of each polyurethane soft segment. The mixing strategies combine these segments in three different ways, altering the composition of the scaffold fibers. This final objective is meant to investigate the mixing strategies, which produce polymer chains and fibers with different chemistries, on blood compatibility.

2.0 MATERIALS AND METHODS

2.1 MATERIALS

Polycaprolactone diol (PCL diol, M_n = ~2,000 g/mol, Sigma, Burlington, MA) and poly(hexamethylene carbonate) diol (PHC diol, M_n = ~2,000 g/mol, Scientific Polymer Products, Ontario, NY) were dried using toluene distillation prior to use. Putrescine (Sigma) and 1,4-diisocyanatobutane (BDI, Sigma) were purified with vacuum distillation. Anhydrous toluene (Sigma), anhydrous dimethyl sulfoxide (DMSO, Sigma), tin(II) 2-ethylhexanoate ($Sn(Oct)_2$, Sigma), 2-propanol (Sigma), and 1,1,1,3,3,3-hexafluoro-2-propanol (HFIP, Oakwood Chemical, Estill, SC) were used as received. Phosphate buffered saline (PBS) tablets (Sigma) were dissolved in deionized water to form a 1x PBS solution. Lipase from porcine pancreas (Sigma) was used as received.

2.2 POLYURETHANE SYNTHESIS

Biodegradable polyurethanes elastomers were synthesized using a two-step polymerization process shown in **Figure 13**. Prior to synthesis, BDI and putrescine were vacuum distilled to remove any remaining impurities. Poly(ester urethane)urea (PEUU), poly(carbonate urethane)urea (PCUU), and poly(ester carbonate urethane)urea (PECUU) were synthesized using

PCL diol and/or PHC diol as the soft segment, BDI as the hard segment, and putrescine as the chain extender. The ratio of (PCL diol):(PHC diol) in the synthesis of PEUU, PECUU, and PCUU were 100:0, 50:50, and 0:100, respectively. A 1:2:1 molar ratio of (PCL diol/PHC diol):BDI:putrescine was used in the synthesis as reported in Hong et al. [64]. In the first polymerization step, diol was added to a triple-neck flask and dried using toluene distillation with a vacuum pump. Anhydrous DMSO was then added to the diol and the flask was submerged in an oil bath with argon protection. BDI was added dropwise to the flask followed by six drops of $Sn(Oct)_2$. After reacting for 3 hours at 70°C, the prepolymer solution was cooled to room temperature. Next, putrescine mixed with DMSO was slowly added dropwise to the prepolymer solution with constant stirring. This chain extension reaction proceeded overnight at 50°C. An excess volume of cool deionized water was used for polymer precipitation. Finally, the polymer underwent multiple water exchanges to remove any remaining solvent, followed by a wash with 2-propanol, before drying for 2 days in a vacuum oven at 50°C.

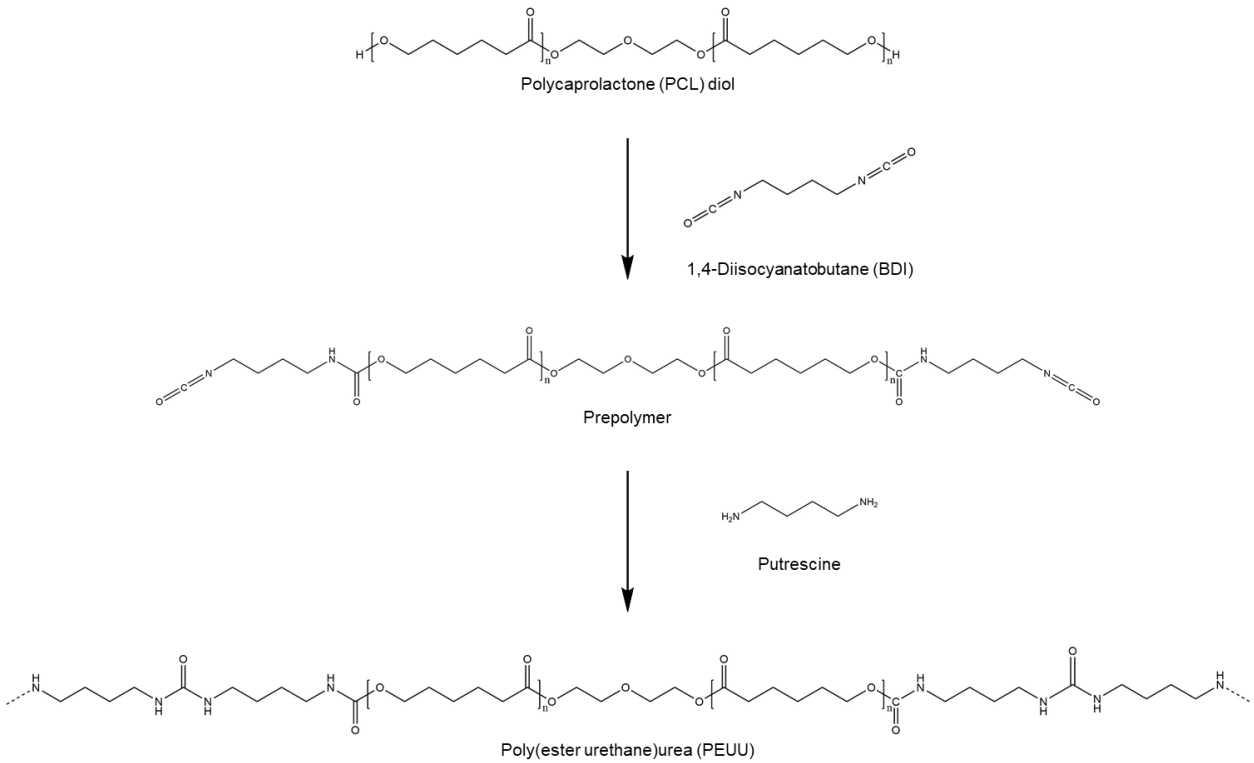

Figure 13. Two-step polyurethane synthesis schematic for PEUU. The same two-step polyurethane synthesis schematic was used for PCUU and PECUU by exchanging the PCL diol for PHC diol or PCL diol/PHC diol, respectively.

2.3 TISSUE ENGINEERED HEART VALVE SCAFFOLD FABRICATION

Fully assembled, stentless, trileaflet heart valves were fabricated by an electrospinning process, described in Section 1.3, to deposit biodegradable polyurethanes onto a rotating mandrel (i.e. collecting surface) developed by D'Amore et al. [51]. Briefly, the mandrel shown in **Figure 14**, was designed in SolidWorks (Dassault Systèmes, Vélizy-Villacoublay, France) and consisted of two components: a conductive aluminum alloy machined into the shape of a heart valve and a non-conductive acrylonitrile butadiene styrene (ABS) shield produced by injection molding. This double component deposition (DCD) technique exploits the differences in the material

conductivities to selectively redirect fiber deposition to more inaccessible areas on a complex surface geometry.

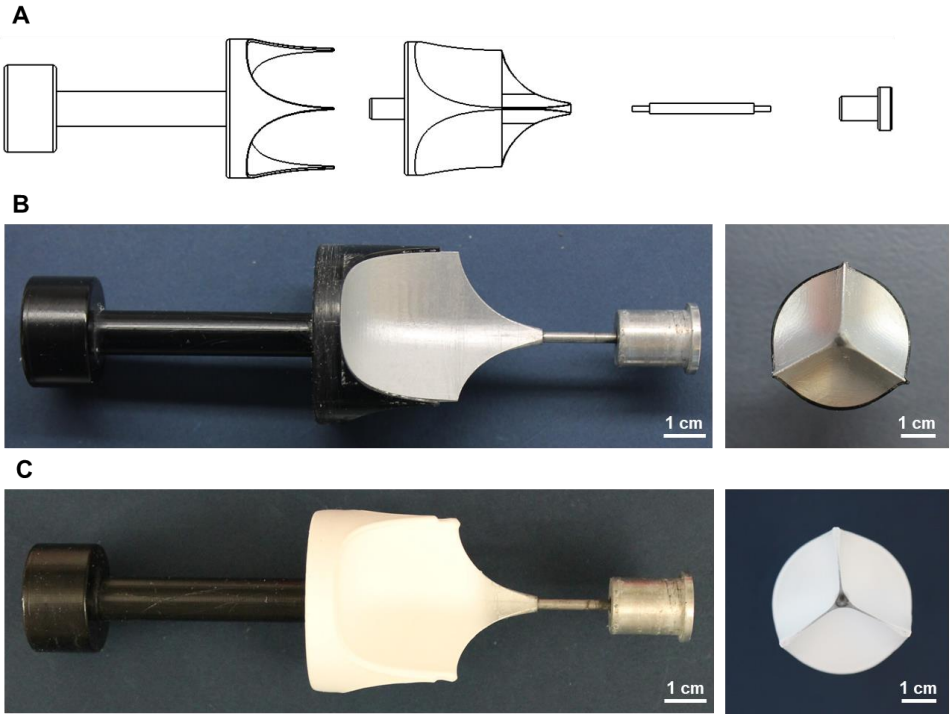

Figure 14. Double component deposition (DCD) mandrel for electrospinning heart valves. A) SolidWorks drawing of the assembly, B) assembled DCD mandrel, and C) mandrel with deposited electrospun fibers.

Experimental groups combined polyester and polycarbonate soft segments into a polyurethane by three different mixing strategies. Soft segment mixed valves were produced through electrospinning a 12% w/v PECUU in HFIP solution; physically blended valves were produced by dissolving 6% w/v PEUU and 6% w/v PCUU together in HFIP and electrospinning a single solution; and co-stream electrospun valves were produced via two independent streams of 12% w/v PEUU in HFIP and 12% w/v PCUU in HFIP. A schematic of the one- and two-stream electrospinning setup is shown in **Figure 15** with high voltage power sources (Gamma High Voltage Research, Ormond Beach, FL), syringe pumps (Harvard Apparatus, Holliston,

MA), stepper motor (Oriental Motor, Tokyo, Japan) for rotation, and stepper motor (Velmex, Bloomfield, NY) for rastering. Each polyurethane group was dissolved in HFIP overnight at an equivalent concentration of 12% w/v. The mandrel was rotated at 250 rpm and polymer deposition was concentrated on the conductive leaflets by limiting the rastering span to 3.5 cm. Each polymer solution was loaded into a 10 mL syringe (Becton Dickinson, Franklin Lakes, NJ), and the conditions for electrodeposition were: polymer flow rate of 1.5 mL/hr, polymer voltage of +12 kV, gap distance of 4.5 cm, and mandrel voltage of -5 kV.

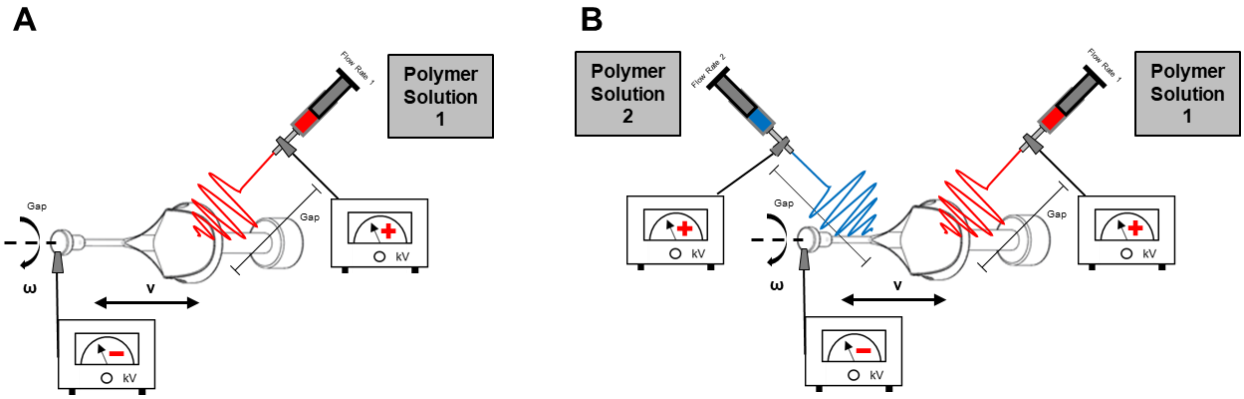

Figure 15. Schematic of the electrospinning setup for A) one-stream and B) two-stream fabrications.

Valve scaffold thickness was controlled by polymer deposition time and was targeted for the reported native porcine tricuspid valve thickness of 227 μm [51]. Polymer deposition was studied for each experimental group by electrospinning valves at three different time points for up to 4 hours, performing a linear interpolation of the polymer dipositive vs. time, and calculating the required deposition time to achieve a thickness of 227 μm. Electrospun heart valves were then fabricated using the calculated deposition time for each experimental group. **Video 1** in the supplemental materials is an example of the TEHV electrospinning setup, deposition process, and removal from the mandrel.

2.4 PULSE DUPLICATOR DESIGN

A custom designed pulse duplicator [51] was used to test the degradation rates of the engineered heart valves under mechanical stresses. Modifications were made to the system to allow for control over the fluid temperature, with the new setup shown in **Figure 12**. Electrospun valves (**Figure 16A**) were prepared for testing by using Ti-Cron™ 0 braided polyester sutures (Medtronic, Minneapolis, MN) to suture along each commissure and create ~1 cm loop at the top (**Figure 16B**). Another ~2 cm loop was tied between each initial loop and one of the three equally-spaced stainless steel posts (**Figure 16C**) to function as chordae tendineae for an atrioventricular valve in the native heart before loading into the valve holder (**Figure 16D**). A Thoratec® TLC-II® Portable VAD Driver (Thoratec Corporation, Pleasanton, CA) was used to control a Thoratec® Paracorporeal Ventricular Assist Device (PVAD, Thoratec Corporation) which generated pulsatile flow across the valve. The PVAD functioned at 80 beats per minute and had a stroke volume on 65 mL. System pressure was collected from K1VAC/30PSI sealed SS compound transducers (Cole Parmer, Vernon Hills, IL) and flow was measured with a PXL Clamp-on Flowsensor (11XL, Transonic Systems Inc., Ithaca, NY). A 3MP USB2.0 Microscope Digital Camera (AmScope) equipped with a EF 50mm f/2.5 Compact Macro Lens (Canon Inc., Melville, NY) faced the ventricular side of the valve positioning apparatus and recorded videos of the valve hemodynamic performance. A custom-made LabVIEW (National Instruments, Austin, TX) program was used in conjunction with a USB-6009 data acquisition (DAQ) unit (National Instruments) to display and record synchronized hemodynamic data and videos of valve motion. A SC100 Immersion Circulator (Thermo Fisher Scientific, Pittsburgh, PA) was combined with the compliance chamber to provide a heat source and maintain control over the temperature of the system.

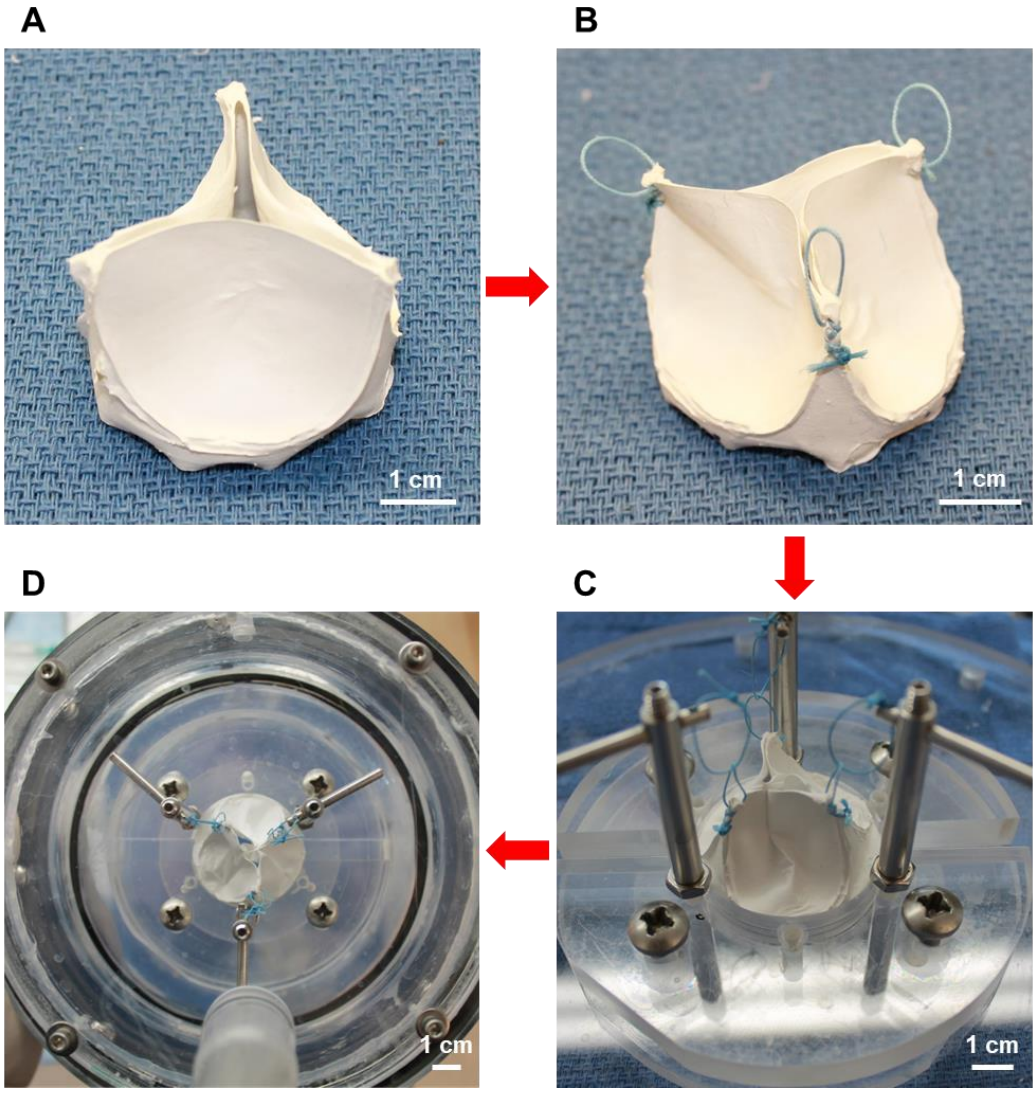

Figure 16. Process of loading the valve into the pulse duplicator. A) Electrospun valve, B) valve with sutures along commissure with ~1 cm loop, C) valve connected to post with ~2 cm loop on valve positioning apparatus, and D) valve positioning apparatus loaded into the valve holder.

2.5 TISSUE ENGINEERED HEART VALVE ACCELERATED *IN VITRO* DEGRADATION

Electrospun trileaflet valves were subjected to enzymatic, hydrolytic, and mechanical degradation in the pulsatile flow system with an enzymatic solution at physiological temperature for up to 2 weeks [33]. Prior to degradation, the valves were weighed and the leaflet thicknesses were measured. Valves were sutured to the posts as described in Section 2.3 and loaded into the valve holder of the pulse duplicator. Engineered valve scaffolds were immersed in 4 L of 100 unit/mL lipase/PBS at 37°C [66, 105] and experienced pulsatile flow at 80 beats per minute. Enzymatic solution was changed twice per week [99, 104], momentarily stopping the pulsatile flow. Degraded valves were removed for evaluation at three timepoints: 3 days, 7 days, and 14 days. Sutures in the commissures were carefully removed and valves were rinsed 3x with deionized water followed by 3 days of drying in a lyophilizer (Labconco, Kansas City, MO).

To understand how mechanical loading affected the degradation rate, valve leaflets were also degraded in an enzymatic solution without mechanical loading. Single leaflets were excised from the fully assembled construct and immersed in 15 mL of 100 unit/mL lipase/PBS in 20 mL glass vials. Vials were slowly rocked on a rocking platform shaker (VWR Scientific, Radnor, PA) in an incubator (Fisher Scientific, Hampton, NH) to maintain a constant temperature of 37°C. Timepoints, rinsing, and drying were the same as described above.

2.5.1 Valve visual inspection

Qualitative analysis of the degraded scaffold macrostructure was conducted to understand areas of significant degradation within the valve and to compare the soft segment mixing strategies.

An EOS Rebel T3 camera (Canon, Melville, NY) equipped with a EF-S 18–55mm lens (Canon) was used to photograph the assembled valve construct. A blade was used to open the valve along one commissure, and additional images of the atrial and ventricular surfaces of all valves were captured.

2.5.2 Valve mass loss

Mass loss was evaluated for both the mechanically loaded valves (n = 3/group/timepoint) and unloaded leaflets (n = 3/group/timepoint) according to [99, 104, 105]. Sample mass before degradation (m_0) and mass following degradation and drying (m_1) were recorded from a balance (OHAUS, Parsippany, NJ) and used to calculate mass remaining according to **Equation 1**:

$$mass\ remaining = \left(\frac{m_1}{m_0}\right) \cdot 100\%$$

2.5.3 Leaflet thickness loss

Leaflet thickness loss (n = 3/group/timepoint) was visualized for the mechanically loaded valves using an interpolation tool introduced in [51]. Leaflet thickness was measured with a dial indicator gage (Starrett, Athol, MA) at fifteen locations [122]: five in the belly region and ten distributed around the free edge, commissures, and annulus of the valve leaflet to serve as boundary values, as depicted in **Figure 17A**. Thicknesses prior to degradation (t_0) and after drying post-degradation (t_1) were used to calculate the thickness remaining with **Equation 2**:

$$thickness\ remaining = \left(\frac{t_1}{t_0}\right) \cdot 100\%$$

A surface map of leaflet thickness remaining was generated using a biquintic numerical interpolation in MATLAB (MathWorks, Natick, MA) with a custom-made script [51]. Thickness loss was also quantitatively compared (n = 3/group/timepoint) for the mechanically loaded valves using the leaflet thickness measured at five points in the belly region with a dial indicator gage (Starrett) as shown in **Figure 17B**. Thickness measurements from each of the three leaflets were averaged before (t_0) and after degradation (t_1) and calculated according to **Equation 2**.

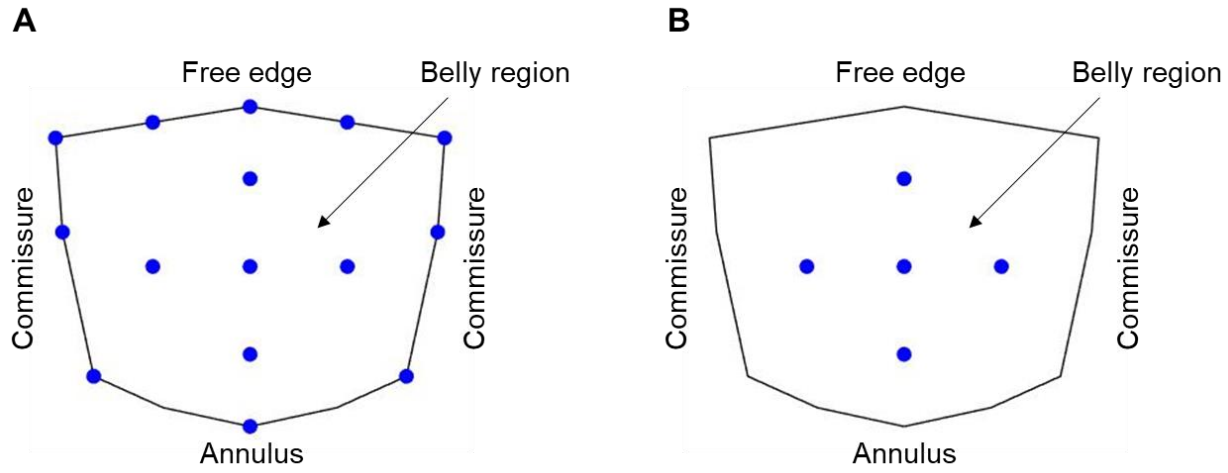

Figure 17. Location of valve thickness measurements for A) fifteen points and B) five points.

2.6 SURFACE MORPHOLOGY OF DEGRADED TISSUE ENGINEERED HEART VALVES

Scanning electron microscopy (SEM) was employed to observe the surface morphology of the degraded valves (n = 3/group/timepoint). A small rectangle with the longer edge oriented in the circumferential direction of the leaflet, shown in **Figure 18A**, was removed from the belly region

of each degraded valve, slightly offset to account for leaflet tears or holes. Samples were attached to metal stubs with double-sided copper tape, and sputter coated with gold/palladium to 4.5 nm before imaging with the SEM (JSM-6335F, JEOL USA, Peabody, MA) shown in **Figure 18B**. Images were collected at 25x, 250x, and 1500x to qualitatively analyze surface and fiber characteristics of the degraded leaflets.

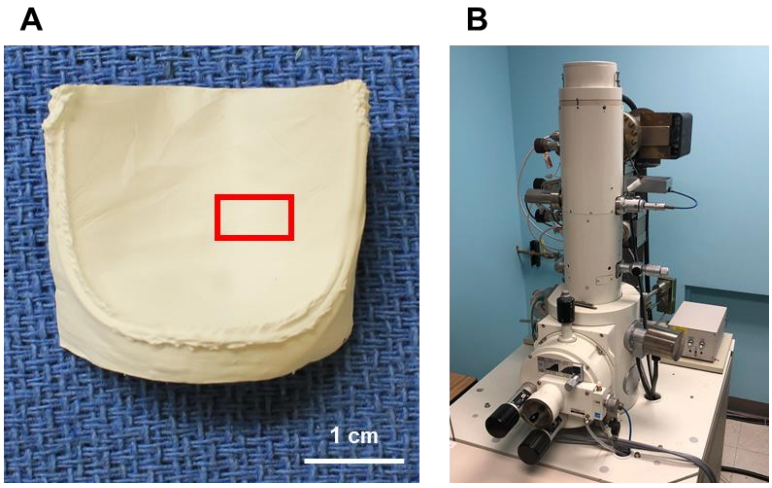

Figure 18. A) Electrospun valve with a red box indicating the location of the excised piece for SEM imaging. B) SEM at the University of Pittsburgh, Center for Biologic Imaging (CBI) used for imaging.

2.7 BIAXIAL MECHANICAL RESPONSE OF DEGRADED TISSUE ENGINEERED HEART VALVES

To understand the effects of degradation on the mechanical response of the valves, biaxial mechanical testing was performed on the degraded leaflets (n = 3/group/timepoint) according to [123]. A square ranging from 6 mm x 6 mm to 10 mm x 10 mm was removed from the belly region of the valve leaflet (**Figure 19A**), and sample thickness was determined by averaging five

thickness measurements from a dial indicator gage (Starrett). A Sharpie was used to make four dots in an approximate 3 mm x 3 mm square in the middle of the sample to measure the deformation gradient tensor, and four hooks attached to two strings were inserted along each side of the sample. After loading into a biaxial testing device (**Figure 19B**), samples were preconditioned and tested in a PBS solution at room temperature for ten cycles of 15 seconds. A Lagrangian equi-stress protocol was used for testing to a peak stress of 400 kPa and membrane tension of 120 N/m, physiologically relevant values for heart valve leaflets as reported in [51, 54, 57, 58]. Mechanical responses were post-processed with a custom-made MATLAB (MathWorks) script, using the free-float marker configuration following preconditioning as the reference state. The MATLAB script also performed strain energy calculations for the equi-stress test by fitting a fifth-degree polynomial to the stress-strain curve of each axis between 5 kPa and 400 kPa and integrating the area below the polynomial equation.

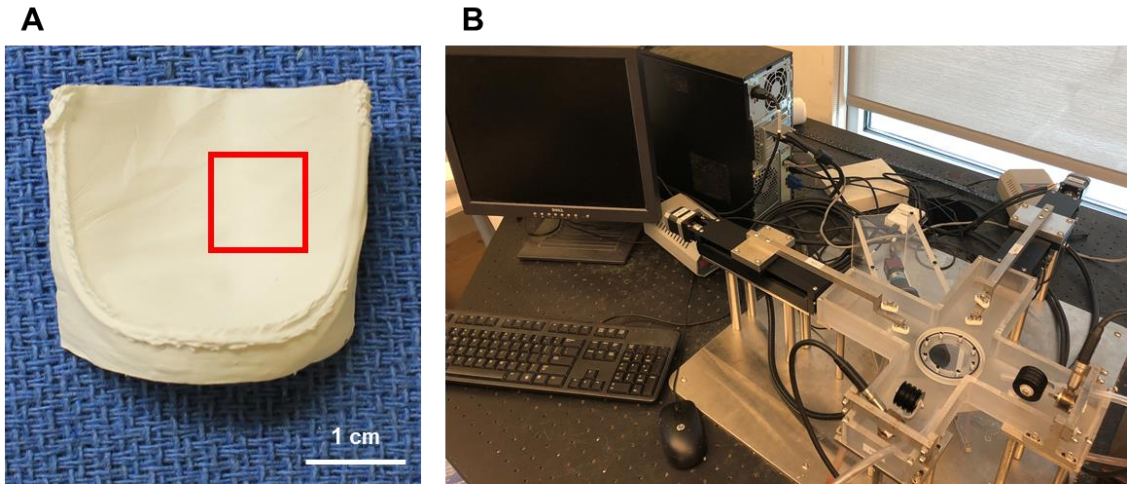

Figure 19. A) Electrospun valve with a red box indicating the location of the excised piece for biaxial mechanical testing. B) Biaxial testing device for in-plane mechanical characterization.

2.8 POLYMER VISCOSITY OF DEGRADED TISSUE ENGINEERED HEART VALVES

Relative viscosity of the degraded polymer valves was measured at 21°C using an Ubbelohde viscometer (Ace Glass, Inc., Vineland, NJ) with the method described in [89]. Following degradation, the dried valve leaflets were dissolved in 15 mL of HFIP at a concentration of 0.4 g/dL. The solution was filtered using a 10 mL syringe (Becton Dickinson) and a 0.22 μm polyethersulfone syringe filter (MilliporeSigma, Burlington, MA) before loading into the Ubbelohde viscometer. The efflux time of HFIP and each polymer solution was measured five times and averaged. Inherent viscosity (IV) of the polymer valves (n = 3/group/timepoint) was calculated from the relative polymer viscosity and the concentration of the solution with **Equation 3**:

$$IV = \ln\left(\frac{t_p}{t_s}\right) \Big/ C_p$$

where t_p is the polymer solution efflux time, t_s is the HFIP efflux time, and C_p is the concentration of polymer solution. IV at each degradation timepoint was then normalized with respect to the 0 days degradation valves of that group.

2.9 BLOOD COMPATIBILITY OF TISSUE ENGINEERED HEART VALVES

Ovine were used as a source for whole blood which was collected by jugular venipuncture. Guidelines presented by the National Institute of Health (NIH) for the care and use of laboratory animals were observed, and the animal protocol was approved by the Institutional Animal Care

and Use Committee (IACUC) at the University of Pittsburgh. A simple rocking test [124] was used to evaluate the thrombotic deposition on the electrospun polymer surface. Whole ovine blood was immediately mixed with 10% sodium citrate. A punch (Acuderm, Fort Lauderdale, FL) was used to cut 8 mm disks from the valve leaflets. The disks were sterilized using 70% ethanol and placed in a Vacutainer blood collection tube (Becton Dickinson) where 5 mL of ovine blood was added to each tube and rocked gently on a hematology mixer (Fisher Scientific, Hampton, NH) for 1.5 hours at 37°C. After rocking, the samples were rinsed in DPBS (Dulbecco's phosphate buffered saline) 10x to remove any blood not adhering to the surface.

Lactate dehydrogenase (LDH) assay [124] was used to quantify platelet deposition on the valve leaflet surface (n = 3/group) with a LDH Cytotoxicity Detection Kit (Takara Bio USA, Mountain View, CA). Briefly, following DPBS rinsing, samples were dried and added to vials filled with 500 μL Triton X solution. Whole ovine blood was centrifuged (Sorvall Legend RT, Thermo Fisher Scientific, Pittsburgh, PA) at 250 g for 20 minutes, and the supernatant was also added to a vial with Triton X solution. After 20 minutes in the Triton X solution, 500 μL of solution from the vials was added to an Eppendorf tube (Hauppauge, NY) and centrifuged at 250 g for 10 minutes. For each sample, 100 μL of the supernatant was added to a 96-well plate (Fisher Scientific), and the supernatant of the standard was diluted to 6000k, 3000k, 600k, 300k, 60k, 30k, and 0 platelets for the standard curve. From the kit, 11.25 mL dye was added to 250 μL catalyst and mixed, and 10 μL of this solution was added to each well. After reacting for one hour in the dark, the 96-well plate was loaded into a SpectraMax M2 microplate reader (Molecular Devices, San Jose, CA) and analyzed with SoftMax Pro 5 software (Molecular Devices). The equation from the linear interpolation of the standard curve absorbance values was used to determine platelet adhesion for the experimental leaflets divided by disk surface area.

2.10 STATISTICAL ANALYSIS

Statistical analysis of the data was performed with SigmaPlot (Systat Software, San Jose, CA). All results in tables and graphs are presented as mean ± standard error of the mean. T-tests were used when comparing two groups, and one-way analysis of variance (ANOVA) with Tukey post-hoc testing for multiple comparisons was applied to many groups. Differences were determined to be statistically significant if $p < 0.05$.

3.0 RESULTS

3.1 POLYMER SYNTHESIS

Biodegradable polyurethane elastomers (PEUU, PECUU, and PCUU) were synthesized with the two-step polymerization method. Variations in the chemistry of the three polyurethanes involved substitution of polyester and/or polycarbonate into the polyurethane backbone. **Figure 20** shows the degradable PEUU, PECUU, and PCUU after synthesis and dissolved in HFIP at an equivalent 12% w/v for the three mixing strategies. Inherent viscosity for each polyurethane is listed in **Table 1** and each was higher than the literature value in [64] with large variations in the PECUU.

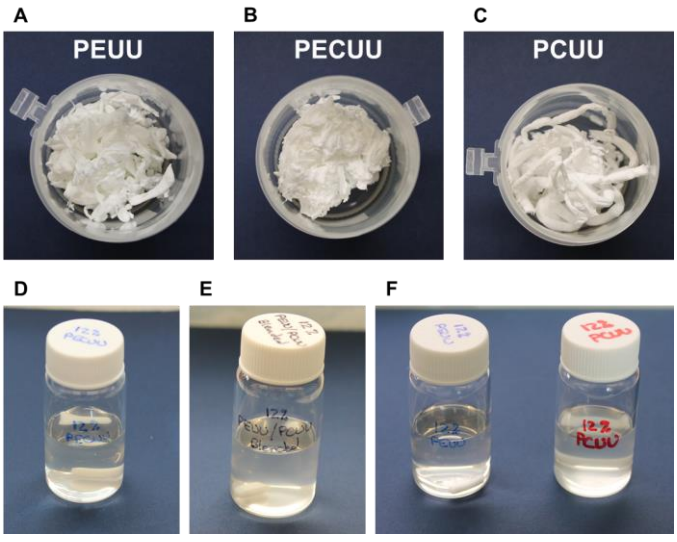

Figure 20. Synthesized A) PEUU, B) PECUU, and C) PCUU. Dissolved polyurethanes for the D) soft segment mixed, E) physically blended, and F) co-steam electrospun mixing strategies.

Table 1. Synthesized polyurethane inherent viscosity compared to literature.

	Inherent Viscosity (dL/g)	Hong et al. [64] (dL/g)
PEUU	1.42 ± 0.02	1.38
PECUU	1.18 ± 0.25	0.96
PCUU	1.02 ± 0.07	0.80

3.2 TISSUE ENGINEERED HEART VALVE SCAFFOLD FABRICATION

Fully assembled, stentless, trileaflet heart valves were fabricated from the biodegradable polyurethanes through electrodeposition onto the valve-shaped mandrel. **Figure 21A-C** shows the relationship of deposition time vs. valve leaflet thickness for each of the processing conditions. A desired thickness of 227 μm required 3.51 hours, 4.13 hours, and 2.46 hours of fabrication for the soft segment mixed, physically blended, and co-spun valves, respectively. There was no significant difference in initial valve thickness between the mixing strategies for valves used in the degradation study (**Figure 21D**). Representative valves from the soft segment mixed group, physically blended group, and co-stream electrospun group are shown in **Figure 22**. Electrospun valves used in the degradation study demonstrated proper coaptation at rest after removal from the mandrel.

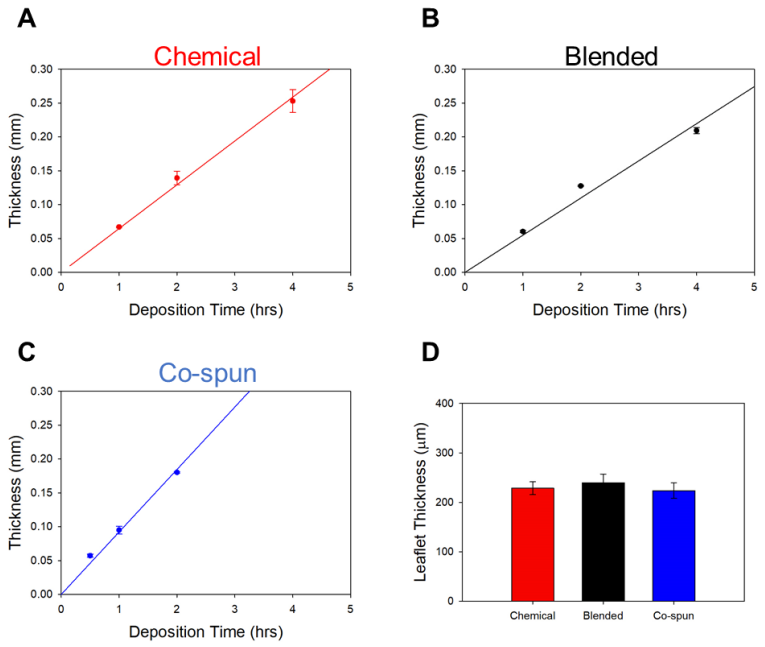

Figure 21. Characterization of the electrospinning deposition time vs. leaflet thickness for the mixing strategies A) soft segment mixing, B) physically blending, and C) co-stream electrospinning. D) Initial leaflet thickness of the degraded valves.

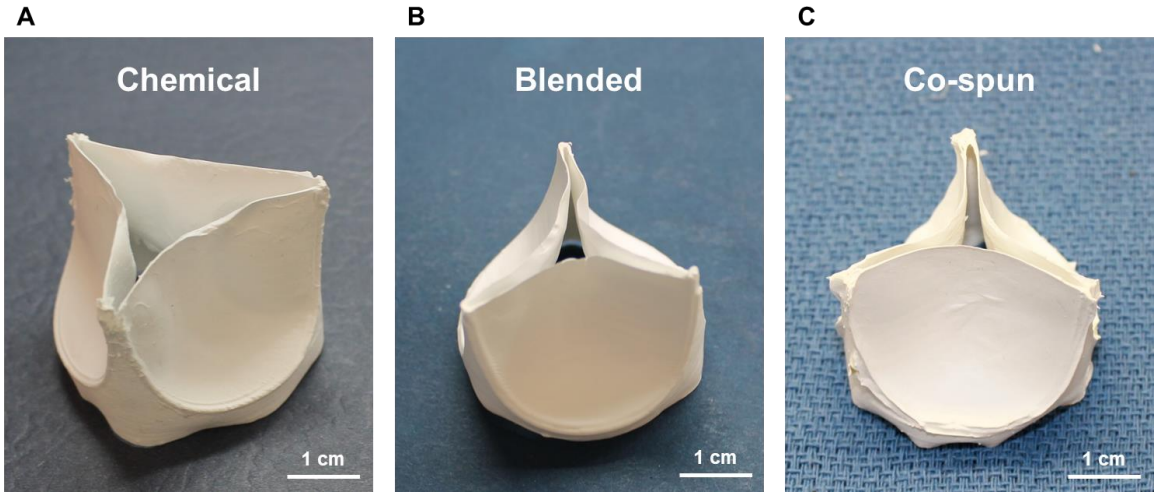

Figure 22. Electrospun, biodegradable, fully assembled tissue engineered heart valves fabricated with each of the mixing strategies A) soft segment mixing, B) physical blending, and C) co-stream electrospinning.

3.3 TISSUE ENGINEERED HEART VALVE ACCELERATED *IN VITRO* DEGRADATION

Scaffold polymer degradation was evaluated in a lipase solution at 37°C with mechanically loaded and unloaded environments. Videos of valve function in the pulse duplicator for all three experimental groups and at each timepoint can be found in the supplemental materials, with a brief description of the videos in Appendix A.1. Valve visual inspection, mass loss, and leaflet thickness loss were all used to evaluate the degradation. Lipase solution was changed twice per week to maintain consistent enzyme concentration and mitigate significant changes in pH [66].

3.3.1 Valve visual inspection

Figure 23 shows the fully assembled valves following degradation in the pulse duplicator. Valves displayed little to no tearing at the commissures or annulus, but nearly all degraded valves had tearing in the belly region of the leaflet which extended up to the free edge in some cases. The spliced valve photos in **Figure 24** further confirm this observation where some valves had tears down the middle of the leaflet which was fairly similar between the three leaflets. The co-spun valves displayed less tearing compared to the other two groups. Valve leaflets from the degradation experiment without mechanical loading had no tearing or hole formation, in any group, up to 14 days (**Figure 25**).

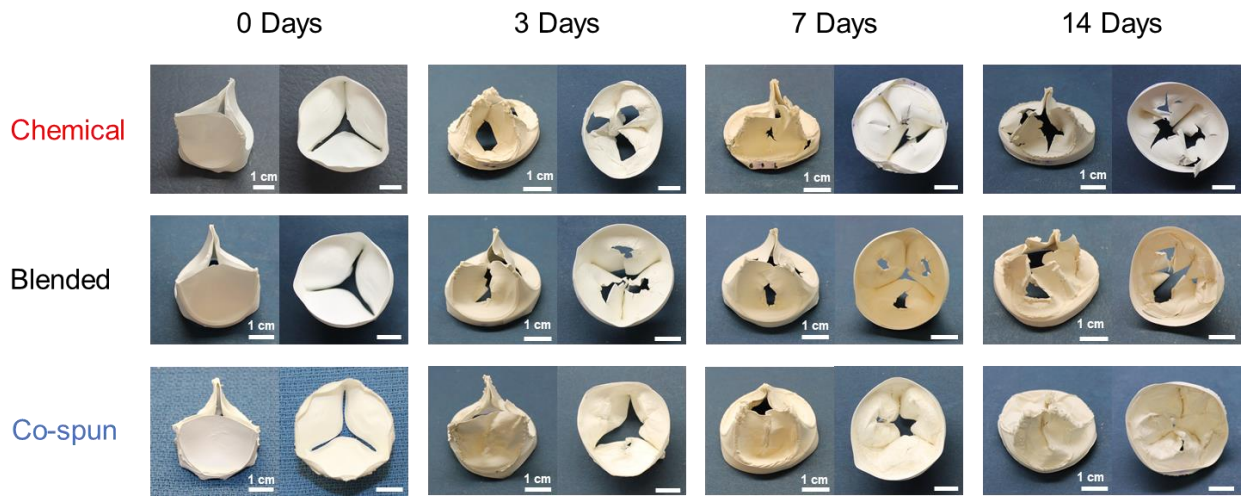

Figure 23. Visual inspection of the fully assembled valves following degradation in a mechanically demanding environment.

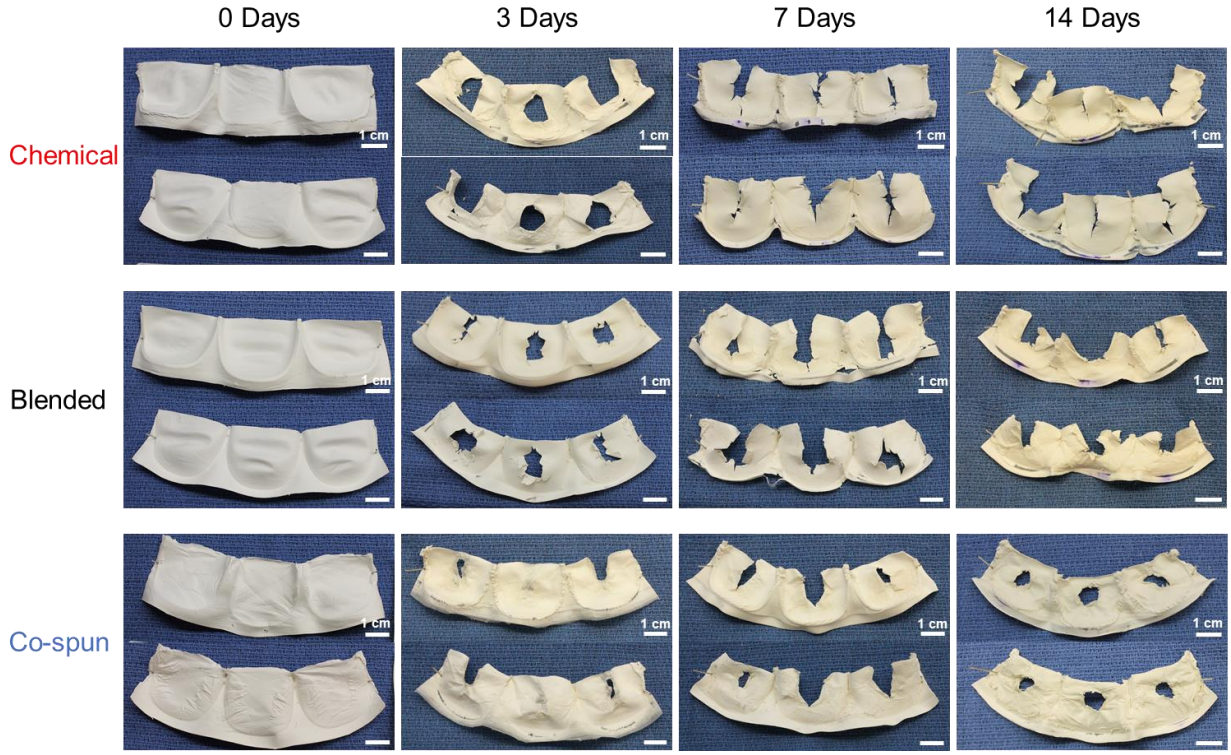

Figure 24. Visual inspection of the spliced valves following degradation in a mechanically demanding environment.

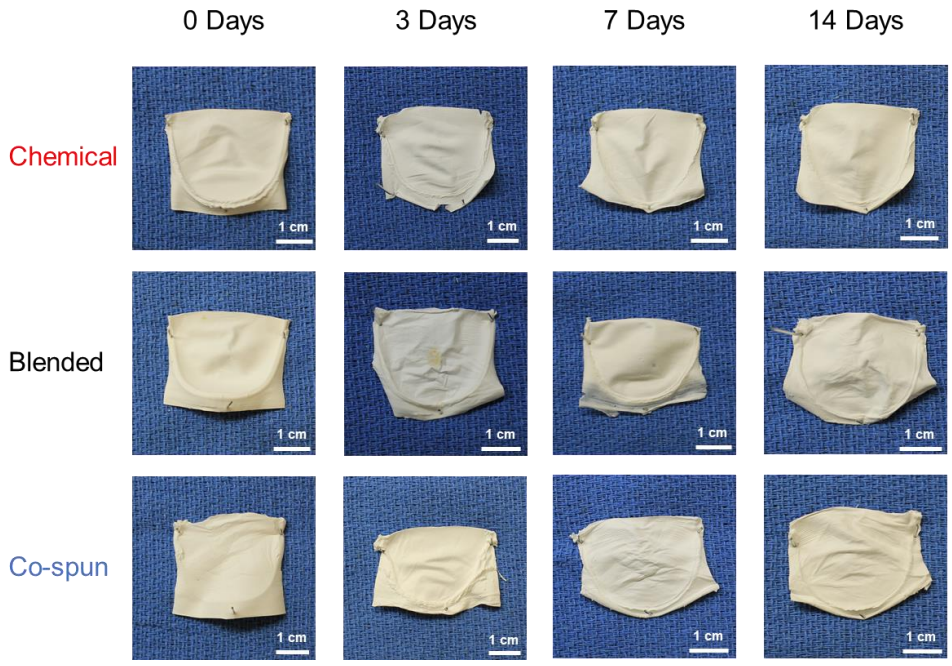

Figure 25. Visual inspection of the leaflets following degradation without mechanical loading.

3.3.2 Valve mass loss

Results from the valve mass loss accelerated degradation study with lipase and a mechanically demanding environment are presented in **Figure 26**. Mass remaining was significantly less for the soft segment mixed group (78.2%) than the physically blended (87.8%) or co-spun (87.9%) groups at 14 days. Both soft segment mixed and physically blended valves showed gradual decreases in mass remaining, while the co-spun valves increased in mass remaining at 14 days compared to 7 days.

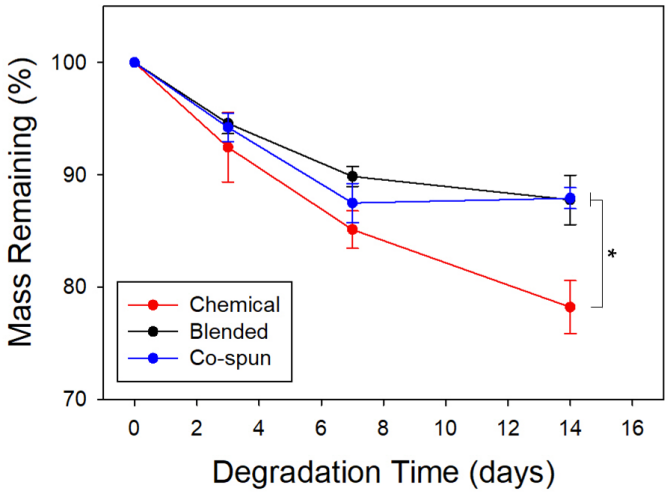

Figure 26. Valve mass remaining for electrospun tissue engineered heart valves fabricated with different mixing strategies and degraded in the pulse duplicator with mechanical loading and an enzymatic solution.

Valve leaflets degraded without mechanical loading maintained a similar trend for mass remaining, with the soft segment mixed group degrading significantly faster than the co-spun group. All valve leaflets experienced a gradual loss of mass shown in **Figure 27**, with the mass remaining ranging from 91.8% to 94.2% for the three groups. In a degradation comparison between the mechanically loaded and unloaded valves, each mixing strategy showed faster degradation in a mechanically demanding environment at both 7 and 14 days (**Figure 28**).

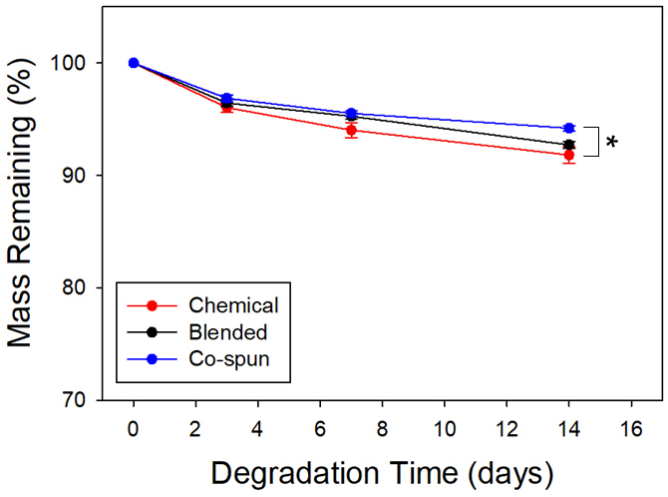

Figure 27. Valve leaflet mass remaining for electrospun tissue engineered heart valves fabricated with different mixing strategies and degraded in an enzymatic solution without mechanical loading.

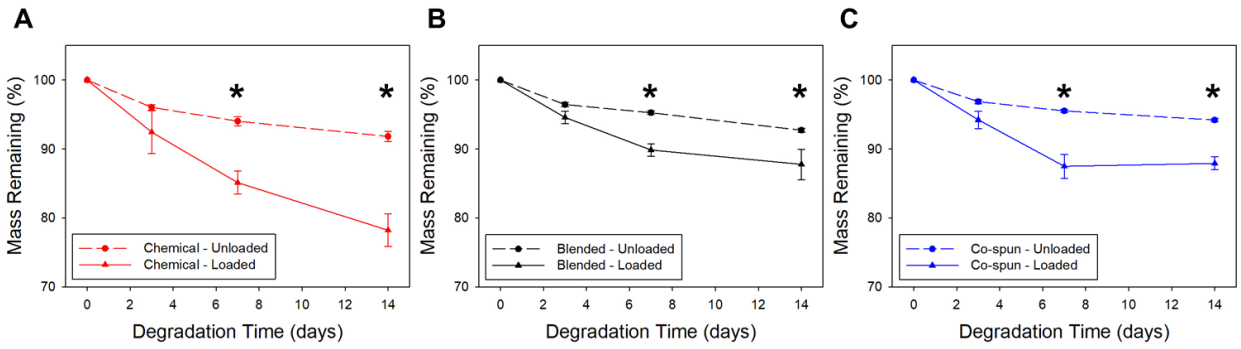

Figure 28. Valve mass remaining degradation profiles of tissue engineered heart valves processed with A) soft segment mixing, B) physical blending, and C) co-stream electrospinning, with (loaded) and without (unloaded) a mechanically demanding environment.

3.3.3 Leaflet thickness loss

Polymer valve degradation was also evaluated from its effect on leaflet thickness. Interpolation of thickness remaining at fifteen points on the leaflet surface is shown in **Figure 29**. Most degraded valves showed a loss of thickness in the belly region and up to the free edge, consistent with the visual inspection. The soft segment mixed leaflets had lost significantly more thickness

at 14 days than the others. Co-spun leaflets had degradation that was more random throughout the study, consistent with mass loss and had lost the least thickness at 14 days.

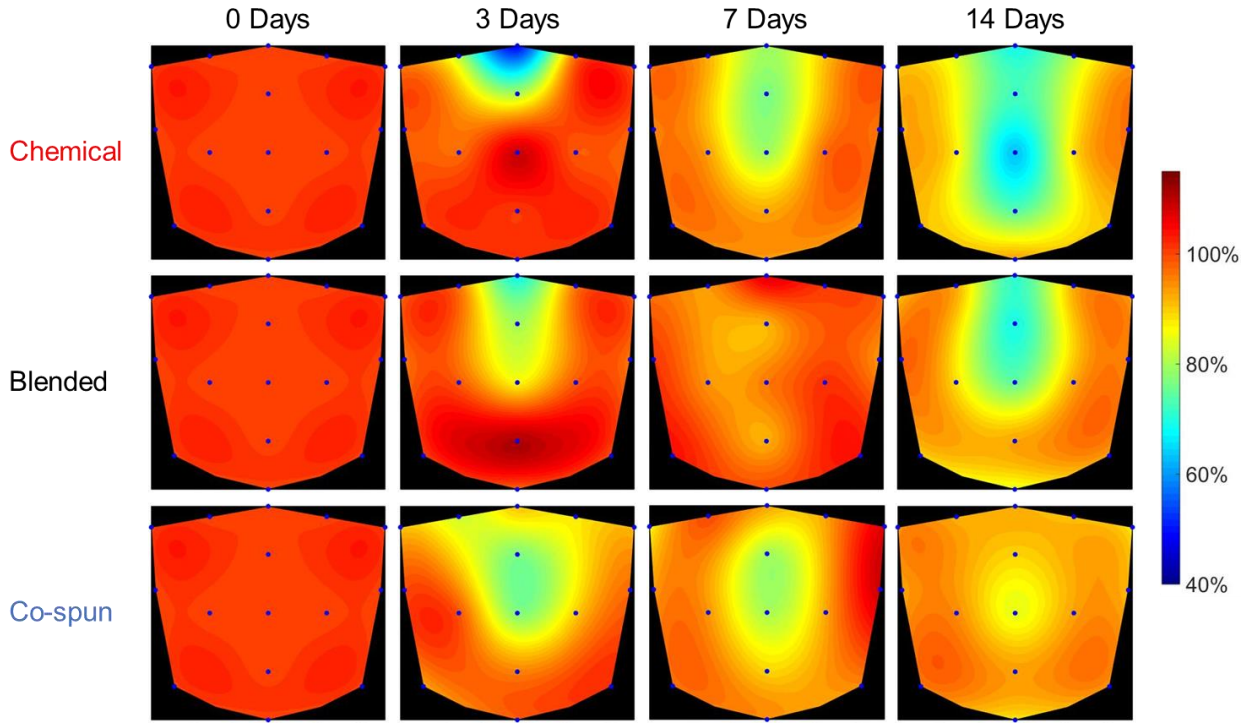

Figure 29. Degraded tissue engineered heart valve leaflet thickness remaining interpolation for fifteen points along the free edge, commissures, annulus, and in the belly region for valves degraded in the pulse duplicator with a mechanically demanding environment and enzymatic solution.

The *in vitro* degradation of the leaflet thickness was also quantified and compared (**Figure 30**). Thickness loss maintained the same general order as the other degradation parameters, with soft segment mixed valves having experienced significantly more degradation than the co-spun valves, and thickness remaining ranging from 83.5% to 92.6%. Again, the co-spun valves experienced more random degradation throughout the 14 days and increased in thickness remaining at 14 days compared to 3 days and 7 days.

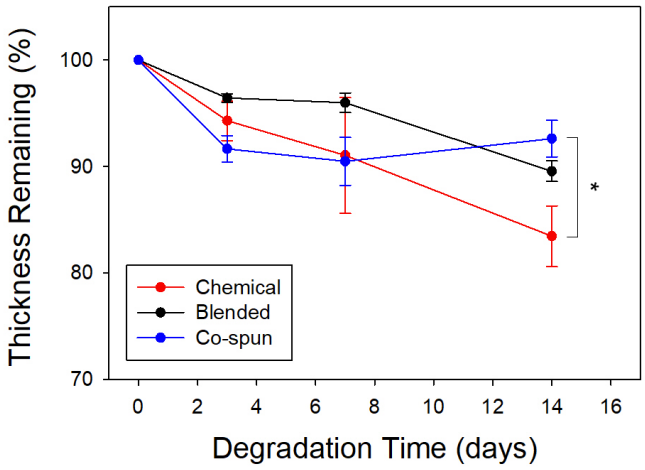

Figure 30. Valve leaflet thickness remaining for electrospun tissue engineered heart valves fabricated through different mixing strategies and degraded in the pulse duplicator with a mechanically demanding environment and enzymatic solution.

3.4 SURFACE MORPHOLOGY OF DEGRADED TISSUE ENGINEERED HEART VALVES

Valve leaflet surface morphology was observed with a SEM for the mechanically loaded scaffolds. SEM images of the atrial and ventricular surfaces of the valve leaflets are shown in **Figures 31-33** and **Figure 34-36**, respectively. Qualitative analysis confirms an initial fibrous scaffold on both surfaces for each experimental group. At low magnification, the soft segment mixed leaflet surface is noticeably broken apart with increasing prevalence at later timepoints. There is no major damage to the physically blended or co-spun leaflet surfaces up to 14 days. At a more moderate magnification where fibers appear, the soft segment mixed surface breaking apart becomes more apparent and the physically blended surface also appears to have a few areas which are broken. At high magnification, all groups maintained a fibrous structure and most

appeared to have fibers fraying, especially at the later timepoints. There was noticeably more damage on the soft segment mixed and physically blended surfaces at 14 days degradation. There were no major differences between the atrial and ventricular surfaces at any magnification.

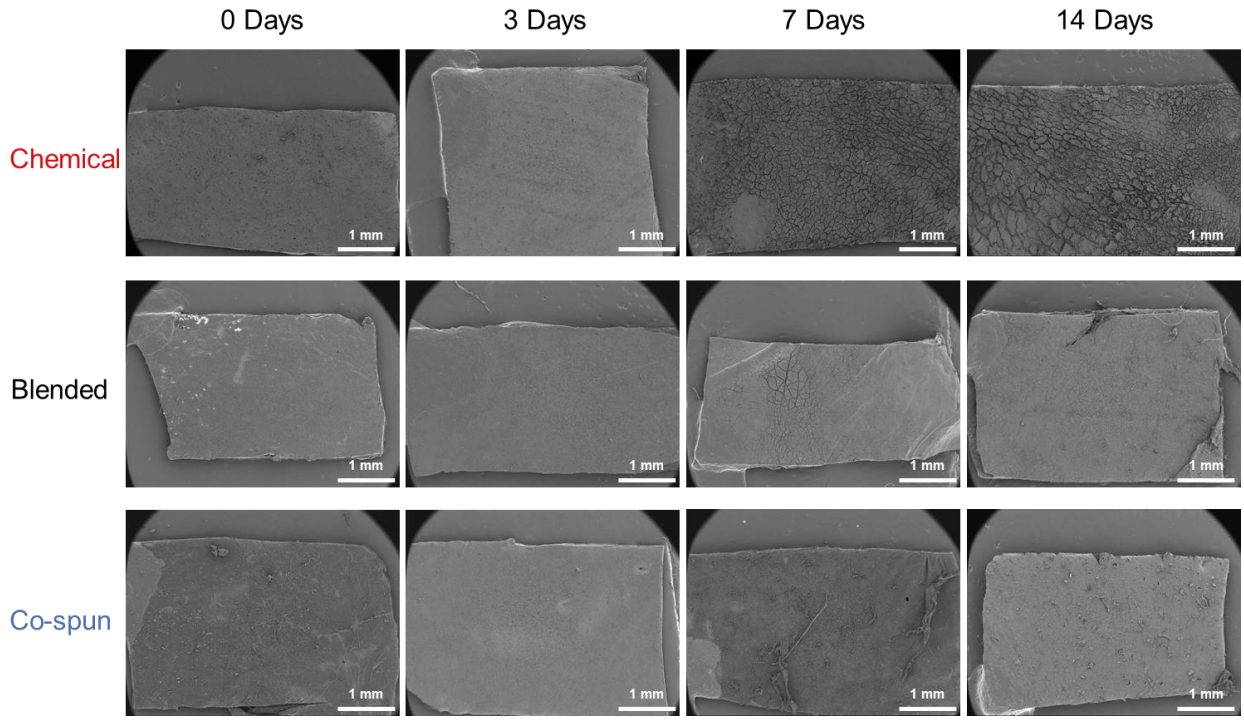

Figure 31. SEM images of the surface morphology of degraded leaflet atrial side at low magnification (25x).

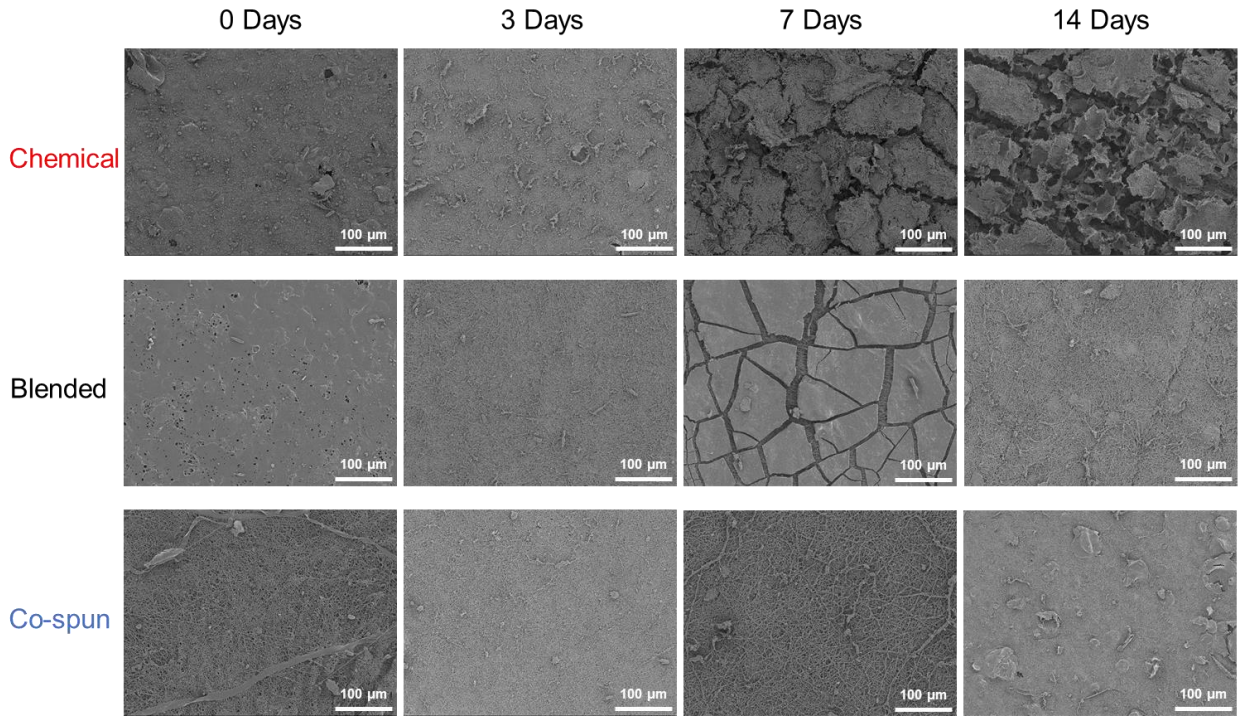

Figure 32. SEM images of the surface morphology of degraded leaflet atrial side at moderate magnification (250x).

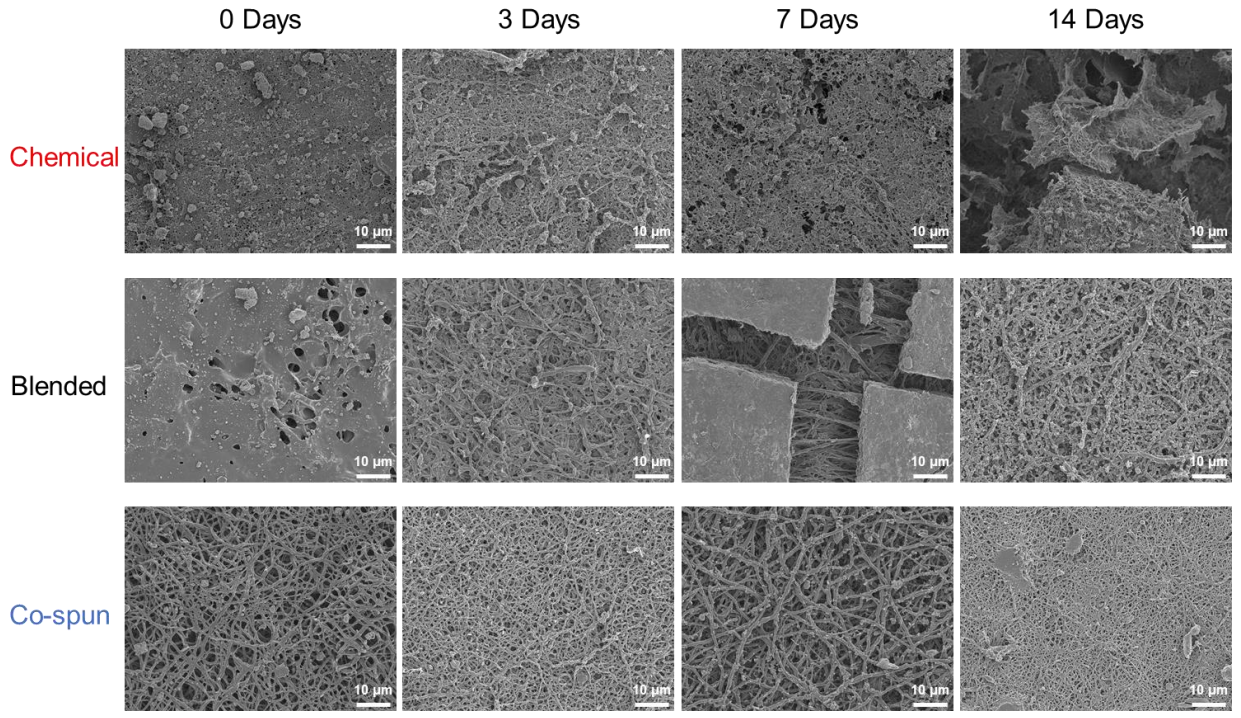

Figure 33. SEM images of the surface morphology of degraded leaflet atrial side at high magnification (1500x).

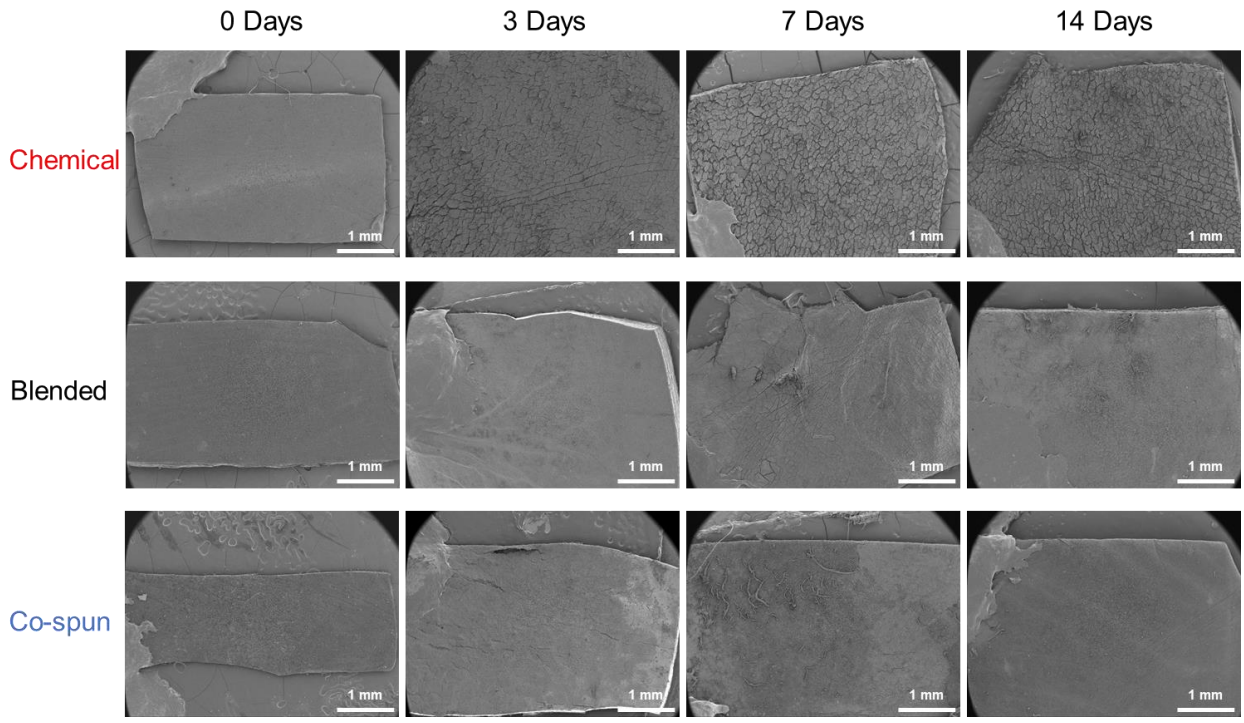

Figure 34. SEM images of the surface morphology of degraded leaflet ventricular side at low magnification (25x).

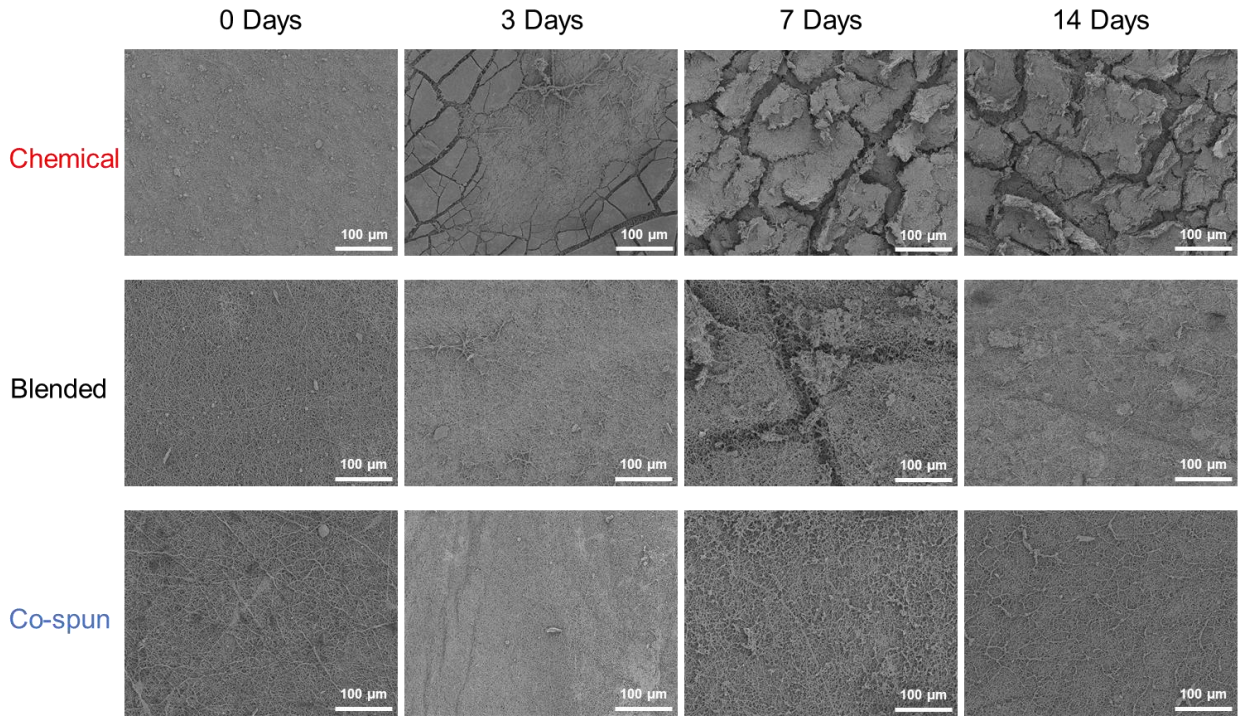

Figure 35. SEM images of the surface morphology of degraded leaflet ventricular side at moderate magnification (250x).

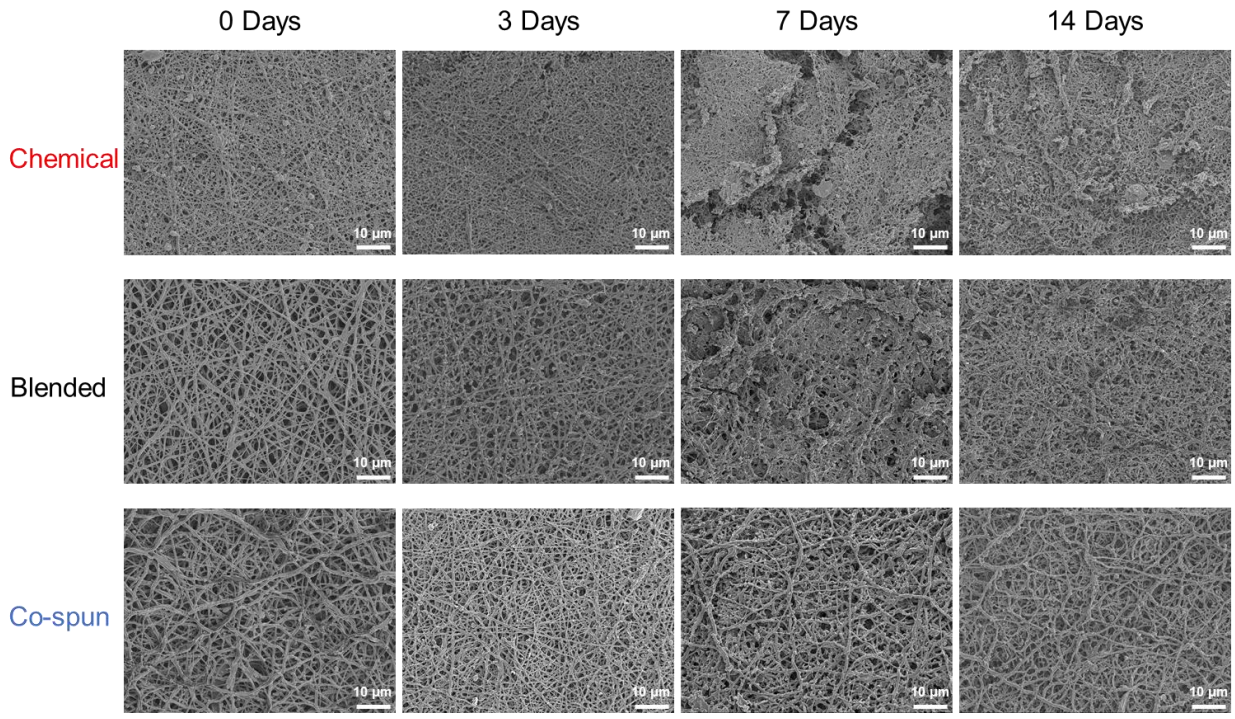

Figure 36. SEM images of the surface morphology of degraded leaflet ventricular side at high magnification (1500x).

3.5 BIAXIAL MECHANICAL RESPONSE OF DEGRADED TISSUE ENGINEERED HEART VALVES

Degraded valves biaxial mechanical response was evaluated for the valve leaflets at each timepoint. **Figure 37** shows the equi-stress biaxial response in the radial and circumferential directions over time. While there were no significant differences in compliance in any group throughout the degradation, the physically blended and co-spun groups trended toward increased compliance with longer degradation. The strain energy (**Figure 38**) was also calculated for each group over time without any significant results. In general, there was very little change in the soft

segment mixed group and slight increases in strain energy for the blended and co-spun groups. Leaflets were also evaluated under equi-tension testing, and the results in **Figure 39** were similar to those of the equi-stress test.

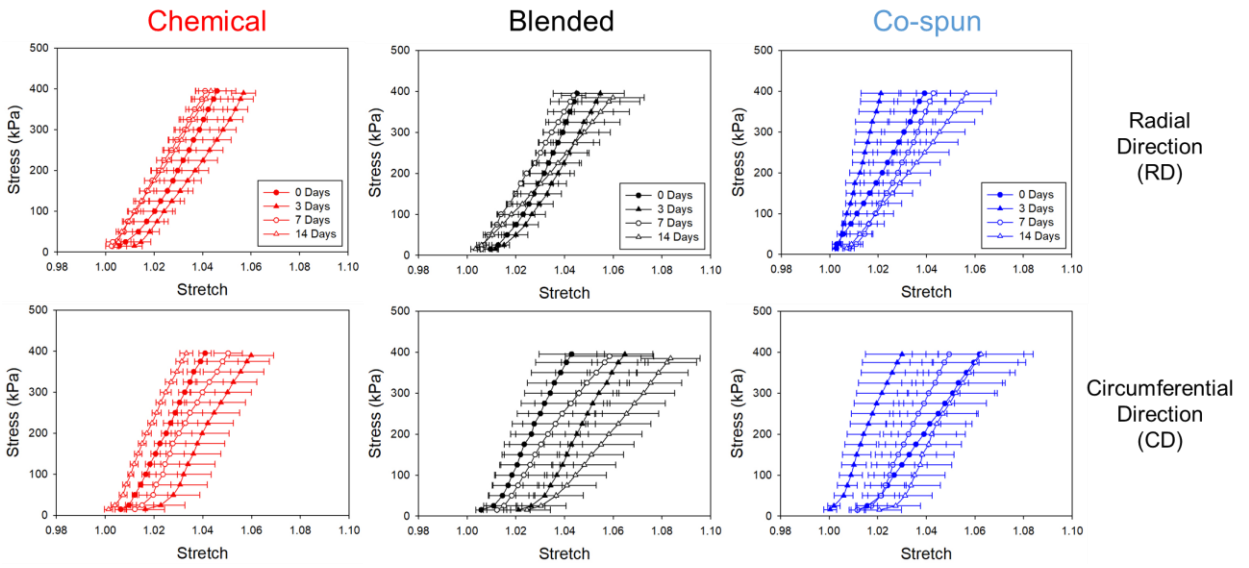

Figure 37. Equi-stress biaxial mechanical response of tissue engineered heart valve leaflets which were mechanically loaded and degraded in the pulse duplicator.

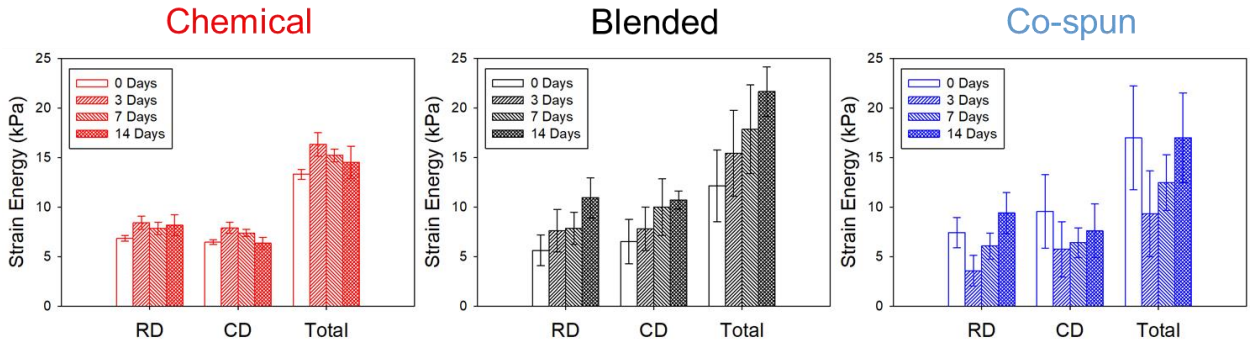

Figure 38. Strain energy calculations from the equi-stress biaxial mechanical response in the previous figure for the degraded tissue engineered heart valve leaflets.

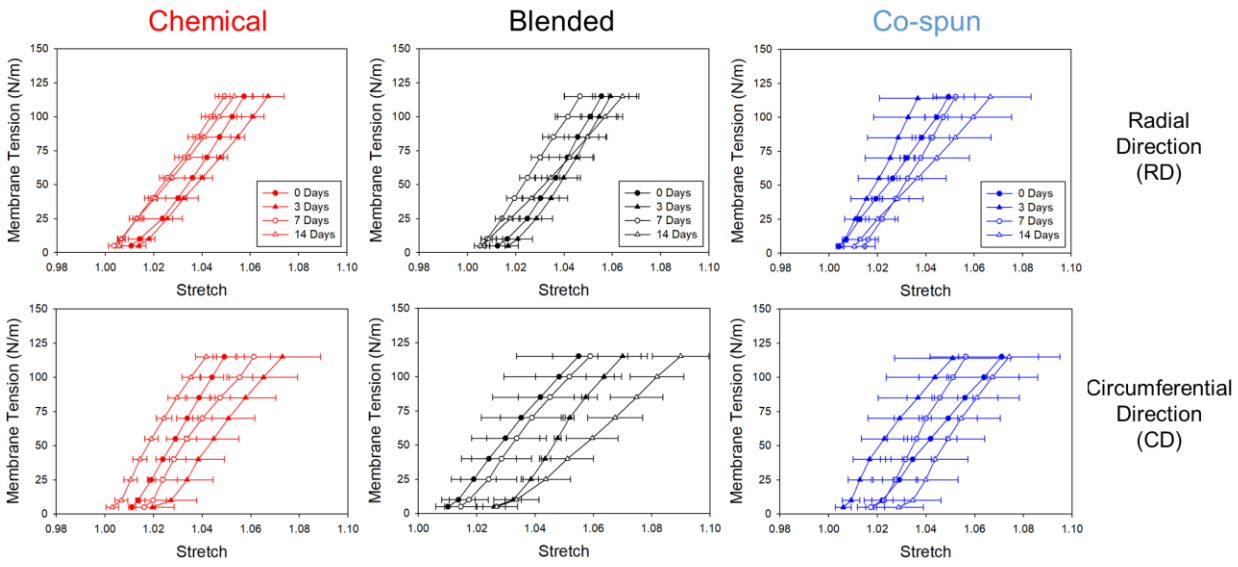

Figure 39. Equi-tension biaxial mechanical response of tissue engineered heart valve leaflets which were mechanically loaded and degraded in the pulse duplicator.

3.6 POLYMER VISCOSITY OF DEGRADED TISSUE ENGINEERED HEART VALVES

Inherent viscosity of the degraded polyurethane valves was calculated from the relative viscosity measured with an Ubbelohde viscometer and the solution concentration. **Figure 40** shows the results of the normalized inherent viscosity of the degraded polyurethane valves with mechanical loading. Both the soft segment mixed (83.3%) and physically blended (90.6%) groups had significant decreases in viscosity as compared to the co-spun (98.3%) group at 14 days. Additionally, the co-spun group indicated nearly no loss in viscosity throughout the study while the soft segment mixed group had high variation at 3 days and 7 days. The inherent viscosity of the polyurethane valves can be found in **Table 2**.

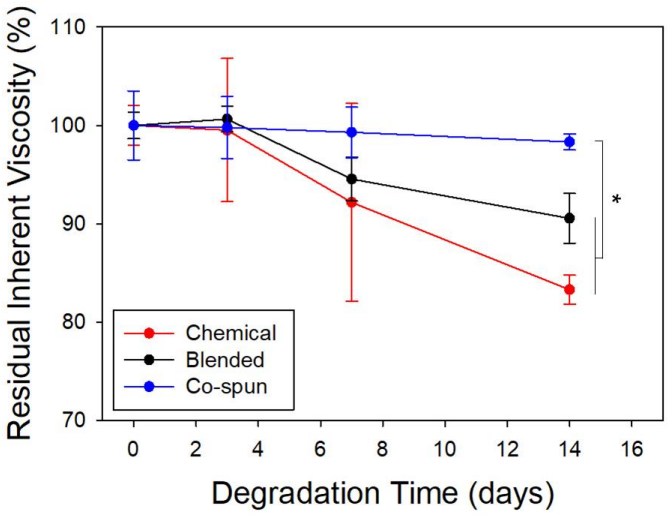

Figure 40. Residual inherent polymer viscosity from the tissue engineered heart valves degraded in the pulse duplicator with mechanical loading and an enzymatic solution.

Table 2. Degraded valve polymer inherent viscosity.

	0 Days (dL/g)	3 Days (dL/g)	7 Days (dL/g)	14 Days (dL/g)
Chemical	1.12 ± 0.02	1.12 ± 0.08	1.04 ± 0.11	0.94 ± 0.02
Blended	1.30 ± 0.02	1.31 ± 0.02	1.23 ± 0.03	1.18 ± 0.03
Co-spun	1.26 ± 0.04	1.26 ± 0.04	1.26 ± 0.03	1.24 ± 0.01

3.7 BLOOD COMPATIBILITY OF TISSUE ENGINEERED HEART VALVES

To evaluate platelet deposition onto the surface of the electrospun leaflets, a simple rocking test was performed with electrospun samples from each mixing strategy for 1.5 hours and platelets were quantified with a LDH assay, shown in **Figure 41**. Although the physically blended leaflets had a lower number of deposited platelets than the soft segment mixed and co-spun leaflets, the

results were not statistically significant. There was also high variability in the platelet quantification for the co-spun group compared to the other two groups.

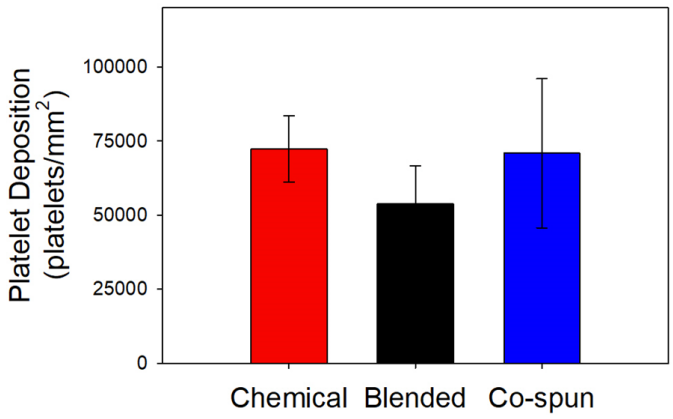

Figure 41. Platelet deposition quantified by a lactate dehydrogenase assay for the electrospun tissue engineered heart valves with the three mixing strategies.

4.0 DISCUSSION

TEHVs offer the potential to overcome many of the drawbacks which exist with mechanical or bioprosthetic heart valves, namely chronic anticoagulation therapy and limited durability, and the related morbidity. The ability to degrade and regenerate living, functional tissue makes the pediatric population a target of this therapy. While biodegradable materials are typically used in the design of tissue engineered valves, specific degradation rates for those scaffolds are often unknown. In order to de-risk preclinical studies and provide controllable rates of scaffold degradation, furthers studies were needed to characterize the materials being used in the valve constructs.

4.1 TISSUE ENGINEERED HEART VALVE DEGRADATION WITH POLYURETHANE SOFT SEGMENT MIXING STRATEGIES

The rate at which a TEHV degrades *in vivo* is important to the formation of new functional tissue. Degradability of the scaffold should be tuned to match new tissue formation by ECM synthesis [92, 109]. Heart valve tissue is subjected to cyclic opening and closing more than 30 million times each year, and the mechanical stresses of this motion can fatigue and degrade the valve. Continuous contact with blood and other factors can also influence the degradation rate, which also varies depending on other comorbidities.

Biodegradable polyurethanes have been established by incorporating segments with labile bonds into the polyurethane backbone [85]. Other studies have shown the ability to integrate polyether [86] or polycarbonate [64] along with polyester into the polyurethane to tune degradability. Electrospun scaffolds have been produced from the combination of multiple polymers that were mixed through soft segment mixing during synthesis to form a copolymer [76], physically blending in a common solvent [70], or co-stream electrospinning to produce a scaffold with two different fiber populations [73], although there has been no comparison between the three methods.

The purpose of this study was to analyze the relative degradation rates of these three mixing strategies with a 50/50 ratio of polyester and polycarbonate soft segments in the polyurethane scaffolds. Of the two segments, polyesters have been shown to have a faster degradation rate than polycarbonates [64, 81, 99]. In this thesis, degradation rates were found to be significantly faster for the soft segment mixed valves (**Figure 26**) which had the more labile ester bonds integrated into every polymer chain and electrospun fiber. Unlike the other two groups which had polymer chains consisting of only polyester or only polycarbonate segments, theoretically each polymer chain in the soft segment mixed group contained polyester segments. Similar results were found with thickness loss (**Figure 30**) as the soft segment mixed group lost a greater amount of thickness during degradation. Entire polymer chains and fibers consisting of the slower degrading polycarbonate segments were present in the physically bended and co-spun groups, respectively, providing a level of structure during degradation that the soft segment mixed group did not have.

Additional analysis of leaflet thickness using the interpolation maps (**Figure 29**) showed more degradation for the soft segment mixed group at 14 days, as well as significant degradation

in the belly region and up to the free edge for all groups. This corresponds to the images of the spliced valves (**Figure 24**) which display tears in the degraded valves extending from the belly region to the free edge. These tears typically began forming in the valves within a few hours of initiating the degradation study and were likely a result of valve contraction and enzymatic activity, further discussed in Appendix A.2 and A.3. The appearance of holes were not pieces of leaflet lost during the study, but rather tears that pulled apart due to the stresses on the leaflet. This shows the significance of fatigue testing [15, 33] prior to preclinical studies in order to de-risk valve failure and harm to the animal.

Previous studies with lipase enzyme and biodegradable polyurethanes [66, 99, 104, 105] showed rapid degradation with respect to the control in just a few days. This may account for the initial tearing of the valves at the thinnest locations on the leaflets. While the degradation of the three groups in this study was significantly slower than most of the groups in the previous studies, those studies mostly involved PEUU or a derivative. However, in the study by Ma et al. [99], a polyurethane with polycarbonate in the backbone showed little degradation in an lipase solution at 4 weeks. Hong et al. [64] reported no degradation of 50/50 PECUU scaffolds at 8 weeks *in vitro* without an enzyme. Other factors such as solution volume, contact surfaces, and high pressures and fluid movement may have affected enzymatic degradation in the system.

Co-spun TEHVs may have displayed more random degradation properties due to their fabrication process. Rather than an equal distribution of polyester and polycarbonate segments in the polymer chain or blended solution as the other two groups had, the co-spun group required equal deposition of the PEUU and PCUU fibers onto the mandrel during electrospinning. Unlike previous degradation studies [85, 87, 100] where multiple samples could be made simultaneously for a group, this study required each sample to be fabricated independently, increasing the

variation of the samples. Because the two polymer streams were originating from opposite sides of the rotating mandrel, one polymer stream experienced an upward tangential velocity of the mandrel while the other stream experienced a downward tangential velocity, potentially affecting the electrodeposition process. These concerns will be further addressed in the limitations, Section 5.2.

Surface morphology from the SEM images showed significant degradation on the surface of the soft segment mixed valves (**Figures 31, 34**). These images at the surface level showed the valve breaking apart on both sides, atrial and ventricle, as degradation progressed. Physically blended and co-spun valves did not show significant fractures, all of which corresponds with the mass loss of the scaffold. At the fiber level (**Figures 33, 36**), fibers appear to be broken in both the soft segment mixed and physically blended groups. Additionally, the fractures from the low magnification image of the soft segment mixed valve surface can be clearly seen.

Results from the inherent viscosity tests (**Figure 39**) generally agree with the results from the mass loss (**Figure 26**) as the degradation order of the three mixing strategies is maintained at 14 days. Loss of molecular weight in the degraded polymer scaffolds is indicated by loss in inherent viscosity [64]. Therefore, significantly lower inherent viscosity for the soft segment mixed and physical blended scaffold indicate more chain scission. Theoretically, with perfect mixing, each of these groups had both polyester and polycarbonate groups in every electrospun fiber. Meanwhile, the co-spun scaffold had two different polyurethane fiber populations, one with polyester segments and one with polycarbonate segments, which could maintain the viscosity during degradation. All experiments in the degradation analysis had soft segment mixed valves degrading significantly faster than the co-spun valves, with blended valves

somewhere in between the two. Extending this study out to longer timepoints may provide more clarity on the relationship between the three mixing strategies.

This is the first study to characterize and compare the relative degradation profile of the three mixing strategies: soft segment mixing, physical blending, and co-spinning, for two different polymers. Guan et al. [86] and Hong et al. [64] studied the ratio of labile segments incorporated into the polyurethane backbone, but did not consider other strategies to combine the segments. Previous studies have considered each of these three strategies independently [70, 73, 76], but there has yet to be a comparative study. This work provides a way to tune degradability of polymers without having to alter the polymer chemistry. Additionally, alternative mixing strategies are presented as possibilities when working with two desirable polymers which could not be combined using a different method.

4.2 EFFECTS OF MECHANICAL LOADING AND PULSATILE FLOW ON TISSUE ENGINEERED HEART VALVE DEGRADATION

The *in vivo* degradation rates of polymers are typically faster than the *in vitro* degradation in a PBS solution. Enzymes such as lipase [66, 99, 104, 105, 107], elastase [90], and collagenase [101] have been added to *in vitro* studies to create accelerated degradation studies which more accurately represent the *in vivo* environment. Lipases have been used to a great effect, significantly degrading polyurethanes with polyester segments as compared to PBS alone. These studies consider hydrolytic and enzymatic degradation with the polymer scaffold, but often neglect the effects of mechanical degradation.

Cyclical opening and closing of the heart valves occurs more than 30 million times each year, causing the valves to experience high pressure and mechanical fatigue [15]. While some TEHV studies evaluate the degradation of the construct *in vitro*, mechanical degradation is usually ignored as flat sheets of polymer are degraded in solution [109, 111]. This study advances those shortcomings by introducing a pulse duplicator to simulate the effects of mechanical degradation in addition to subjecting the fully assembled TEHVs to hydrolytic and enzymatic degradation. To recapitulate the *in vivo* experience of an atrioventricular valve, sutures were used to connect the valve commissures with the posts to represent the chordae tendineae and papillary muscles in the heart.

Comparing the images of the mechanically loaded and unloaded degraded valve leaflets (**Figures 24, 25**), significant differences in valve leaflet tearing is present at all timepoints, indicating that mechanical stresses played a role in leaflet tearing. At the 14 day timepoint in the unloaded leaflet, no tears had occurred in any group, yet all groups in the mechanically loaded valves formed holes or tears at 3 days. Two other experiments to analyze the causes of leaflet tearing are presented in Appendix A.2 and A.3. Contraction of the electrospun fibers followed by stretching in the pulse duplicator may have contributed to this effect. To prevent similar valve failure during the *in vivo* studies, valves should not be stretched to fit the annulus; rather, a broader range of mandrel diameters should be used to increase the available valve sizes.

The relative degradation rates of the three mixing strategies maintained the same general order without mechanical loading as they did in the mechanically demanding environment (**Figure 27**). Co-spun valves degraded significantly less than the soft segment mixed valves, reinforcing the initial findings described in the previous section. With respect to each mixing strategy, the valves in the pulse duplicator had degraded significantly faster at the 7 and 14 day

timepoints than the leaflet without mechanical stimulation (**Figure 28**). This could be an effect of the mechanical stresses experienced by the valve as well as fluid flowing past at a higher velocity removing degraded polymer. Regardless, this emphasizes the importance of replicating the mechanical stresses that would normally be experienced by a TEHV construct in the heart during an *in vitro* degradation study.

This is the first study to perform a degradation analysis on fully assembled TEHVs in a pulse duplicator which attempts to mimic the native conditions of the heart. Reimer et al. [33] performed a fatigue test in a pulse duplicator, but did not specifically evaluate scaffold degradation. Sant et al. [109] and Brugmans et al. [111] evaluated the degradation of heart valve leaflet material, but did not evaluate the material as an assembled scaffold in a pulse duplicator. In conclusion, this work demonstrates the need to create a mechanically demanding environment when performing degradation studies on dynamic tissues and provides a method for long term degradation studies with TEHVs.

4.3 MECHANICAL STABILITY OF TISSUE ENGINEERED HEART VALVES FOLLOWING DEGRADATION

The importance of mechanical properties in the design of TEHVs has been introduced in [15, 51, 54]. Mechanical properties of TEHVs are generally evaluated through tensile testing, biaxial testing, flexural testing, and fatigue testing. From a mechanics approach, in-plane biaxial properties relate to proper valve coaptation and reduced regurgitation while out-of-plane flexure properties are important for the valve opening and closing millions of times per year [54].

Additionally, these mechanical signals are important for cell migration, alignment, and differentiation on the scaffold, all of which are required for endogenous tissue growth.

To accommodate these mechanical requirements in a biodegradable scaffold, proper stress transfer from the degrading valve to newly formed tissue is required. Success in this transfer is a function of the valve degradation rate matching the rate of newly synthesized ECM [92]. As the scaffold degrades, there should be a loss in mechanical strength leading to increased compliance of the scaffold material; *in vivo*, this would be augmented by new tissue providing increased mechanical strength over time. Consequences of early degradation are failure of the tissue at the site, which can be traumatic in heart valve applications, while late degradation can result in fibrosis and stiffening of the leaflets [64, 92]. Additionally, inappropriate mismatch in mechanical properties can hinder proper cell function.

This study characterized the biaxial mechanical properties of the degraded valve from the pulse duplicator to determine the effect of degradation on mechanical compliance. The isotropic valves showed no significant changes in mechanical response during the 14 day degradation study (**Figures 37, 39**). However, the physically blended and co-spun valves appeared to have a slight increase in compliance as degradation progressed. The soft segment mixed valves had essentially no change in compliance at 14 days which is contrary to what would be predicted. Because this group had the most scaffold degradation, it would be expected that the mechanical strength would decrease and result in increased in-plane mechanical compliance. Additionally, the compliance in the radial and circumferential directions are similar throughout the degradation for all groups, indicating that the tissue maintains isotropy and that the direction of degraded fibers is random. Similar results were also observed in the strain energy calculation from the equi-stress biaxial test (**Figure 38**). Although the circumferential direction of the leaflet appears

to be gaining compliance in **Figure 37** as degradation progresses, the strain energy analysis indicates that both directions have approximately the same strain energy and that the difference is an offset in the biaxial response.

While some of these results are counterintuitive, an explanation may be that the slight changes in mechanics at 14 days degradation is simply noise and that longer degradation studies are needed before an accurate evaluation can be made. Regardless, each mixing strategy maintained the mechanical properties of the TEHV up to 14 days, indicating the possibility of using these polyurethanes in long studies without the risk of acute mechanical failure.

4.4 BLOOD COMPATIBILITY WITH POLYURETHANE SOFT SEGMENT MIXING STRATEGIES

TEHVs must have good blood compatibility throughout their temporary use as they will be in constant contact with blood. In fact, many *in situ* approaches to TEHVs, like that of Kluin et al. [50], rely on endogenous cells from the blood to populate the scaffold. Fortunately, the degradable, stentless design of this TEHV will require only short-term contact and will not leave foreign materials in the blood stream. If new tissue successfully forms around the TEHV, less polymer will be exposed to the blood as the valve continues to degrade.

Gu et al. [107] showed a PCUU coating to have relatively less platelet deposition than PEUU, although the results were not significantly different. This study evaluated blood compatibility of TEHV leaflets consisting of equal amounts of polyester and polycarbonate soft segments in polyurethanes, but combined through the three mixing strategies described above. Quantitative platelet deposition (**Figure 41**) showed no significant difference between the

mixing strategies, indicating the position of the polyester and polycarbonate segments in the same polymer chain, in different polymer chains in the same electrospun fiber, and in different electrospun fibers did not affect blood compatibility. Considering this, selection of the mixing strategy to control degradation will not affect the blood compatibility of the valve. The high variability within the co-spun group is again reflective of the more significant sample to sample variation with this dual-stream electrospinning method. However, due to the small sample size and variation within the groups, further testing of the scaffolds produced in a more controlled manner should be performed to verify blood compatibility.

5.0 CONCLUSIONS

TEHVs could one day offer a promising solution for those suffering from VHD in need of a replacement valve. As an alternative to the current clinical technologies (mechanical and bioprosthetic heart valves), TEHVs have the potential to regenerate functional, native tissue that overcomes many of the limitations of the current technology and reduces the need for future surgery. Electrospun heart valves are fibrous structures that have been shown to have controllable anatomical geometry, submicron fiber diameter, and mechanical properties [51]. These scaffolds are fully assembled, stentless, trileaflet valves made from biodegradable polyurethane elastomers without a cellular component. As an acellular scaffold, endogenous tissue growth would be required by cells populating the polymeric scaffold from either the circulating blood or the walls of the heart. It is desirable for scaffold degradation to evenly match new tissue growth, while maintaining sufficient mechanical strength to avoid tissue failure at the site. This thesis focused on the degradation effects that the three mixing strategies for polyurethanes with polyester and polycarbonate soft segments would have on TEHVs. Further assessment of ECM production and new tissue formation on the TEHV *in vivo* is needed before selecting the appropriate mixing strategy to match the degradation rate with new tissue formation.

5.1 SUMMARY OF CONCLUSIONS

Three different mixing strategies of polyester and polycarbonate segments in a polyurethane were used to electrospin fully assembled, biodegradable TEHVs. An accelerated degradation study of these TEHVs performed *in vitro* in a pulse duplicator found that mixing both polyester and polycarbonate segments into the polyurethane backbone during synthesis had the fastest degradation rate. Meanwhile, the TEHVs produced from independent electrospun streams of PEUU and PCUU had the least amount of degradation at 14 days, although there was more variability within the group. TEHVs produced from electrospun blends of PEUU and PCUU in solvent were between the other two groups and significantly different depending on the experiment, giving it a moderate degradation rate.

TEHVs were degraded in a pulse duplicator with the cyclical stresses of a valve opening and closing and sutures to replicate the chordae tendineae of the atrioventricular valves. These factors were intended to more accurately represent the native environment of a heart valve, and increased degradation rates of TEHVs from all mixing strategies were shown at 7 and 14 days. This result indicates that mechanical as well as enzymatic and hydrolytic degradation should be considered in degradation studies of dynamic tissue scaffolds like heart valves.

Biaxial mechanical properties of the TEHVs from each mixing strategy were maintained up to the 14 day timepoint. TEHVs produced through blending PEUU and PCUU into a solvent or electrospinning with two independent streams of PEUU and PCUU had a slight increase in compliance at the 14 day timepoint. Although this increase was not significant, it was contrary to what would be expected based on the scaffold degradation. These findings indicate that although the scaffolds have begun to degrade and lose mass, the mechanical properties are being maintained until new tissue could putatively support the stresses.

The mixing strategies of the polyurethane soft segments were not significantly different with regard to platelet deposition. Therefore, blood compatibility of the material will not need to be a selection factor for the appropriate polyurethane soft segment mixing strategy when attempting to match degradation rate with new tissue formation.

5.2 STUDY LIMITATIONS

One of the main limitations of this study is the sample to sample variability produced by the electrospinning process [125]. Variability can result from environmental factors such as humidity and temperature, and although the temperature during the fabrications remained constant at ~21°C, humidity would vary between 9% to 45%. Small differences in polymer concentration or variable loss in continuity of the mandrel and electrode could also alter the fabrications. Unlike previous degradation studies [85, 87, 104] which could generate all of the samples from a group in one fabrication, each sample had to be fabricated independently in this study, amplifying the effects described above. These repeatability issues of electrospinning are acknowledged as a concern for using this method to produce TEHVs.

The design of the mandrel was another limitation in the study. Although the mandrel consisted of a conductive and a non-conductive component, fibers would not always deposit on the collecting surface, but would form a bridge between the commissures of the mandrel. Utilizing a material like copper as the conductive component may increase deposition onto the concave surface. Additionally, the high rotational speeds required for anisotropy [51, 67] could not be achieved as fibers had more difficulty depositing on the surface with high tangential velocity; therefore, rotational speed was modified to produce isotropic leaflets.

Another limitation to this study was the small sample size (n = 3/group/timepoint) and the fairly short degradation timepoints. Although longer timepoints [66, 104, 105] would have been beneficial to understanding the long-term performance of the valves, previous studies [66, 99, 104, 105] using lipase with the biodegradable polyurethanes were performed for only a few weeks with significant degradation. Two weeks was selected as the final timepoint based on these previous enzymatic studies along with the study by Reimer et al. [33] which fatigue tested valves for 2 weeks. Experimentally, testing a single valve at a time in the pulse duplicator limited the number and length of experiments. This, along with the amount of material required for each scaffold, prevented the testing of fast degrading PEUU valves and slow degrading PCUU valves as controls.

Due to the number of fabrications and required polymer for each valve, several different batches of each polyurethane had to be synthesized to complete this study. Therefore, polymer batch to batch variability may have also contributed to the experimental variation. Although the viscosity was evaluated for each batch, and the results for each polyurethane type (PEUU, PECUU, PCUU) were relatively similar to, but slightly higher than, previously reported literature values [64], changes in solution viscosity can vary the electrospinning process and fiber diameter of the scaffold [65].

Characterization methods such as proton nuclear magnetic resonance (^{1}H NMR), Fourier transform infrared (FTIR) spectroscopy, differential scanning calorimetry (DSC), and size-exclusion chromatography are other methods that have been used to characterize the series of degradable polyurethanes (PEUU, PECUU, PCUU) [64, 85, 86]. Because the synthesis has been extensively repeated and characterized, and in the interest of conserving resources, these experiments were not included in this study. However, the lack of these experiments potentially

limit the study in that the molecular weight, presence of monomers, or functional groups are not identified after synthesis or throughout the degradation study.

A more philosophical limitation to this study is the ability to accurately replicate the *in vivo* environment experienced by heart valves. Solution contents and viscosity in the pulse duplicator varied from the blood in the circulatory system. Viscosity is higher for blood than the PBS solution and can be represented with a 40% glycerol solution as used in [51]. The proteins (enzymes) and cells (macrophages) in the circulatory system likely cause different degradation rates with the TEHVs than the lipase enzyme typically found in the pancreas. Additionally, the valve positioning apparatus and holder did not replicate the hemodynamics of the native heart, and the pressures from the PVAD exceeded those experienced in the human body.

5.3 FUTURE DIRECTIONS

The results from the degradation study presented in the previous sections add to the scientific knowledge of designed degradability of polyurethanes and specifically to biodegradable TEHVs. This work contributes to the development of a novel TEHV that supports endogenous tissue growth by degrading at a controlled rate which can be tuned to match new tissue formation. The following are ongoing research opportunities outside of the objectives of this thesis that both inspired and may benefit from this study and the results herein.

5.3.1 Development of a novel tissue engineered heart valve

Inspiration for this study stemmed from the concept of a novel method for producing TEHVs presented by D'Amore et al. [51]. As previously mentioned, the concept of double component deposition was introduced with a complex, anatomically inspired mandrel to produce electrospun heart valves. The two-component mandrel used conductive and non-conductive materials to direct electrospun fiber deposition onto the surface of a complex geometry. As a result, a fully assembled, stentless, trileaflet heart valve with microscopic fibers could be produced.

The acellular scaffold was fabricated with a biodegradable polyurethane with the intention of being a temporary mechanical support while providing a matrix with aligned fibers for new tissue growth. Lacking a cellular component, this construct was intended to rely on endogenous tissue growth by recruiting local and circulating cells to populate the scaffold. The study employed PEUU, a stronger yet fast degrading polyurethane, as mentioned in Section 1.4.3, to prevent mechanical failure.

This study further characterized important mechanical properties defined by [54] as well as macro- and micro-structure of native porcine heart valves and implemented these same properties into the novel TEHV. In-plane biaxial mechanical properties were tuned to match the native valve anisotropy by modifying the rotational speed of the mandrel [67] while out-of-plane flexural properties were matched by altering the translational speed [68]. Native leaflet thickness was matched by controlling the deposition time of polymer onto the mandrel, while fiber diameter was defined by voltage difference, polymer concentration, and gap distance, also defined in [65]. Functionally, the performance of the engineered valve *in situ* and *in vitro* was similar to that of a native porcine tricuspid valve coaptation and a state-of-the-art bioprosthetic in a pulse duplicator, respectively. Finally, the ability to apply the DCD technique to each heart

valve geometry was exemplified through the production of a TEHV with the various geometries and sizes.

The results from the degradation study in the previous sections have the ability to augment this study by D'Amore et al. [51] by providing a method for tuning the degradation rates of the construct to match the rate of endogenous tissue growth. While it is recognized that this study was limited to 2 weeks and performed *in vitro*, it provides a starting point for tweaking the degradation rate of the engineered valves. Similar to how mechanics and structure were controlled through the fabrication process [51], this study indicates a way for controlling the degradation in a similar approach.

5.3.2 Ongoing *in vivo* studies with the tissue engineered heart valves

There are several current ongoing *in vivo* studies evaluating the TEHVs introduced by D'Amore et al. [51]. Current studies use an acute porcine model ($\leq$ 24 hours) to understand the valve functionality and surgical approach to the different engineered heart valves. To date, there have been four approaches attempted with this electrospun valve construct: pulmonary valve with a magnesium stent (n = 5), stentless tricuspid valve (n = 8), mitral valve with a nitinol stent (n = 1), and stentless mitral valve (n = 4). Surgical methods for performing the valve replacement with each engineered construct have been improved to minimize cardiopulmonary bypass time. Stented pulmonary valves and stentless tricuspid valves have been successful in the acute *in vivo* setting with three animals surviving up to 24 hours. Additionally, the valves showed no to mild regurgitation from epicardial echocardiography, and leaflets displayed no thrombus formation, no mechanical failure, and no degradation. Mitral valve replacements were not as successful, due in large part to a small, stiff anterior leaflet which lacked sufficient function.

Valve leaflets for the acute *in vivo* studies were fabricated from PCUU, a mechanically weaker, but less thrombogenic polyurethane. This slower degrading polyurethane was sufficient for an acute study where tissue growth was not expected, but longer chronic studies will require appropriate degradation rates to account for new tissue growth. Hashizume et al. [82] concluded that PECUU (i.e. the soft segment mixed group in this thesis) produced the optimal outcome in a cardiac patch study. Success in the acute valve studies indicates the potential for chronic animal studies to characterize the construct performance over several months as well as endogenous tissue growth, scaffold degradation, and mechanical response. As described in Section 5.3.1, this degradation study provides another method for tuning the degradation rates of TEHVs to be used in chronic *in vivo* studies by altering fabrication conditions.

5.3.3 Long term degradation analysis in the pulse duplicator

The degradation study described in this thesis focused on a symmetrical, trileaflet heart valve in a pulse duplicator. As listed in Section 5.3.2, TEHVs with different geometries, sizes, and two or three leaflets will be used in chronic studies. Performance and fatigue of these different valves should be evaluated *in vitro* before performing the chronic studies, and the pulsatile flow system used in this degradation study provides a way to evaluate these constructs.

This study provides the groundwork for degradation testing *in vitro*. Section 3.3.2 indicates the effect of performing degradation analysis in a mechanically demanding environment. The pulse duplicator described in this thesis provides a system with constant pulsatile flow, physiologically relevant temperature, and enzymatic solution to more accurately represent the *in vivo* environment. Additionally, the valve positioning apparatus shown in Section 2.4 contains three metallic posts to which the commissures of the valve are connected by

two loops of suture. These represent the chordae tendineae of the native heart valve which connect the atrioventricular valves with the papillary muscles in the ventricles. This is an important feature when considering the stresses, and consequent degradation, applied to the engineered valves. **Figure 42** shows two additional valve positioning apparatuses which have been designed according to the size and geometry of the valves for the *in vivo* studies. These are intended to evaluate the performance, fatigue, and degradability of the TEHVs before chronic studies by studying the valves in the pulse duplicator for several months.

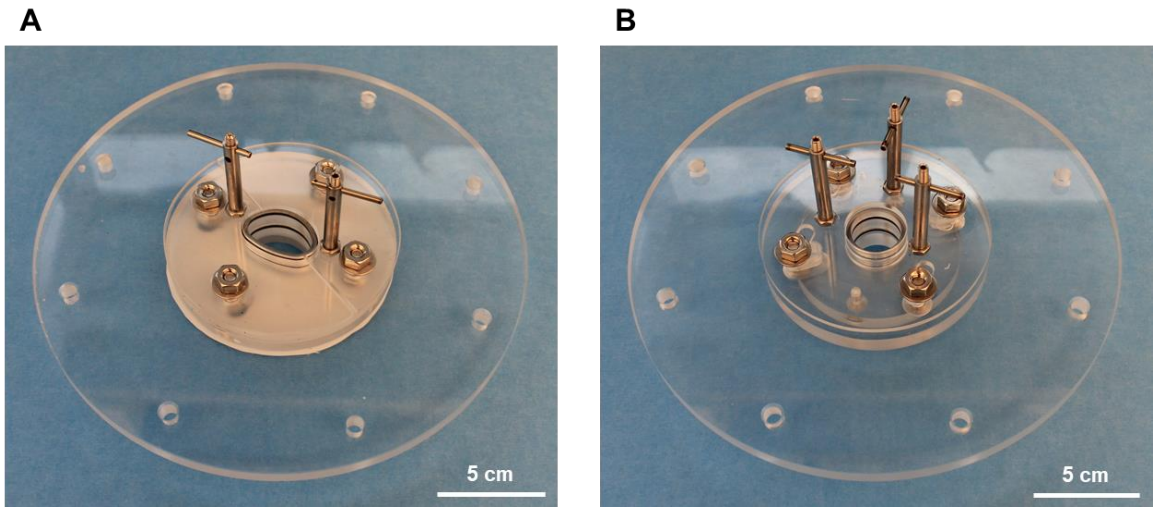

Figure 42. New valve positioning apparatuses for A) mitral valve geometries and B) tricuspid valve geometries with a larger anterior leaflet.

APPENDIX A

ADDITIONAL VALVE DEGRADATION VIDEOS AND STUDIES

Descriptions of the videos of valve function in the pulse duplicator as well as two additional experiments to assess the rapid leaflet tearing and hole formation are included in this appendix.

A.1 REPRESENTATIVE VALVE FABRICATION, PULSE DUPLICATOR, AND DEGRADATION VIDEOS

Representative videos for the TEHV electrospinning process, pulse duplicator side and front views, and degraded valve function in the pulsatile duplicator are available in the supplemental material. Brief, accompanying descriptions of the videos are provided in this section.

Video 1: Representative video showing the electrospinning process to fabricate fully assembled, trileaflet, biodegradable heart valves using the heart valve-shaped mandrel.

Video 2: Representative video of an electrospun TEHV in the pulse duplicator; front view showing the leaflet coaptation at the free edge during pulsatile flow.

Video 3: Representative video of an electrospun TEHV in the pulse duplicator; side view showing the sutures from the commissures to the posts to simulate chordae tendineae.

Video 4: Soft segment mixed electrospun TEHV at 0 days of degradation.

Video 5: Soft segment mixed electrospun TEHV at 3 days of degradation.

Video 6: Soft segment mixed electrospun TEHV at 7 days of degradation.

Video 7: Soft segment mixed electrospun TEHV at 14 days of degradation.

Video 8: Physically blended electrospun TEHV at 0 days of degradation.

Video 9: Physically blended electrospun TEHV at 3 days of degradation.

Video 10: Physically blended electrospun TEHV at 7 days of degradation.

Video 11: Physically blended electrospun TEHV at 14 days of degradation.

Video 12: Co-stream electrospun TEHV at 0 days of degradation.

Video 13: Co-stream electrospun TEHV at 3 days of degradation.

Video 14: Co-stream electrospun TEHV at 7 days of degradation.

Video 15: Co-stream electrospun TEHV at 14 days of degradation.

A.2 ANALYSIS OF LEAFLET TEARS AND HOLE FORMATION

Within a few hours from the start of the degradation study, holes would begin forming in the belly region of the leaflets. A brief experiment was conducted to gain some insight into this phenomenon and to understand if certain factors (e.g. buffer solution, solution temperature, enzyme, degradability of polymer) or combinations of factors were causing this effect. Six conditions were tested: 1) deionized water, room temperature, and a PEUU TEHV, 2) deionized water, physiological temperature, and a PEUU TEHV, 3) tap water, physiological temperature,

and a PEUU TEHV, 4) PBS, physiological temperature, and a PEUU TEHV, 5) PBS, lipase, physiological temperature, and a PEUU TEHV, and 6) PBS, lipase, physiological temperature, and a nondegradable Tecoflex™ polyurethane (Lubrizol, Wickliffe, OH) TEHV. PEUU was selected as the degradable polymer since it has the fastest degradation rate. TEHVs were tested for 3 hours in the pulse duplicator under the conditions listed above. Videos of valve function for the six conditions can be found in the supplemental materials and a description of each is provided below. **Figure 43** shows the six valves, and only the PEUU valve with lipase had tears and holes in the leaflets at 3 hours. While the tearing may result from the interplay of several factors, the enzyme appears to have a significant role in initiating this effect.

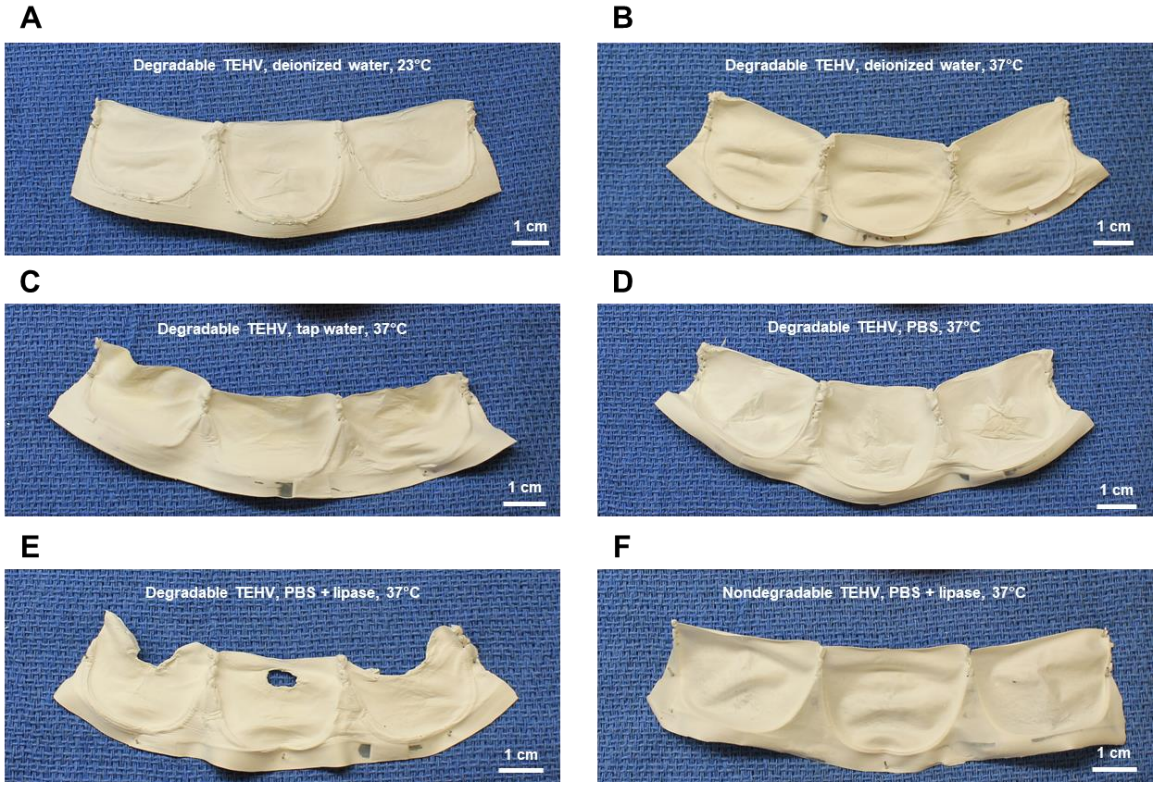

Figure 43. Visual inspection of spliced valves after 3 hours of degradation with A) degradable polyurethane in deionized water at 23°C, B) degradable polyurethane in deionized water at 37°C, C) degradable polyurethane in tap water at 37°C, D) degradable polyurethane in PBS at 37°C, E) degradable polyurethane in PBS + lipase at 37°C, and F) nondegradable polyurethane in PBS + lipase at 37°C.

Video 16: PEUU TEHV in deionized water at 23°C at 3 hours.

Video 17: PEUU TEHV in deionized water at 37°C at 3 hours.

Video 18: PEUU TEHV in tap water at 37°C at 3 hours.

Video 19: PEUU TEHV in PBS at 37°C at 3 hours.

Video 20: PEUU TEHV in PBS with lipase at 37°C at 3 hours.

Video 21: Nondegradable polyurethane TEHV in PBS with lipase at 37°C at 3 hours.

A.3 ANALYSIS OF VALVE CONTRACTION FOLLOWING FABRICATION

Contraction of the valve construct [126] may have been another factor in the formation of holes and tearing in the leaflet. During fabrication of valves for the *in vivo* studies described in Section 5.3.2, it was noted that the diameter of the annulus is smaller than the mandrel dimensions. The mandrel used in this thesis had a diameter of 40 mm, and the valve positioning apparatus contained a 40 mm ring which the valve had to be stretched over when loading it into the system. Valve contraction by just a few millimeters in diameter may have put an unnecessary stress concentration on the valve scaffold, which may have assisted in the hole formation at the thinnest locations: the belly region and free edge of the leaflets. **Table 3** below lists the mixing strategies and the true valve scaffold diameter for the symmetrical 40 mm tricuspid mandrel, while **Table 4** compares the valve mandrel diameters used for the *in vivo* studies to the true valve diameter using PCUU. To compensate for the contraction and provide the correct annulus dimensions, the valve positioning apparatuses shown in Section 5.3.3 **Figure 42** were scaled to match the true valve diameter.

Table 3. Electrospun valve diameter and contraction following fabrication for the three mixing strategies.

Mixing Strategy	Mandrel Diameter (mm)	Valve Diameter (mm)	Contraction (%)
Chemical	40.0	37.3 ± 0.2	6.7 ± 0.5
Blended	40.0	37.9 ± 0.4	5.1 ± 1.1
Co-spun	40.0	37.4 ± 0.3	6.5 ± 0.8

Table 4. Electrospun valve diameter and contraction following fabrication with the new mandrels for *in vivo* studies.

Mandrel Geometry	Mandrel Diameter (mm)	Valve Diameter (mm)	Contraction (%)
Tricuspid	26.0	24.0 ± 0.3	7.7 ± 1.1
Tricuspid	30.0	26.9 ± 0.2	10.3 ± 0.6
Tricuspid	34.0	31.1 ± 0.6	8.6 ± 1.7
Mitral	24.0	22.4 ± 0.2	6.8 ± 1.7
Mitral	30.0	26.8 ± 0.2	10.7 ± 0.7
Mitral	34.0	31.0 ± 0.7	8.9 ± 0.2
Aortic/Pulmonary	20.0	18.5 ± 0.4	7.5 ± 1.9
Aortic/Pulmonary	23.0	21.6 ± 0.2	6.2 ± 0.7

BIBLIOGRAPHY

1. Benjamin, E.J., et al., *Heart disease and stroke statistics-2017 update: a report from the American Heart Association.* Circulation, 2017. **135**(10): p. e146-e603.

2. Nkomo, V.T., et al., *Burden of valvular heart diseases: a population-based study.* The Lancet, 2006. **368**(9540): p. 1005-1011.

3. Pibarot, P. and J.G. Dumesnil, *Prosthetic heart valves.* Circulation, 2009. **119**(7): p. 1034-1048.

4. Yacoub, M. and J. Takkenberg, *Will heart valve tissue engineering change the world?* Nature clinical practice cardiovascular medicine, 2005. **2**(2): p. 60-61.

5. Fallahiarezoudar, E., et al., *A review of: application of synthetic scaffold in tissue engineering heart valves.* Materials Science and Engineering: C, 2015. **48**: p. 556-565.

6. *Edwards Lifesciences 2015 year report.*

7. Cheung, D.Y., B. Duan, and J.T. Butcher, *Current progress in tissue engineering of heart valves: multiscale problems, multiscale solutions.* Expert opinion on biological therapy, 2015. **15**(8): p. 1155-1172.

8. Iung, B., et al., *A prospective survey of patients with valvular heart disease in Europe: The Euro Heart Survey on Valvular Heart Disease.* European heart journal, 2003. **24**(13): p. 1231-1243.

9. Soler-Soler, J. and E. Galve, *Worldwide perspective of valve disease.* Heart, 2000. **83**(6): p. 721-725.

10. Yacoub, M.H. and L.H. Cohn, *Novel approaches to cardiac valve repair.* Circulation, 2004. **109**(9): p. 1064-1072.

11. Bloomfield, P., *Choice of heart valve prosthesis.* Heart, 2002. **87**(6): p. 583-589.

12. Singhal, P., A. Luk, and J. Butany, *Bioprosthetic heart valves: impact of implantation on biomaterials.* ISRN Biomaterials, 2013. **2013**.

13. Bapat, V.N., R. Attia, and M. Thomas, *Effect of valve design on the stent internal diameter of a bioprosthetic valve: a concept of true internal diameter and its implications for the valve-in-valve procedure.* JACC: Cardiovascular Interventions, 2014. **7**(2): p. 115-127.

14. Puvimanasinghe, J., et al., *Comparison of outcomes after aortic valve replacement with a mechanical valve or a bioprosthesis using microsimulation.* Heart, 2004. **90**(10): p. 1172-1178.

15. Hasan, A., et al., *Biomechanical properties of native and tissue engineered heart valve constructs.* Journal of biomechanics, 2014. **47**(9): p. 1949-1963.

16. Schoen, F.J. and R.J. Levy, *Tissue heart valves: current challenges and future research perspectives.* Journal of Biomedical Materials Research Part A, 1999. **47**(4): p. 439-465.

17. Siddiqui, R.F., J.R. Abraham, and J. Butany, *Bioprosthetic heart valves: modes of failure.* Histopathology, 2009. **55**(2): p. 135-144.

18. Nejad, S.P., et al., *Biomechanical conditioning of tissue engineered heart valves: Too much of a good thing?* Advanced drug delivery reviews, 2016. **96**: p. 161-175.

19. Kehl, D., B. Weber, and S.P. Hoerstrup, *Bioengineered living cardiac and venous valve replacements: current status and future prospects.* Cardiovascular Pathology, 2016. **25**(4): p. 300-305.

20. Flanagan, T.C., et al., *The in vitro development of autologous fibrin-based tissue-engineered heart valves through optimised dynamic conditioning.* Biomaterials, 2007. **28**(23): p. 3388-3397.

21. Emmert, M.Y., et al., *Stem cell–based transcatheter aortic valve implantation: first experiences in a pre-clinical model.* JACC: Cardiovascular Interventions, 2012. **5**(8): p. 874-883.

22. Dohmen, P.M., et al., *In-vivo repopularization of a tissue-engineered heart valve in a human subject.* JOURNAL OF HEART VALVE DISEASE, 2007. **16**(4): p. 447.

23. Dohmen, P.M., et al., *Ross operation with a tissue-engineered heart valve.* The Annals of thoracic surgery, 2002. **74**(5): p. 1438-1442.

24. Tedder, M.E., et al., *Stabilized collagen scaffolds for heart valve tissue engineering.* Tissue Engineering Part A, 2008. **15**(6): p. 1257-1268.

25. Metzner, A., et al., *Percutaneous pulmonary valve replacement: autologous tissue-engineered valved stents.* Cardiovascular research, 2010. **88**(3): p. 453-461.

26. Perri, G., et al., *Early and late failure of tissue-engineered pulmonary valve conduits used for right ventricular outflow tract reconstruction in patients with congenital heart disease.* European Journal of Cardio-Thoracic Surgery, 2012. **41**(6): p. 1320-1325.

27. Simon, P., et al., *Early failure of the tissue engineered porcine heart valve SYNERGRAFT® in pediatric patients.* European journal of cardio-thoracic surgery, 2003. **23**(6): p. 1002-1006.

28. Jana, S., et al., *Scaffolds for tissue engineering of cardiac valves.* Acta biomaterialia, 2014. **10**(7): p. 2877-2893.

29. Badrossamay, M.R., et al., *Engineering hybrid polymer-protein super-aligned nanofibers via rotary jet spinning.* Biomaterials, 2014. **35**(10): p. 3188-3197.

30. Capulli, A.K., et al., *JetValve: Rapid manufacturing of biohybrid scaffolds for biomimetic heart valve replacement.* Biomaterials, 2017. **133**: p. 229-241.

31. Syedain, Z.H., et al., *Implantation of a tissue-engineered heart valve from human fibroblasts exhibiting short term function in the sheep pulmonary artery.* Cardiovascular Engineering and Technology, 2011. **2**(2): p. 101-112.

32. Syedain, Z., et al., *6-month aortic valve implantation of an off-the-shelf tissue-engineered valve in sheep.* Biomaterials, 2015. **73**: p. 175-184.

33. Reimer, J.M., et al., *Pediatric tubular pulmonary heart valve from decellularized engineered tissue tubes.* Biomaterials, 2015. **62**: p. 88-94.

34. Puperi, D.S., et al., *Hyaluronan hydrogels for a biomimetic spongiosa layer of tissue engineered heart valve scaffolds.* Biomacromolecules, 2016. **17**(5): p. 1766-1775.

35. Shinoka, T., et al., *Tissue-engineered heart valve leaflets: does cell origin affect outcome?* Circulation, 1997. **96**(9 Suppl): p. II-102-7.

36. Shinoka, T., et al., *Tissue-engineered heart valves. Autologous valve leaflet replacement study in a lamb model.* Circulation, 1996. **94**(9 Suppl): p. II164-8.

37. Zund, G., et al., *The in vitro construction of a tissue engineered bioprosthetic heart valve.* European journal of cardio-thoracic surgery, 1997. **11**(3): p. 493-497.

38. Sodian, R., et al., *Early in vivo experience with tissue-engineered trileaflet heart valves.* Circulation, 2000. **102**(suppl 3): p. Iii-22-Iii-29.

39. Hoerstrup, S.P., et al., *Tissue engineering of functional trileaflet heart valves from human marrow stromal cells.* Circulation, 2002. **106**(12 suppl 1): p. I-143-I-150.

40. Hoerstrup, S.P., et al., *Functional living trileaflet heart valves grown in vitro.* Circulation, 2000. **102**(suppl 3): p. Iii-44-Iii-49.

41. Mol, A., et al., *Tissue engineering of human heart valve leaflets: a novel bioreactor for a strain-based conditioning approach.* Annals of biomedical engineering, 2005. **33**(12): p. 1778-1788.

42. Emmert, M.Y., et al., *Transcatheter aortic valve implantation using anatomically oriented, marrow stromal cell-based, stented, tissue-engineered heart valves: technical considerations and implications for translational cell-based heart valve concepts.* European Journal of Cardio-Thoracic Surgery, 2013. **45**(1): p. 61-68.

43. Moreira, R., et al., *TexMi: development of tissue-engineered textile-reinforced mitral valve prosthesis.* Tissue Engineering Part C: Methods, 2014. **20**(9): p. 741-748.

44. Kidane, A.G., et al., *A novel nanocomposite polymer for development of synthetic heart valve leaflets.* Acta biomaterialia, 2009. **5**(7): p. 2409-2417.

45. Hockaday, L., et al., *Rapid 3D printing of anatomically accurate and mechanically heterogeneous aortic valve hydrogel scaffolds.* Biofabrication, 2012. **4**(3): p. 035005.

46. Duan, B., et al., *Three-dimensional printed trileaflet valve conduits using biological hydrogels and human valve interstitial cells.* Acta biomaterialia, 2014. **10**(5): p. 1836-1846.

47. Van Lieshout, M., et al., *Electrospinning versus knitting: two scaffolds for tissue engineering of the aortic valve.* Journal of Biomaterials Science, Polymer Edition, 2006. **17**(1-2): p. 77-89.

48. Del Gaudio, C., et al., *Electrospun bioresorbable heart valve scaffold for tissue engineering.* The International journal of artificial organs, 2008. **31**(1): p. 68-75.

49. Tseng, H., et al., *Anisotropic poly (ethylene glycol)/polycaprolactone hydrogel–fiber composites for heart valve tissue engineering.* Tissue Engineering Part A, 2014. **20**(19-20): p. 2634-2645.

50. Kluin, J., et al., *In situ heart valve tissue engineering using a bioresorbable elastomeric implant – From material design to 12 months follow-up in sheep.* Biomaterials, 2017. **125**: p. 101-117.

51. D'Amore, A., et al., *Heart valve scaffold fabrication: Bioinspired control of macro-scale morphology, mechanics and micro-structure.* Biomaterials, 2018. **150**: p. 25-37.

52. Tudorache, I., et al., *Decellularized aortic allografts versus pulmonary autografts for aortic valve replacement in the growing sheep model: haemodynamic and morphological results at 20 months after implantation.* European Journal of Cardio-Thoracic Surgery, 2016. **49**(4): p. 1228-1238.

53. Sohier, J., et al., *The potential of anisotropic matrices as substrate for heart valve engineering.* Biomaterials, 2014. **35**(6): p. 1833-1844.

54. Merryman, W.D., et al., *Defining biomechanical endpoints for tissue engineered heart valve leaflets from native leaflet properties.* Progress in Pediatric cardiology, 2006. **21**(2): p. 153-160.

55. Stradins, P., et al., *Comparison of biomechanical and structural properties between human aortic and pulmonary valve.* European Journal of Cardio-thoracic Surgery, 2004. **26**(3): p. 634-639.

56. Balguid, A., et al., *The role of collagen cross-links in biomechanical behavior of human aortic heart valve leaflets—relevance for tissue engineering.* Tissue engineering, 2007. **13**(7): p. 1501-1511.

57. Christie, G.W. and B.G. Barratt-Boyes, *Mechanical properties of porcine pulmonary valve leaflets: how do they differ from aortic leaflets?* The Annals of thoracic surgery, 1995. **60**: p. S195-S199.

58. Christie, G.W. and B.G. Barratt-Boyes, *Age-dependent changes in the radial stretch of human aortic valve leaflets determined by biaxial testing.* The Annals of thoracic surgery, 1995. **60**: p. S156-S159.

59. Merryman, W.D., et al., *The effects of cellular contraction on aortic valve leaflet flexural stiffness.* Journal of biomechanics, 2006. **39**(1): p. 88-96.

60. Mirnajafi, A., et al., *The flexural rigidity of the aortic valve leaflet in the commissural region.* Journal of biomechanics, 2006. **39**(16): p. 2966-2973.

61. Brazile, B., et al., *On the bending properties of porcine mitral, tricuspid, aortic, and pulmonary valve leaflets.* Journal of long-term effects of medical implants, 2015. **25**(1-2).

62. Gloeckner, D.C., K.L. Billiar, and M.S. Sacks, *Effects of mechanical fatigue on the bending properties of the porcine bioprosthetic heart valve.* ASAIO journal (American Society for Artificial Internal Organs: 1992), 1999. **45**(1): p. 59-63.

63. Göpferich, A., *Mechanisms of polymer degradation and erosion.* Biomaterials, 1996. **17**(2): p. 103-114.

64. Hong, Y., et al., *Tailoring the degradation kinetics of poly (ester carbonate urethane) urea thermoplastic elastomers for tissue engineering scaffolds.* Biomaterials, 2010. **31**(15): p. 4249-4258.

65. Sill, T.J. and H.A. von Recum, *Electrospinning: applications in drug delivery and tissue engineering.* Biomaterials, 2008. **29**(13): p. 1989-2006.

66. Nelson, D.M., et al., *Controlled release of IGF-1 and HGF from a biodegradable polyurethane scaffold.* Pharmaceutical research, 2011. **28**(6): p. 1282-1293.

67. Courtney, T., et al., *Design and analysis of tissue engineering scaffolds that mimic soft tissue mechanical anisotropy.* Biomaterials, 2006. **27**(19): p. 3631-3638.

68. Amoroso, N.J., et al., *Microstructural manipulation of electrospun scaffolds for specific bending stiffness for heart valve tissue engineering.* Acta biomaterialia, 2012. **8**(12): p. 4268-4277.

69. Hinderer, S., et al., *Engineering of a bio-functionalized hybrid off-the-shelf heart valve.* Biomaterials, 2014. **35**(7): p. 2130-2139.

70. Sant, S., et al., *Hybrid PGS–PCL microfibrous scaffolds with improved mechanical and biological properties.* Journal of tissue engineering and regenerative medicine, 2011. **5**(4): p. 283-291.

71. Wang, H., et al., *Co-electrospun blends of PU and PEG as potential biocompatible scaffolds for small-diameter vascular tissue engineering.* Materials Science and Engineering: C, 2012. **32**(8): p. 2306-2315.

72. Kidoaki, S., I.K. Kwon, and T. Matsuda, *Mesoscopic spatial designs of nano-and microfiber meshes for tissue-engineering matrix and scaffold based on newly devised multilayering and mixing electrospinning techniques.* Biomaterials, 2005. **26**(1): p. 37-46.

73. Baker, B.M., et al., *The potential to improve cell infiltration in composite fiber-aligned electrospun scaffolds by the selective removal of sacrificial fibers.* Biomaterials, 2008. **29**(15): p. 2348-2358.

74. Teo, W.E. and S. Ramakrishna, *A review on electrospinning design and nanofibre assemblies.* Nanotechnology, 2006. **17**(14): p. R89.

75. Liang, D., B.S. Hsiao, and B. Chu, *Functional electrospun nanofibrous scaffolds for biomedical applications.* Advanced drug delivery reviews, 2007. **59**(14): p. 1392-1412.

76. D'Amore, A., et al., *Bi-layered polyurethane–Extracellular matrix cardiac patch improves ischemic ventricular wall remodeling in a rat model.* Biomaterials, 2016. **107**: p. 1-14.

77. Shastri, V.P., *Non-degradable biocompatible polymers in medicine: past, present and future.* Current pharmaceutical biotechnology, 2003. **4**(5): p. 331-337.

78. Hoshi, R.A., et al., *The blood and vascular cell compatibility of heparin-modified ePTFE vascular grafts.* Biomaterials, 2013. **34**(1): p. 30-41.

79. Chen, R., et al., *A novel approach via combination of electrospinning and FDM for tri-leaflet heart valve scaffold fabrication.* Frontiers of Materials Science in China, 2009. **3**(4): p. 359-366.

80. Kumar, N., R.S. Langer, and A.J. Domb, *Polyanhydrides: an overview.* Advanced drug delivery reviews, 2002. **54**(7): p. 889-910.

81. Stokes, K., R. McVenes, and J.M. Anderson, *Polyurethane elastomer biostability.* Journal of biomaterials applications, 1995. **9**(4): p. 321-354.

82. Hashizume, R., et al., *The effect of polymer degradation time on functional outcomes of temporary elastic patch support in ischemic cardiomyopathy.* Biomaterials, 2013. **34**(30): p. 7353-7363.

83. Nieponice, A., et al., *In vivo assessment of a tissue-engineered vascular graft combining a biodegradable elastomeric scaffold and muscle-derived stem cells in a rat model.* Tissue Engineering Part A, 2010. **16**(4): p. 1215-1223.

84. Hong, Y., et al., *A small diameter, fibrous vascular conduit generated from a poly (ester urethane) urea and phospholipid polymer blend.* Biomaterials, 2009. **30**(13): p. 2457-2467.

85. Guan, J., et al., *Synthesis, characterization, and cytocompatibility of elastomeric, biodegradable poly (ester-urethane) ureas based on poly (caprolactone) and putrescine.* Journal of Biomedical Materials Research Part A, 2002. **61**(3): p. 493-503.

86. Guan, J., et al., *Biodegradable poly (ether ester urethane) urea elastomers based on poly (ether ester) triblock copolymers and putrescine: synthesis, characterization and cytocompatibility.* Biomaterials, 2004. **25**(1): p. 85-96.

87. Wang, F., et al., *Synthesis, characterization and surface modification of low moduli poly (ether carbonate urethane) ureas for soft tissue engineering.* Acta biomaterialia, 2009. **5**(8): p. 2901-2912.

88. Asplund, B., et al., *In vitro degradation and in vivo biocompatibility study of a new linear poly (urethane urea).* Journal of Biomedical Materials Research Part B: Applied Biomaterials, 2008. **86**(1): p. 45-55.

89. Asplund, J.B., et al., *Synthesis of highly elastic biodegradable poly (urethane urea).* Biomacromolecules, 2007. **8**(3): p. 905-911.

90. Guan, J. and W.R. Wagner, *Synthesis, characterization and cytocompatibility of polyurethaneurea elastomers with designed elastase sensitivity.* Biomacromolecules, 2005. **6**(5): p. 2833-2842.

91. O'brien, F.J., *Biomaterials & scaffolds for tissue engineering.* Materials today, 2011. **14**(3): p. 88-95.

92. Xue, Y., et al., *Biodegradable and biomimetic elastomeric scaffolds for tissue-engineered heart valves.* Acta biomaterialia, 2017. **48**: p. 2-19.

93. Li, P., et al., *Influences of tensile load on in vitro degradation of an electrospun poly (l-lactide-co-glycolide) scaffold.* Acta biomaterialia, 2010. **6**(8): p. 2991-2996.

94. Suriano, F., et al., *Functionalized cyclic carbonates: from synthesis and metal-free catalyzed ring-opening polymerization to applications.* Polymer Chemistry, 2011. **2**(3): p. 528-533.

95. Zhang, H., L. Zhou, and W. Zhang, *Control of scaffold degradation in tissue engineering: a review.* Tissue Engineering Part B: Reviews, 2014. **20**(5): p. 492-502.

96. Place, E.S., et al., *Synthetic polymer scaffolds for tissue engineering.* Chemical Society Reviews, 2009. **38**(4): p. 1139-1151.

97. West, J.L. and J.A. Hubbell, *Polymeric biomaterials with degradation sites for proteases involved in cell migration.* Macromolecules, 1999. **32**(1): p. 241-244.

98. Lutolf, M., et al., *Synthetic matrix metalloproteinase-sensitive hydrogels for the conduction of tissue regeneration: engineering cell-invasion characteristics.* Proceedings of the National Academy of Sciences, 2003. **100**(9): p. 5413-5418.

99. Ma, Z., et al., *Biodegradable polyurethane ureas with variable polyester or polycarbonate soft segments: Effects of crystallinity, molecular weight, and composition on mechanical properties.* Biomacromolecules, 2011. **12**(9): p. 3265-3274.

100. Guan, J., et al., *Preparation and characterization of highly porous, biodegradable polyurethane scaffolds for soft tissue applications.* Biomaterials, 2005. **26**(18): p. 3961-3971.

101. Guan, J., J.J. Stankus, and W.R. Wagner, *Development of composite porous scaffolds based on collagen and biodegradable poly (ester urethane) urea.* Cell transplantation, 2006. **15**(1): p. 17-27.

102. Stankus, J.J., et al., *Hybrid nanofibrous scaffolds from electrospinning of a synthetic biodegradable elastomer and urinary bladder matrix.* Journal of Biomaterials Science, Polymer Edition, 2008. **19**(5): p. 635-652.

103. Wang, F., et al., *Injectable, rapid gelling and highly flexible hydrogel composites as growth factor and cell carriers.* Acta biomaterialia, 2010. **6**(6): p. 1978-1991.

104. Hong, Y., et al., *Synthesis, characterization, and paclitaxel release from a biodegradable, elastomeric, poly (ester urethane) urea bearing phosphorylcholine groups for reduced thrombogenicity.* Biomacromolecules, 2012. **13**(11): p. 3686-3694.

105. Fang, J., et al., *Biodegradable poly (ester urethane) urea elastomers with variable amino content for subsequent functionalization with phosphorylcholine.* Acta biomaterialia, 2014. **10**(11): p. 4639-4649.

106. Guan, J., J.J. Stankus, and W.R. Wagner, *Biodegradable elastomeric scaffolds with basic fibroblast growth factor release.* Journal of Controlled Release, 2007. **120**(1-2): p. 70-78.

107. Gu, X., et al., *Biodegradable, elastomeric coatings with controlled anti-proliferative agent release for magnesium-based cardiovascular stents.* Colloids and Surfaces B: Biointerfaces, 2016. **144**: p. 170-179.

108. Guan, J., et al., *Protein-reactive, thermoresponsive copolymers with high flexibility and biodegradability.* Biomacromolecules, 2008. **9**(4): p. 1283-1292.

109. Sant, S., et al., *Effect of biodegradation and de novo matrix synthesis on the mechanical properties of valvular interstitial cell-seeded polyglycerol sebacate–polycaprolactone scaffolds.* Acta biomaterialia, 2013. **9**(4): p. 5963-5973.

110. Brugmans, M.M., et al., *Poly-ε-caprolactone scaffold and reduced in vitro cell culture: beneficial effect on compaction and improved valvular tissue formation.* Journal of tissue engineering and regenerative medicine, 2015. **9**(12).

111. Brugmans, M.M., et al., *Superior tissue evolution in slow-degrading scaffolds for valvular tissue engineering.* Tissue Engineering Part A, 2015. **22**(1-2): p. 123-132.

112. Hobson, C.M., et al., *Fabrication of elastomeric scaffolds with curvilinear fibrous structures for heart valve leaflet engineering.* Journal of Biomedical Materials Research Part A, 2015. **103**(9): p. 3101-3106.

113. Kucinska-Lipka, J., et al., *Fabrication of polyurethane and polyurethane based composite fibres by the electrospinning technique for soft tissue engineering of cardiovascular system.* Materials Science and Engineering: C, 2015. **46**: p. 166-176.

114. Makadia, H.K. and S.J. Siegel, *Poly lactic-co-glycolic acid (PLGA) as biodegradable controlled drug delivery carrier.* Polymers, 2011. **3**(3): p. 1377-1397.

115. Hong, H., et al., *Fabrication of a novel hybrid heart valve leaflet for tissue engineering: an in vitro study.* Artificial organs, 2009. **33**(7): p. 554-558.

116. Huang, C., et al., *Electrospun collagen–chitosan–TPU nanofibrous scaffolds for tissue engineered tubular grafts.* Colloids and Surfaces B: Biointerfaces, 2011. **82**(2): p. 307-315.

117. Gupta, P. and G.L. Wilkes, *Some investigations on the fiber formation by utilizing a side-by-side bicomponent electrospinning approach.* Polymer, 2003. **44**(20): p. 6353-6359.

118. Theron, S., et al., *Multiple jets in electrospinning: experiment and modeling.* Polymer, 2005. **46**(9): p. 2889-2899.

119. Ding, B., et al., *Fabrication of blend biodegradable nanofibrous nonwoven mats via multi-jet electrospinning.* Polymer, 2004. **45**(6): p. 1895-1902.

120. Hashizume, R., et al., *Morphological and mechanical characteristics of the reconstructed rat abdominal wall following use of a wet electrospun biodegradable polyurethane elastomer scaffold.* Biomaterials, 2010. **31**(12): p. 3253-3265.

121. Stankus, J.J., et al., *Microintegrating smooth muscle cells into a biodegradable, elastomeric fiber matrix.* Biomaterials, 2006. **27**(5): p. 735-744.

122. Mackay, T., et al., *New polyurethane heart valve prosthesis: design, manufacture and evaluation.* Biomaterials, 1996. **17**(19): p. 1857-1863.

123. Sacks, M.S., *Biaxial mechanical evaluation of planar biological materials.* Journal of elasticity and the physical science of solids, 2000. **61**(1-3): p. 199.

124. Ye, S.-H., et al., *Simple surface modification of a titanium alloy with silanated zwitterionic phosphorylcholine or sulfobetaine modifiers to reduce thrombogenicity*. Colloids and Surfaces B: Biointerfaces, 2010. **79**(2): p. 357-364.

125. Walser, J. and S.J. Ferguson, *Oriented nanofibrous membranes for tissue engineering applications: Electrospinning with secondary field control.* Journal of the mechanical behavior of biomedical materials, 2016. **58**: p. 188-198.

126. Ru, C., et al., *Suspended, shrinkage-free, electrospun PLGA nanofibrous scaffold for skin tissue engineering.* ACS applied materials & interfaces, 2015. **7**(20): p. 10872-10877.